AWARD NUMBER: W81XWH-13-1-0090

TITLE: Targeting Androgen Receptor in Breast Cancer: Enzalutamide as a Novel Breast Cancer Therapeutic

PRINCIPAL INVESTIGATOR: Jennifer Richer, Ph.D.

CONTRACTING ORGANIZATION: The Regents of the University of Colorado
Aurora, CO 80045

REPORT DATE: September 2014

TYPE OF REPORT: Annual Progress Report

PREPARED FOR: U.S. Army Medical Research and Materiel Command
Fort Detrick, Maryland 21702-5012

REPORT DOCUMENTATION PAGE

Form Approved
OMB No. 0704-0188

1. REPORT DATE	2. REPORT TYPE	3. DATES COVERED
September 2014	Annual	15Aug2013-14Aug2014

4. TITLE AND SUBTITLE
Targeting Androgen Receptor in Breast Cancer: Enzalutamide as a Novel Breast Cancer Therapeutic

5a. CONTRACT NUMBER

5b. GRANT NUMBER
W81XWH-13-1-0090

5c. PROGRAM ELEMENT NUMBER

6. AUTHOR(S)

Jennifer K. Richer, Ph.D.

E-Mail: Jennifer.richer@ucdenver.edu

5d. PROJECT NUMBER

5e. TASK NUMBER

5f. WORK UNIT NUMBER

7. PERFORMING ORGANIZATION NAME(S) AND ADDRESS(ES)

The Regents of the University of Colorado

Aurora, CO 90010

8. PERFORMING ORGANIZATION REPORT NUMBER

9. SPONSORING / MONITORING AGENCY NAME(S) AND ADDRESS(ES)

U.S. Army Medical Research and Materiel Command
Fort Detrick, Maryland 21702-5012

10. SPONSOR/MONITOR'S ACRONYM(S)

11. SPONSOR/MONITOR'S REPORT NUMBER(S)

12. DISTRIBUTION / AVAILABILITY STATEMENT

Approved for Public Release; Distribution Unlimited

13. SUPPLEMENTARY NOTES

14. ABSTRACT

In breast cancers, the androgen receptor (AR) is more widely expressed than estrogen receptor alpha (ER) or the progesterone receptor (PR) (1), which are used as therapeutic targets and biomarkers, suggesting a potential role for AR in BC. To explore the function of AR in models of the three main subtypes of breast cancer (ER positive, ER negative and Her2+), we are using a new-generation AR inhibitor, enzalutamide, which impairs nuclear localization of AR. This is a very different mode of action than previous generation anti-androgens such as bicalutamide (Casodex), which is a competitive inhibitor of endogenous androgens that allows ligand-mediated nuclear localization of AR. Enzalutamide has shown success in the clinic in patients with late stage prostate cancer. The research in this proposal seeks to determine whether inhibition of AR with enzalutamide will be effective in breast cancer and utilize preclinical models to determine if and how it should be combined with currently used standard of care treatments in the three main types of breast cancer, with the primary objectives of the research being to guide the design of future clinical trials with enzalutamide.

15. SUBJECT TERMS
Breast cancer, androgen receptor, estrogen receptor, growth factors, enzalutamide, endocrine resistance, targeted therapy

16. SECURITY CLASSIFICATION OF:			17. LIMITATION OF ABSTRACT	18. NUMBER OF PAGES	19a. NAME OF RESPONSIBLE PERSON
					USAMRMC
a. REPORT	b. ABSTRACT	c. THIS PAGE			19b. TELEPHONE NUMBER *(include area code)*
U Unclassified	U Unclassified	U Unclassified	U Unclassified	104	

Standard Form 298 (Rev. 8-98)
Prescribed by ANSI Std. Z39.18

Table of Contents

Page

INTRODUCTION:

In breast cancers, the androgen receptor (AR) is more widely expressed than estrogen receptor alpha (ER) or the progesterone receptor (PR) (1), which are used as therapeutic targets and biomarkers, suggesting a potential role for AR in BC. We examined the primary tumors of women treated with tamoxifen or aromatase inhibitor therapy and found that a higher AR to ER protein ratio correlates with worse response to traditional the anti-estrogen tamoxifen (see figure 1 in our published manuscript Cochrane et al in the appendix) (2). To explore the function of AR in models of the three main subtypes of breast cancer (ER positive, ER negative and Her2+), we are using a new-generation AR inhibitor, enzalutamide, which impairs nuclear localization of AR. This is a very different mode of action than previous generation anti-androgens such as bicalutamide (Casodex), which is a competitive inhibitor of endogenous androgens that allows ligand-mediated nuclear localization of AR. Enzalutamide has shown success in the clinic in patients with late stage prostate cancer refractory to bicalutamide (3) and is now FDA approved as a prostate cancer therapy. The research in this proposal seeks to determine whether inhibition of AR with enzalutamide will be effective in breast cancer and utilize preclinical models to determine if and how it should be combined with currently used standard of care treatments in the three main types of breast cancer, with the primary objectives of the research being to guide the design of future clinical trials with enzalutamide.

KEYWORDS: Breast cancer, androgen receptor, estrogen receptor, growth factors, enzalutamide, endocrine resistance, targeted therapy

ACCOMPLISHMENTS: Below we describe for each task in the official statement of work the major activities; specific objectives; significant results or key outcomes, including major findings, developments, or conclusions (both positive and negative); and/or other achievements. We include a discussion of stated goals not met or tasks not fully completed. For some of the tasks we are ahead of schedule. We include pertinent data and graphs in sufficient detail to explain significant results achieved. Detailed description of the methodology used is provided in the methods section of two manuscripts in the appendix. The first manuscript was published in January of 2014 and the second one is about to be sent out for review, likely this week.

The objective of Stage I of this proposal is to rapidly generate preclinical data testing enza alone or in combination with standard of care therapeutics in different subtypes of BC to help guide the clinical trials described in **Stage II** (PI clinical partner Anthony Elias, M.D.) and steer the rational design and focus on patients most likely to benefit from enzalutamide alone or in combination with currently used therapeutics.

Preclinical Aim 1. **To test enzalutamide (enza) in combination with currently approved therapies for breast cancer (BC) in the various subtypes of BC. Year 1, months 1-12**

Task 1 – Evaluate enzalutamide in ER+/AR+ BC lines (MCF7, BCK4) and explant (PT15) in combination with anti-estrogen therapy. Months 1-4. 75% completed.

Task 2. Test enza in three different tamoxifen resistance models *in vitro.* Months 1-4 (30% complete)

Task 3. Test enzalutamide in combination with Her2 directed therapy in ER+ and ER- Her2+ models Months 13-18 (25% complete)

Task 4. Examine enzalutamide in combination with an mTOR inhibitor (Afinitor/everolimus) Months 7-10 (25% complete)

Task 5. In true TNBC cell lines and explants that retain AR, enzalutamide will be evaluated alone and in combination with chemotherapy and everolimus, *in vitro* and *in vivo*. Months 12-15 (30% completed ahead of schedule).

What was accomplished under these goals?

Task 1 – Evaluate enzalutamide in ER+/AR+ BC lines (MCF7, BCK4) and explant (PT15) in combination with anti-estrogen therapy. Months 1-4. (75% completed).

For this task we have performed *in vitro* and *in vivo* experiments with MCF7 cells in our published paper (Cochrane, D.R. et al Breast Cancer Research) (2) and in unpublished work described below. We find that enzalutamide (Enz) effectively inhibits androgen-stimulated growth of ER+/AR+ xenograft models (Figure 2 and 3 in Cochrane DR et al 2014 in appendix) and is as effective as tamoxifen at reducing the viability of estradiol (E2)-driven MCF7 xenografts (Figures 5 and 6 in Cochrane et al 2014 in appendix). This is very important since we also demonstrated that women whose primary tumors express a high percentage of AR+ nuclei as compared to ER+ nuclei have significantly higher likelihood of recurrent disease while on the anti-estrogen tamoxifen and shorter disease free survival (Figure 1 of Cochrane et al 2014 in appendix).

Since we demonstrated in our published work that Tam and Enz work equally well to inhibit growth of estradiol (E2) induced ER+/AR+ breast cancer xenoograft tumors (2), we performed an experiment with Enz and Tam combined as compared to either drug alone *in vivo* in nude mice and find that Tam and Enz combined are superior to either drug alone (Figure 1).

Figure1. Combination of enzalutamide plus tamoxifen inhibits estrogen-stimulated growth of MCF7 tumors more effectively than either drug alone*. MCF7-TGL cells stably expressing luciferase were implanted orthotopically in the mammary gland of ovariectomized female nude mice. E2 pellets were implanted SQ in all mice at the time of injection. Tumor growth was monitored by caliper and IVIS measurement. When tumors reached an average of 100mm^3, mice were randomized into four groups given either: control chow (E2), chow containing 50 mg/kg enzalutamide (E2 + enza), control chow plus a tamoxifen pellet implanted SQ (E2 + tam), or chow containing enzalutamide plus a tamoxifen pellet (E2 + tam + enza). Tumor burden was measured by whole body luminescence.* ***A.*** *Mean total flux. Mice were matched on day -4 and readings taken on the indicated days following beginning of treatment (day 0). * p<0.05, *** p<0.001, ANOVA with Bonferroni's multiple comparison test correction.* ***B.*** *The total luminescent flux is shown for individual mice (two tumors per mouse) at day of matching (day -4) and weekly thereafter through day 24. Treatment began on day 0 (arrow). * p<0.05, ANOVA with Bonferroni's multiple comparison test correction.* ***C.*** *Images of luminescent signal in the mice at day 24 post-treatment.*

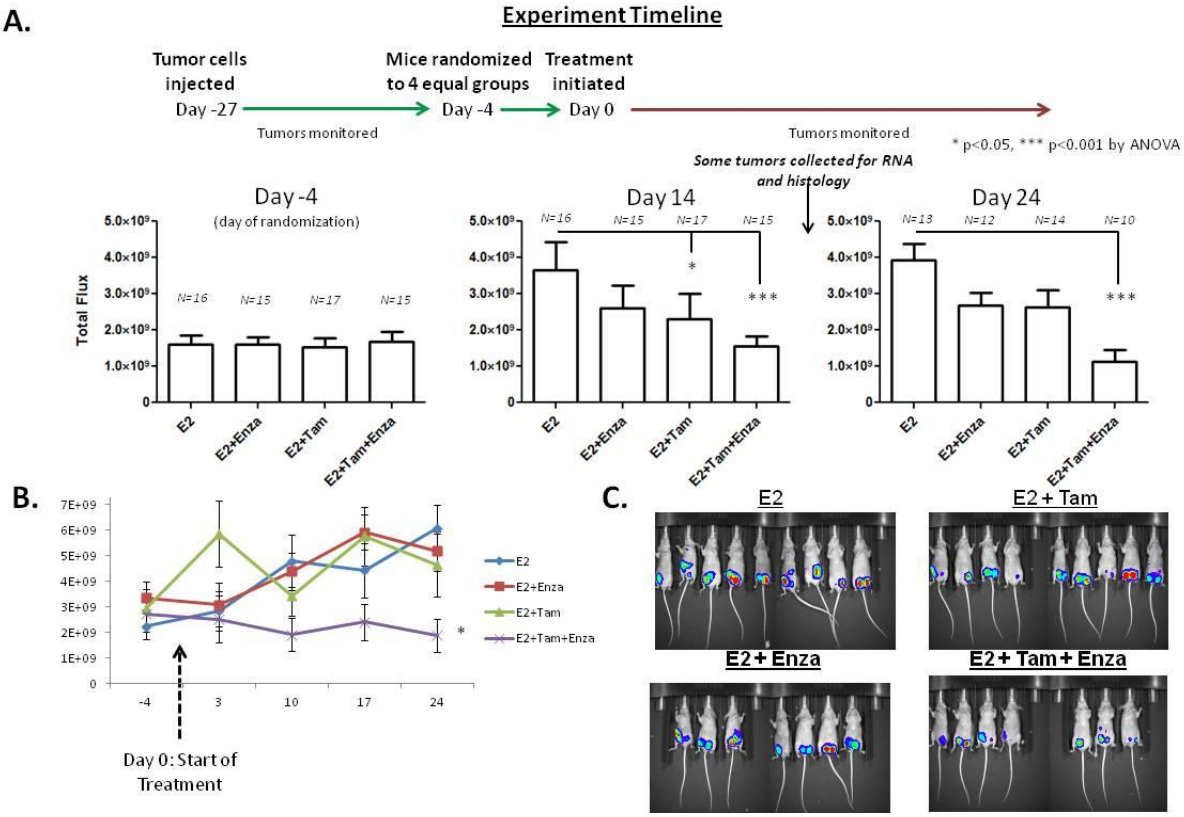

Because we observe that drugs like Enz and MJC13 (4), that keep AR out of the nucleus, inhibit estrogen-mediated tumor growth, whereas the older generation anti-androgens such as bicalutamide do not, our overarching hypothesis for ER+/AR+ breast cancers is that AR actually helps ER to regulate certain genes or that AR regulates genes necessary for estradiol-mediated growth, and therefore inhibiting AR nuclear localization decreases E2/ER-mediated tumor growth. Consequently, we believe both Tam, working as a competitive inhibitor of endogenous estrogen for binding to ER, and Enz, which keeps AR out of the nucleus and seems to thereby affect ER, would work well together to inhibit E2-mediated tumor growth by two different mechanisms. In order to demonstrate true drug synergy, postdoctoral fellow Dr. Nicholas D'Amato sought to evaluate Tam and Enz or another anti-androgen that keeps AR out of the nucleus, MJC13 *in vitro* (Figure 2) to test whether enzalutamide combined with tamoxifen would inhibit proliferation of ER+/AR+ cells. The ability of Enz to synergize with tamoxifen and the ER degrader fulvestrant, were then tested formally with multiple doses using a program called Calcusyn (Figures 3 and 4).

Figure 2. Tamoxifen combined with either enzalutamide or another anti-androgen that keeps AR out of the nucleus, MJC13, works better than tamoxifen alone. *MCF7 cells were cultured in phenol red-free MEM with 5% DCC for 3 days. Cells were then treated with the indicated compounds for 6 days, and cell growth (as measured by percent confluence) was monitored over time (left panel). Data from Day 5 is show as bar graphs (right panel).*

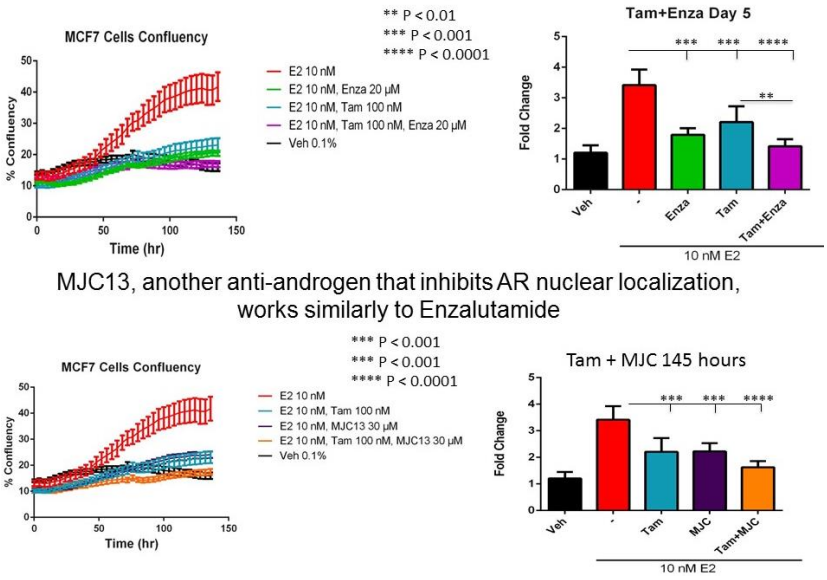

Figure 3. Tamoxifen and Enzalutamide act synergistically in ER+AR+ MCF7 breast cancer cells. *MCF7 cells were treated with multiple doses of Enzalutamide and Tamoxifen alone or together for 72 hrs and proliferation measured by percent confluence by Incucyte (Essen Bioscience). Combination Index analysis was performed using Calcusyn, with a CI index under 1.0 indicative of synergistic drug activity.*

Enzalutamide

Enza (uM)	% Inhibition
3.16	7.72%
10	13.91%
31.6	75.25%

Tamoxifen

Tam (nM)	% Inhibition
31.6	12.56%
100	3.99%
316	40.51%

Enza + Tam

Enza (uM)	Tras (nM)	% Inhibition	Combination Index
3.16	31.6	35.28%	0.287
10	100	28.26%	1.182
31.6	316	79.21%	0.707

CI < 1 indicative of synergistic activity

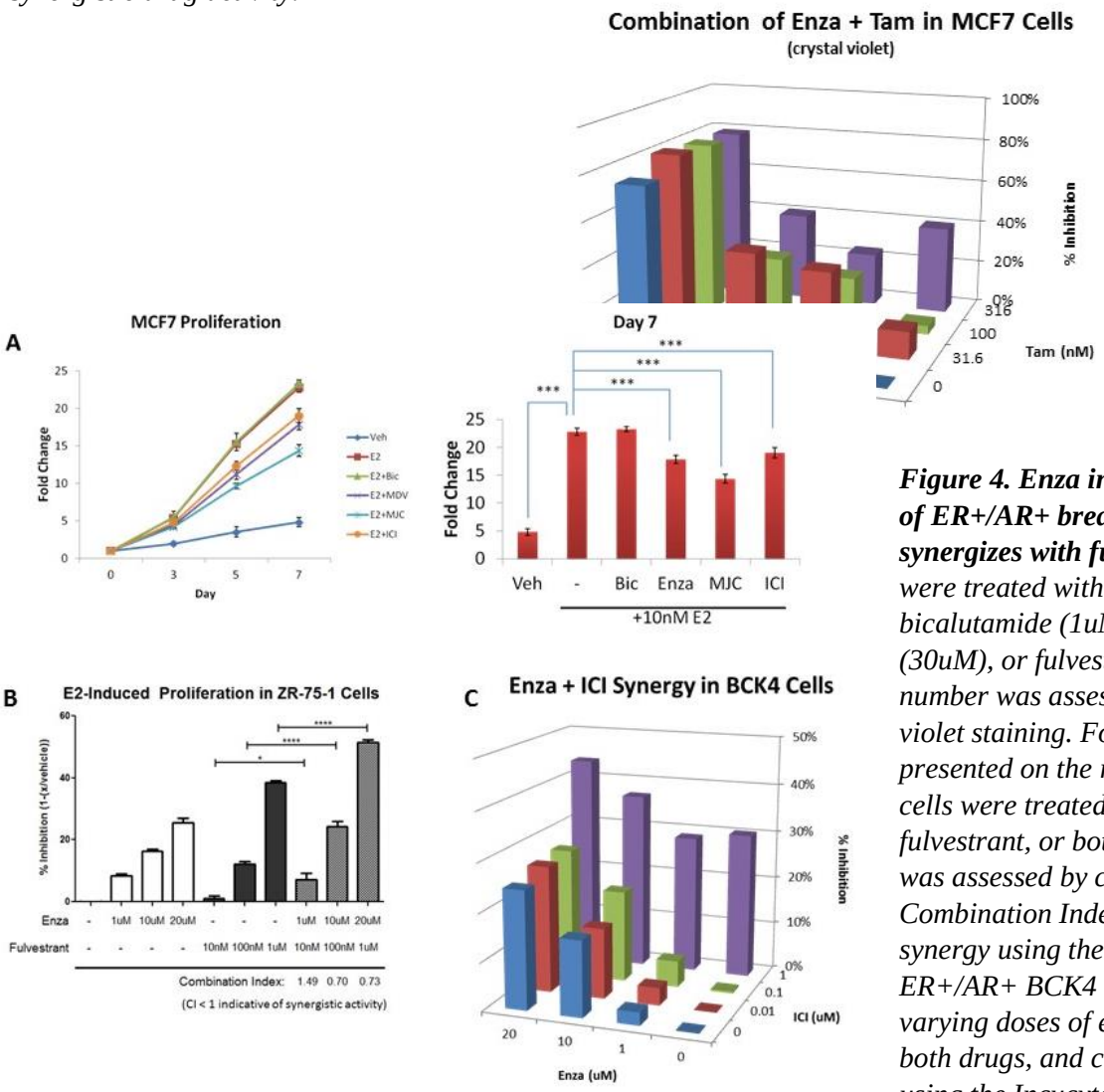

Figure 4. Enza inhibits E2-induced growth of ER+/AR+ breast cancer cells and synergizes with fulvestrant. *(A) MCF7 cells were treated with vehicle control, E2, bicalutamide (1uM), Enza (10uM), MJC13 (30uM), or fulvestrant (ICI, 100nM) and cell number was assessed over 7 days by crystal violet staining. Fold change at Day 7 is presented on the right. (B) ER+/AR+ ZR-75-1 cells were treated with varying doses of enza, fulvestrant, or both drugs, and cell number was assessed by crestal violet staining. Combination Index was calculated to measure synergy using the Calcusyn program. (C) ER+/AR+ BCK4 cells were treated with varying doses of enza, fulvestrant (ICI), or both drugs, and cell number was assessed using the Incucyte ZOOM kinetic live-cell imager.*

Because the ER degrader, Fulvestrant is used clinically after resistance to tamoxifen or aromatase inhibitors, we decided to determine if there was any added benefit or synergy achieved by adding enzalutamide with fulvestrant. We find synergy between these two drugs in two other ER+/AR+ breast cancer cell lines (BCK4 and ZR75) and that the effective dose of fulvestrant can be reduced by adding Enza (Figure 4 and 5). Clinically, this would be beneficial since Fulvestrant is given IM currently and it is difficult to achieve the effective dose, so being able to give a lower dose with just as good response or better would be very beneficial.

Figure 5. Enza and fulvestrant synergize to oppose E2-mediated proliferation in ER+AR+ ZR75-1 cells. *Cells were plated in phenol red-free media containing 5% charcoal-stripped FBS for 72hrs, then treated with varying doses of Enzalutamide and Fulvestrant (ICI) for 5 days and cell number was measured by crystal violet staining. %Inhibition was calculated compared to Vehicle control, and Combination Index analysis calculated in Calcusyn.*

Enzalutamide

Enza (uM)	% Inhibition
1	8.40%
10	16.43%
20	25.60%

ICI

ICI (uM)	% Inhibition
0.01	1.02%
0.10	12.17%
1.00	38.47%

Enza + ICI

Enza (uM)	Tras (uM)	% Inhibition	Combination Index
1	0.01	7.22%	1.493
10	0.1	24.30%	**0.703** ←
20	1	51.55%	**0.726** ←

CI < 1 indicative of synergistic activity

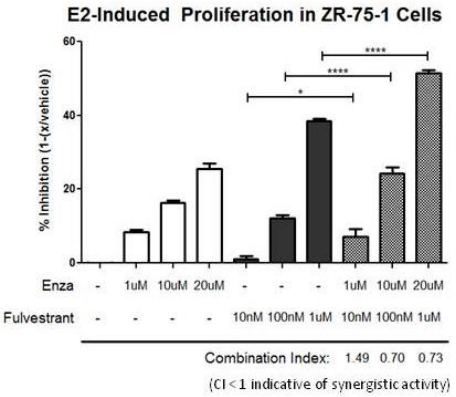

Dose Reduction Index

Combination		Drug alone		Dose Reduction Index (DRI)	
Dose Enza / ICI	% Inhibition	Dose Enza	Dose ICI	Enza	ICI
1uM / .01uM	7.22%	0.73uM	78.85nM	0.73	7.885
10uM / .1uM	24.30%	22.51uM	385.99nM	2.25	3.86
20uM / 1uM	51.55%	407.78uM	1.48uM	20.39	1.48

As outlined in Task 1, we have also put the PT15 patient derived xenograft (PDX) explant tumor into mice. We chose this tumor because it was ER+PR+ and AR+ and relatively fast as compared to other PDX. This tumor was described by collaborator, Dr. Carol Sartorius as having low ER (8% cell staining) in the original clinical sample and even lower in the 5% in the mouse xenografts (5) (Figure 6 top). We gave 10 mice an estradiol pellet and 10 without and both of those groups had 5 mice given chow containing 50mg/kg Enz and 5 were given control chow. This experiment was recently completed and we do not see any difference in tumor volume or growth/viability between the Enz treated versus control tumors (Figure 7); however we still need to analyze proliferation (by BrdU incorporation) and TUNEL staining for effects on apoptosis.

Table 1 Characteristics and hormone receptor status of patient breast tumors and their corresponding xenografts

Patient tumor			Xenograft[a]					
Sample	Origin	Clinical description	Description	ER (intensity, %)	PR (intensity, %)	AR (%)	HER2 intensity	CK5 (%)
PE4	Pleural effusion	Invasive mammary carcinoma ER+ PR+ HER2−	Poorly differentiated with necrosis	2, 90	3, 75	80	1+	<0.1
AS9	Ascites	Invasive mammary carcinoma ER+ PR+ HER2+	Moderately differentiated with necrosis	3, 99	3, 99	5	3+	0
PT12	Primary tumor	IDC[b] with mucinous features, grade 3, ER+ (93 %), PR+ (15 %), HER2−	IDC with mucinous features	3, 35	3, 1	0	1+	<0.1
PT15	Primary tumor	IDC grade 3, ER+ (8 %), PR (0 %), HER2−	IDC, poorly differentiated	1, 5	1.5, <1	30	1+	30
PT16	Primary tumor	IDC grade 3, ER (74 %), PR (0 %), HER2− (FISH ratio 1.46)	IDC, moderately differentiated	1, 20	1, <1	1	2+	0
PT18	Primary tumor	Metaplastic carcinoma, grade 3, ER− PR− HER2−	Metaplastic carcinoma, poorly differentiated	0	0	0	1+	30

[a] At first passage, estrogen-treated except for PT18
[b] Invasive ductal carcinoma

Kabos et al, Breast Cancer Res Treat. 2012 Sep;135(2):415-32

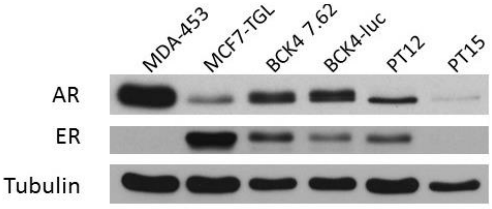

Figure 6. Description of PT15 and PT12 ER+ AR+ patient derived xenografts (PDX). *Table from Kabos et al Breast Cancer Research and Treatment 2012 describing PDX, including PT15 and PT12 (top). Western blot of cell lines isolated from the PT12 and PT15 xenografts (bottom).*

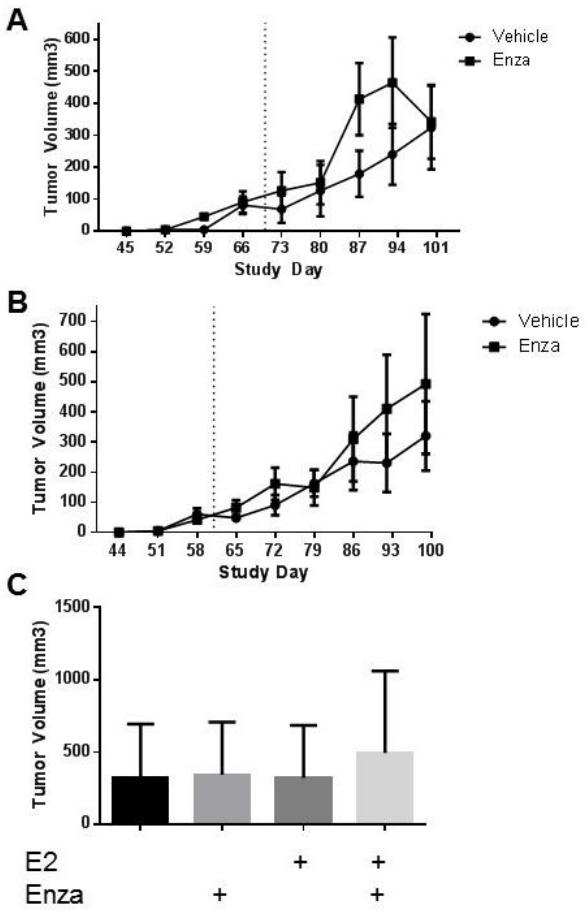

In retrospect, this inconclusive result maybe be due to the fact that this tumor now apparently has undetectable amounts of both ER by IHC and western blot of a cell line from this tumor shows no ER and very little of either receptor (Figure 6 bottom) compared to another explant PT14 or the BCK4 cell line which was recently established from a ER+/PR+ patient by our collaborator, Dr. Britta Jacobsen (6). Although PT12 grows slower in culture it is more E2-dependent and has much higher AR, so in the future we will try to repeat this experiment with the PT12 tumor or the BCK4 cells.

Figure 7. Effects of Enzalutamide and/or Estradiol on the growth of PT15 patient tumor derived xenografts (PDX). *Tumor growth curves of PT15 PDX grown in the absence (**A**) or presence (**B**) of Estradiol (E2) with or without Enza. The dotted line shows the commencement of Enza treatment. **C**) Final tumor volumes for each treatment group are shown. At least 4 tumors are shown per group. There was no statistical significance between groups by ANOVA.*

We now hypothesize that AR helps mediate E2-bound ER to transcribe genes involved in breast cancer cell proliferation of ER+/AR+ tumors. Indeed, we find that estrogen-mediated proliferation is decreased when we knockdown AR in MCF7 cells (Figure 8).

Figure 8. Enza and AR knockdown inhibit growth of ER+/AR+ breast cancer cells. (A) *MCF7 cells were grown in soft agar and treated with enza (10uM), fulvestrant (ICI, 100nM), or both, and colony number was assessed by ImageJ software.* ***(B)*** *Tamoxifen-resistant MCF7 cells from the Yee lab were treated with the indicated drugs for 7 days and cell number was assessed by crystal violet staining.* ***(C)*** *Western blot showing knockdown of AR protein with two different shRNAs in ER+/AR+ MCF7 cells.* ***(D)*** *MCF7 cells with a control shRNA or AR-targeting shRNAs were treated with vehicle or E2 and cell number was measured by crystal violet.*

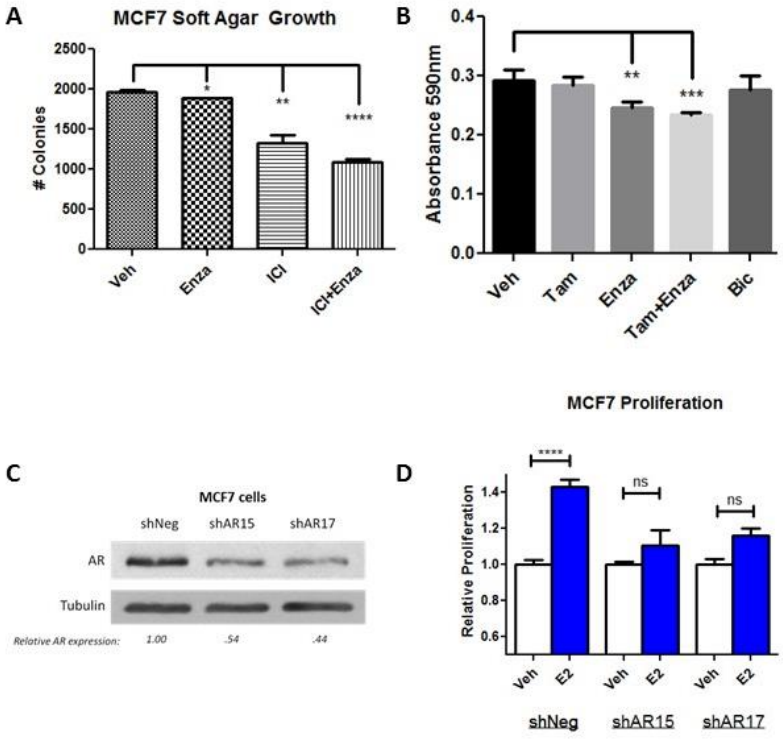

Towards understanding the mechanism whereby inhibition of AR with anti-androgens that inhibit AR nuclear translocation, we find that AR moves to the nucleus with E2 treatment, albeit not as well as it does with its cognate ligand, DHT, and that Enz impedes both DHT and E2 mediated nuclear localization, but bicalutamide does not. This was demonstrated in two different ER+AR+ lines

(MCF7 and ZR75-1) and figure 9 shows a western blot and quantification for ZR75-1 that demonstrate this finding.

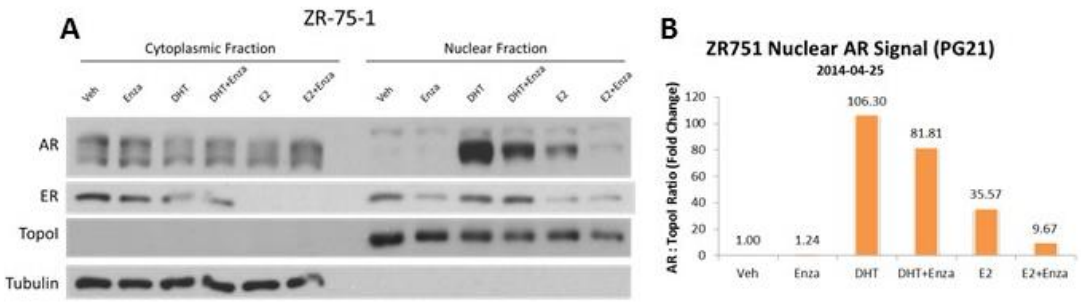

Figure 9: Both DHT and E2 treatment drive AR nuclear translocation. (A) *Western blot of cytoplasmic and nuclear fractions of ZR-751 cells treated with DHT or E2 for 3hrs. Nuclear and cytoplasmic protein fractions were collected using the NE-PER nuclear protein extraction kit (Thermo Scientific). Following western blotting, nuclear AR protein was quantified by densitometry and normalized to TopoI using Image Studio Lite (Li-Cor).* ***(B)*** *Nuclear AR levels were quantified by densitometry normalized to TOPOI loading control and shown relative to vehicle control.*

We next asked whether ER was necessary for E2 to make AR move to the nucleus and we tested for E2 induced nuclear localization of AR in the ER negative breast cancer cell line MDA-MB-453 and do not observe any nuclear localization with E2 treatment, while AR does translocate to the nucleus in the presence of the androgen, DHT (Figure 10).

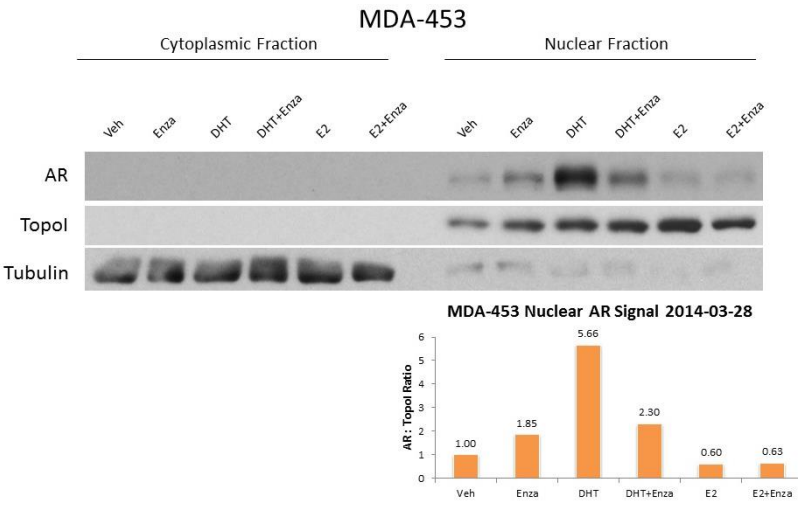

Figure 10. In ER negative MDA-MB-453 cells AR moves to the nucleus with the androgen DHT, but not with E2. *iCells were plated in media containing 5% charcoal-stripped FBS for 72hrs, then treated for 3hrs with Vehicle, 10uM Enza, 10nM DHT, 10nM E2, or the indicated combinations.*

In summary, given that enzalutamide, an AR antagonist that inhibits AR nuclear localization affects E2-driven tumor growth, affects E2-driven proliferation and E2 stimulates movement of AR to the nucleus in an ER-dependent manner, the next logical step towards determining the mechanism by which enzalutamide works in ER+/AR+ breast cancer cells is to perform chromatin immunoprecipitation assay (ChIP) for ER minus and plus estrogen, with and without enzalutamide. We will thereby determine if inhibiting AR nuclear localization affects ER binding to chromatin. These studies are underway and we anticipate having results in the next quarter.

The clinical trial of Enz with the aromatase inhibitor exemestane is currently underway for postmenopausal women diagnosed with ER+AR+ breast cancer. However, it is my opinion, based on our *in vitro* and *in vivo* studies presented above, that Enz may work well in premenopausal women with ER+AR+ tumors when combined with tamoxifen. It should likely at least be utilized in women whose tumors recur while on tamoxifen or then combined with fulvestrant, the standard second line therapy in these cases. Based on our studies examining the ratio of AR to ER and outcome in archival primary breast cancers of women treated with tamoxifen that demonstrated that tumors that had a high amount of AR compared to ER had a > 4 fold increase of recurrence while on tamoxifen (2), it is likely that tumors with a 2 fold or greater percentage of cells positive

for AR as compared to ER, may be excellent candidates for either Enz combined with tamoxifen or fulvestrant. This leads into Task 2.

Task 2. Test enza in three different tamoxifen resistance models *in vitro*. Months 1-4
Institutional Animal Care and Use Committee (IACUC) DoD and ACURO for Tasks 3-5. Months 1-4.

We had a setback in this task because the best model of tamoxifen resistance was the Tam R cells that were made by Dr. Doug Yee at the University of Minnesota Cancer Center (7) since they carried the parental MCF7 cells and treated them the same way except for chronic exposure of the Tam R cells to tamoxifen to generate the resistant cells. Unfortunately, when we tested these cells for mycoplasma contamination upon receiving them, they were positive. Dr. Yee sent an earlier passage, but these were still contaminated, albeit at a lower level. We therefore treated them for mycoplasma and they now test negative. Then we labeled them with a vector containing luciferase to be able to use them in vivo for IVIS imaging in mice. Interestingly these cells have equal amounts of AR and ER, but the transcription factor FOXA1 that serves as a pioneer for both factors is higher in the tamoxifen resistant line (Figure 11A). *In vitro* tests of these cells show that they indeed do not respond to tamoxifen, but are responsive to Enza and MJC13 (anti-androgens that inhibit AR nuclear localization) (Figure 11B).

Figure 11. Tamoxifen resistant MCF7 cells developed in the laboratory of Dr. Doug Yee have increased amounts of FOXA1and are responsive to new generation anti-androgens. (*A) Western blot for AR, ER, and FoxA1 in lysate from MCF7L and MCF7L-TamR (tamoxifen-resistant) cells. (B) MCF7L-TamR (tamoxifen resistant) cells grown in phenol red-free IMEM with 5% charcoal stripped FBS were treated with 100nM Tam, 10uM ENZ, 30uM MJC13, or 1uM Bic for 7 days and cell number was measured by crystal violet staining. *** p<.001 by ANOVA.*

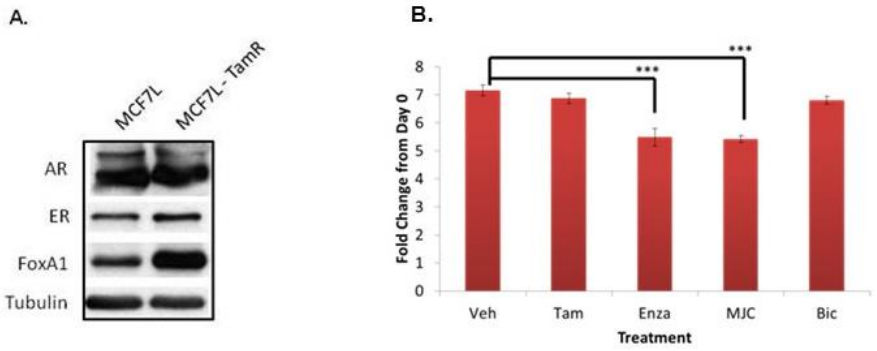

Although we have not met the goal of testing enza in three different tamoxifen resistant models *in vitro*, we think this model is the best and we are ready now to grow these cells as well as the parental as xenograft tumors in nude mice and will do so in the first quarter of the second year. Recently, Dr. Suzanne Fuqua reported that in MCF7 cells engineered to overexpress AR and the enzyme aromatase, sensitivity to the aromatase inhibitor was restored with AR antagonists and they suggest that their results indicate that both AR and ERα must be blocked to restore sensitivity to hormonal therapies in AR-overexpressing ERα-positive breast cancers (8). AR contributed to ERα transcriptional activity in these MCF-7 AR Arom cells, and AR and ERα co-localized, suggesting cooperation between the two receptors. In other words they agree that clinically, blocking both AR and ERα may be necessary in patients whose tumors express elevated levels of AR and lower ER.

We will soon (within the next quarter) put these TamR cells along with parental MCF7 cells into mice and determine if they are responsive to Enz in vivo, while not responding to tamoxifen, or whether Enz combined with tamoxifen will now render the tamoxifen effective. The parental, tamoxifen sensitive cells will serve as a positive control. Recently results on another tamoxifen resistance model have been published and we will try to obtain these cells as well (9). The other model that we were originally thinking of using were the LTED (long term estrogen deprived) cells. However, we have decided that estrogen independence may be a different issue than tamoxifen resistance. We may, however, come back to using that model eventually.

Before we discuss the other tasks in Aim1, we wanted to report findings pertaining to Aim 2 that involve finding the mechanism by which Enz affects E2-driven tumor growth and this data actually

pertains to Preclinical Aim 2 of the grant and was not actually originally scheduled to start until month 12 as stated below. However, in order to publish our findings that the anti-androgen Enz works as well as tamoxifen and in combination with tamoxifen and fulvestrant, we really needed to get to the molecular mechanism by which it does so in order to publish in a high-quality journal.

Preclinical Aim 2. Using samples collected from the xenograft studies, examine if and how the mechanism of action by which enzalutamide works in the various subtypes of breast cancer.

- **Task 1. Perform IHC on xenograft tumors for AR, ER, Her3, BrdU, FOXA1, SDF1, Cyr61 or other potentially relevant proteins. Months 12-18.**
  Our immunostaining of ER in E2 driven MCF7 xenograft tumors demonstrated that the anti-androgen Enz is somehow inhibiting ER nuclear upregulation, whereas Tam causes an increase in ER (a known effect). (Figure 12).

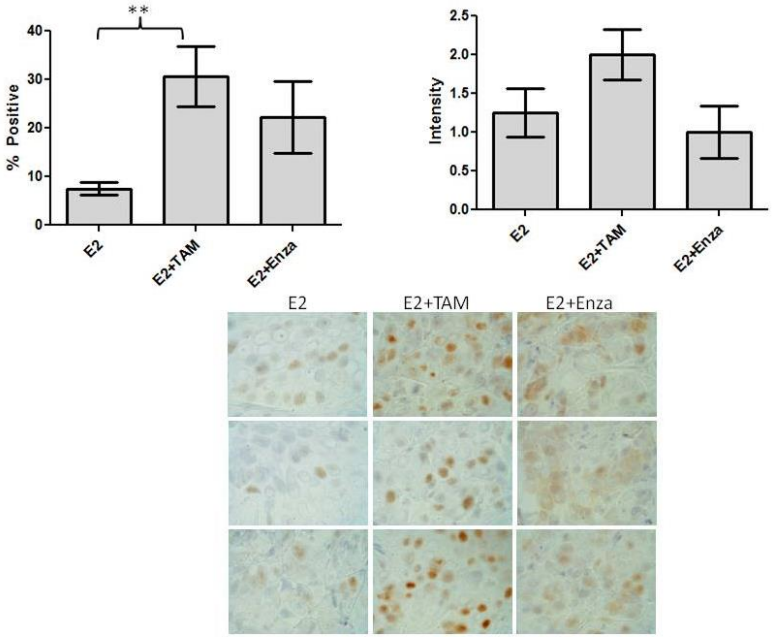

Figure 12. Enzalutamide (Enza) affects ER protein differently than tamoxifen in vivo. *Immunohistochemical staining of ER performed on formalin-fixed paraffin-embedded MCF7 xenograft tumor sections (*n = *8 E2 and E2 + TAM, and* n = *9 E2 + Enza) scored by pathologist for (A) percent positive nuclear staining (**P < *0.005) and (B) intensity. (C) Overall percent positive signal quantified by ImageJ. *P < *0.05. (D) Representative images at 1,000 ×.*

We performed IHC for two E2 regulated proteins that have previously been reported to help mediate E2 proliferative action (SDF1 and Cyr62) and they were not different in the E2 alone versus E2 plus Tam or E2+ Enz MCF7 xenograft tumors (data not shown), so we decided global profiling was necessary and proceeded to make RNA from the frozen tumors as we had proposed to do in Task 2 below.

Task 2. Make RNA from xenografts. Perform profiling. Analyze data. Months 15-18.

In order to determine the mechanism whereby Enz, an anti-androgen that binds to AR but not ER, affects E2-stimulated tumor growth, we made RNA from the MCF7 xenograft tumors stimulated with E2 only as compared to E2 plus Enz or E2 plus tamoxifen and performed gene expression profiling on Affymetric Human Gene Arrays (Figure 13). Again, we are a bit ahead of the game here as we have started to analyze the gene expression profiling data.

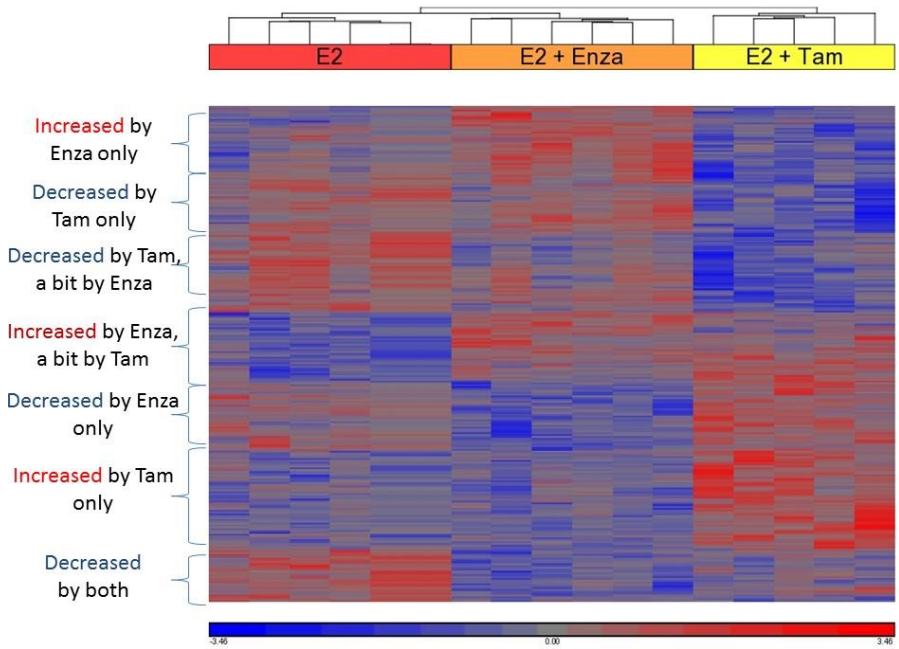

Figure 13. ***Enzalutamide and tamoxifen regulate some of the same genes when they oppose E2 regulated tumor growth in MCF7 xenografts, but other gene clusters are differentially regulated****. RNA was harvested from MCF7 xenograft tumors grown in ovariectomized mice treated with either E2, E2 plus tamoxifen, or E2 plus enzalutamide (6 tumors per group) from a published experiment (Cochrane et al Breast Cancer Research, 2014). We performed mRNA expression profiling on Affymetrix Human Gene 2.0ST arrays to examine potential genes significantly changed by either tamoxifen or enzalutamide treatment. Data analysis was performed using Partek Genomics Suite. One-way ANOVA analysis was performed to identify significant changes in gene expression between the three groups. A p-value cut-off of 0.05 was employed, and a list of genes was generated in which expression was significantly different between treatment groups. Supervised hierarchical clustering analysis of this gene list resulted in separation of the three treatment groups, as shown in the heatmap. Columns represent individual tumors (red=E2 only; orange=E2+Enza; yellow=E2+Tam), and rows indicate individual genes (red=upregulated, blue=downregulated).*

When we examine the data shown in Figure 13 we find that tamoxifen (Tam) and enzalutamide (Enz) are largely affecting different genes. There are only two clusters where genes are either increased by both drugs, or decreased by both; however both drugs are inhibiting the growth of ER+ MCF7 xenograft tumors equally well as we demonstrate in our paper that came out at the beginning of this year (2). When we look specifically at previously identified estrogen regulated genes we observe that Tam is a much stronger inhibitor of E2 regulated genes (as it should be since it is a competitive inhibitor of estradiol) while Enz has only a minimal effect on most known ER regulated genes. This makes sense, because while Enz has been shown to bind AR with high affinity, it does not directly bind to ERalpha or beta.

It is clear that some genes are regulated by both drugs, but many other genes are regulated only by one or the other. Interestingly, three genes that have previously been described as being essential for E2-driven tumor growth were significantly downregulated by enzalutamide, TFF3, SPDEF and CXCR4, but not significantly affected by tamoxifen (Figure 14). The Ets transcription factor SPDEF (also known as PDEF), was previously been identified by the Brugge lab to act as a survival factor for ER positive breast cancer (10). Interestingly, in the Cancer Cell Line Encyclopedia, we find that SPDEF is the gene that correlates best with AR expression in all cancer cell lines and this is also true when only the breast cancer cell lines are examined (Figure 15). We are currently working up a protocol to perform immunohistochemistry for SPDEF, TFF3 and CXCR4 to determine if they are decreased at the protein level by Enz in the xenograft tumors and then ultimately in specimens from the clinical trial in ER+ breast cancers.

Figure 14. Genes significantly affected by enzalutamide but not tamoxifen. *From the same MCF7 xenograft experiment described in figure 1, ANOVA analysis was performed to identify genes that were differentially expressed across treatment groups. Hierarchical clustering was performed to visualize groups of differentially regulated genes. This heatmap depicts genes significantly regulated by enzalutamide, but not tamoxifen. The cutoffs were p<0.04 and fold changes <-1.5 or >1.5 between E2 alone and E2 + Enza. Protein coding genes as well as non-coding RNA's were included in the list. Genes are indicated in rows, and samples are separated by columns. Red indicates and increase in expression, and blue indicates a decrease in expression.*

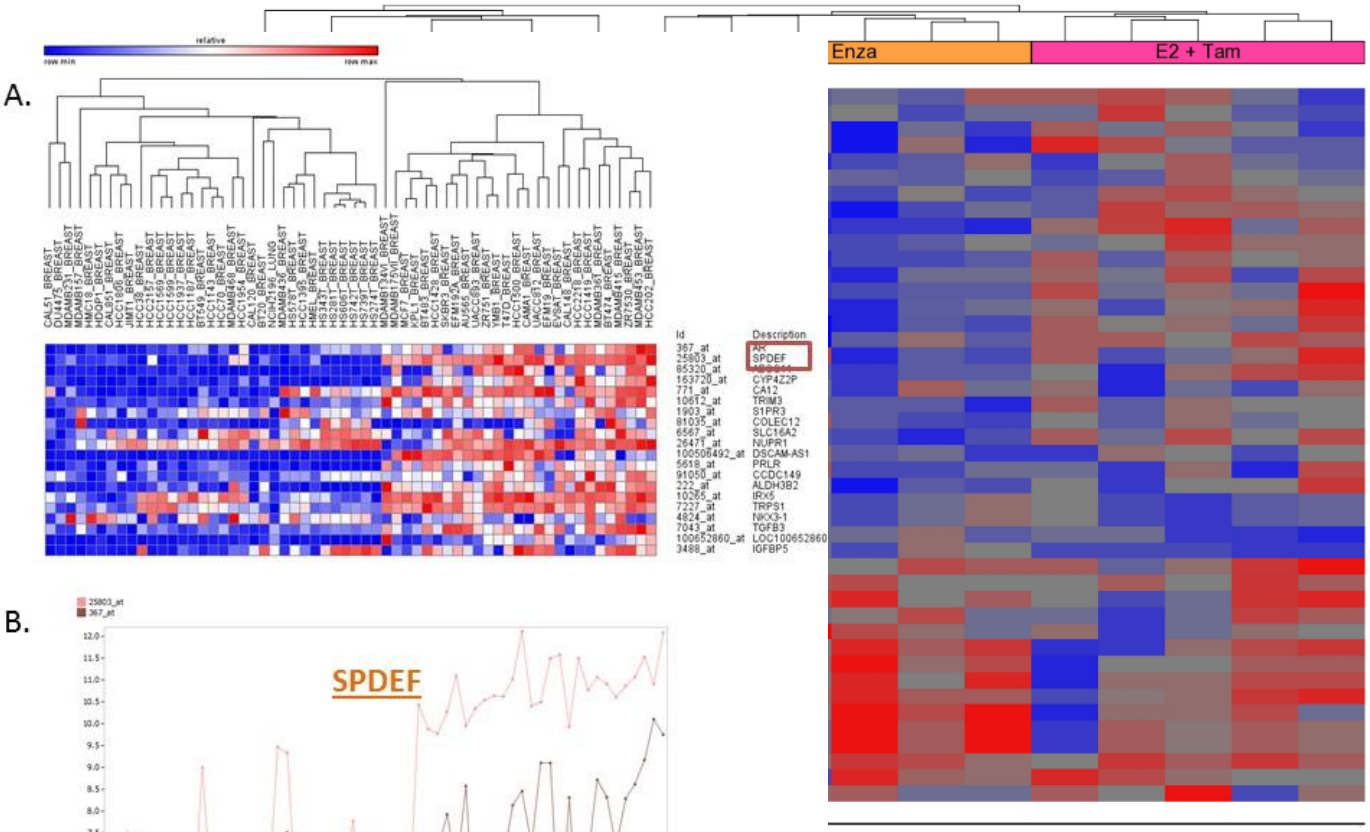

Figure 15. The Ets transcription factor SPDEF is the gene that correlates best with androgen receptor (AR) expression across all cancer cell lines. A. *The Cancer Cell Line Encyclopedia was utilized to determine which genes correlate in expression best to the levels of AR expression in cell lines of various types of cancer. B. Actual plot of SPDEF and AR in breast cancer cell lines specifically*

Preclinical Aim 1

Task 3. Test enzalutamide in combination with Her2 directed therapy in ER+ and ER- Her2+ models. Months 13-18. We are ahead of the game on this task, which involves testing enzalutamide in combination with Her2-directed therapy in models of the Her2+ breast cancer subtype since ~60 % of Her2+ breast cancers are AR positive (1). We have analyzed the combination of Enz with trastuzumab and found that they do act in a synergistic manner. In the MDA-453 cells, which are Her2 overexpressing, but not amplified to the degree to qualify as true Her2 amplified in the clinic, Enza inhibits growth equally as well as trastuzumab, and the combination of Enza plus trastuzumab has a significantly greater effect than either treatment alone (Figure 16, top).One mechanism by which androgens promote growth of Her2+ cell lines is through upregulation of Her3 (11), and we show using antibodies from Cell Signaling pHer3 (Y1197), cat# 4561S; Her3, cat# 4754S that Enz is able to block DHT-mediated increase in both total and phosphor-Her3 in two Her2+ cell lines, the MDA-MB-453, and BT474 (a Her2 amplified line that is also ER+) (Figure 16, bottom).

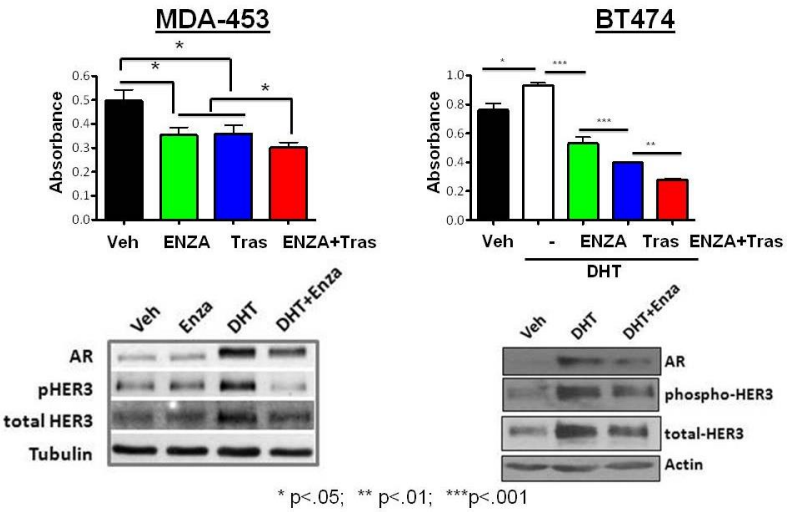

Figure 16. Effects of enzalutamide on Her2+ breast cancer cells. *(A) MDA-453 or BT474 cells were cultured in media containing 1% FBS for 48 hours then treated with Vehicle, 10uM enzalutamide, 20ug/ml trastuzumab, or Enza+Tras for 5 days, and cell number was assessed by MTS. (B) MDA-453 or BT474 cells were cultured in phenol red-free media with 5% CSS for 48 hours then treated with Vehicle, 10uM Enza, 10nM DHT, or DHT+Enza for 48 hours. Lysate was immunoblotted for AR , phospho and total Her3, and tubulin.*

Enz also enhances the effect of trastuzumab in three additional Her2+ cell lines, the SKBR3, SUM-225 (Fig 17) and the ZR75.30 (not shown). However, we were surprised to find that in these lines, androgen treatment does not result in upregulation of either total or phospho Her3. Since inhibition of AR with Enzalutamide is still able to decrease the growth of these cells, this suggests that there must be additional mechanisms by which AR promotes growth. We therefore probed for phosphorylated Her2 and total Her2 (pHer2 (Y1248), cat#2247S; Her2, cat#4290S both from Cell Signaling and indeed found that DHT increase the amount of phosphor Her2 and Enz decreases Her2 phosphorylation, while pHer3 and total Her3 remain unchanged (Figure 17). However, we do not know the mechanism whereby Enz does this yet.

.

Figure 17. Effects of enzalutamide on Her2+ breast cancer cells. *(A) Left, SKBR3 cells were cultured in media containing 1% FBS for 48 hours then treated with Vehicle, 10uM enzalutamide, 20ug/ml trastuzumab, or Enza+Tras for 5 days, and cell number was assessed by MTS. Right, SUM-225 cells were cultured in media containing 5% charcoal stripped serum for 48 hours then treated with Vehicle or DHT plus 10uM enzalutamide, 20ug/ml trastuzumab, or Enza+Tras for 5 days, and cell number was assessed by MTS. (B) SKBR3 and SUM-225 cells were cultured in phenol red-free media with 5% CSS for 48 hours then treated with Vehicle, 10uM Enza, 10nM DHT, or DHT+Enza for 48 hours. Lysate was immunoblotted for AR , phospho and total Her3 and Her2, and tubulin.*

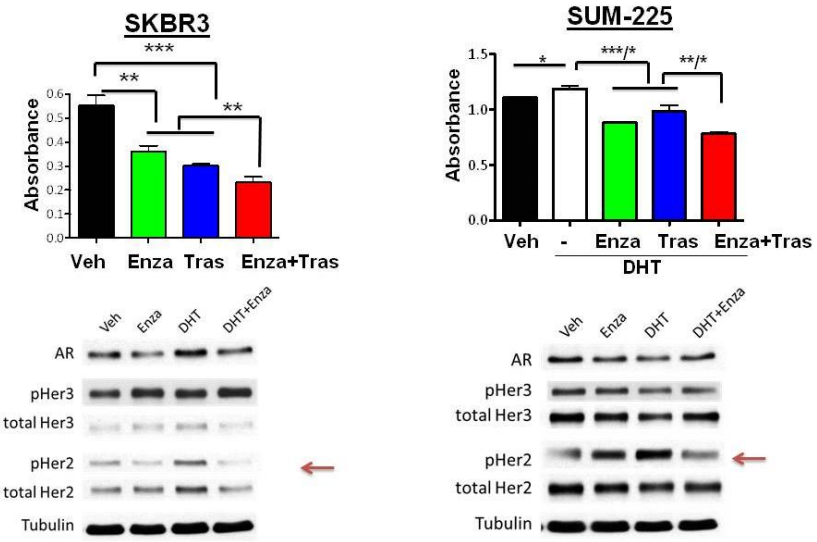

We recently found that enza also inhibits proliferation of trastuzumab resistant SKBR3 cells developed by Dr. Francisco Esteva at MD Anderson Cancer (Figure 18 right).

Figure 18. Enzalutamide synergizes with trastuzumab in SKBR3 (Her2+) breast cancer cells and also is effective at reducing proliferation of trastuzumab-resistant SKBR3 cells*. SKBR3 or Pool2 (trastuzumab-resistant) cells were treated with 10uM ENZ, 20ug/ml Tras, or the combination for 5 days and cell number was measured by crystal violet staining. *p<.05, *** p<.001, ****p<.0001 by ANOVA.*

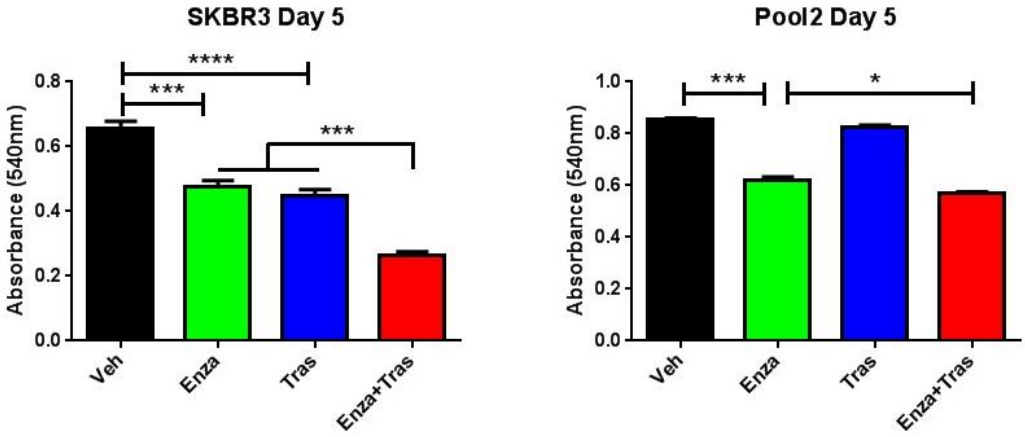

Enzalutamide induces apoptosis in both the parental SKBR3 and the trastuzumab-resistant SKBR3 cells (Figure 19).

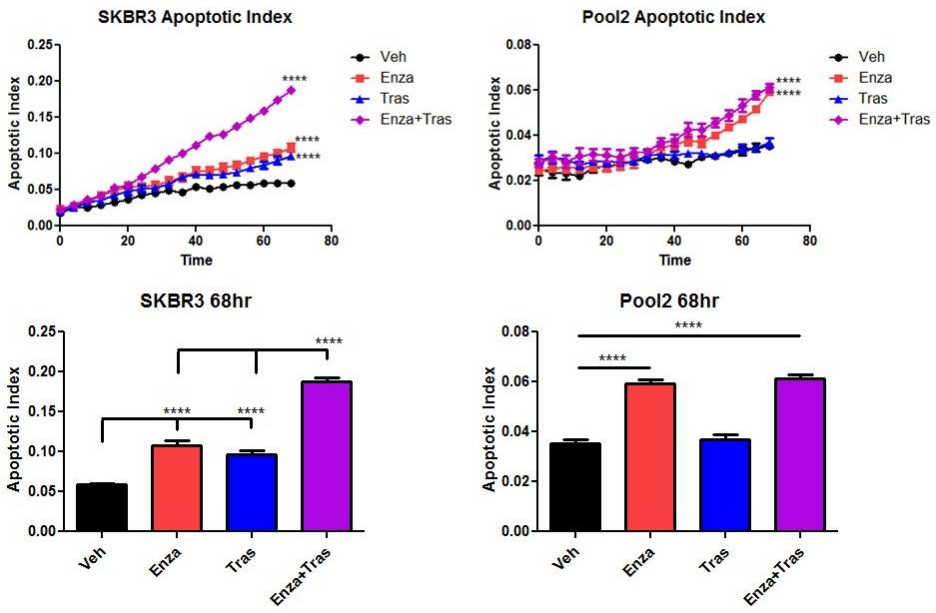

Figure 19. Enzalutamide increases apoptosis in both parental SKBR3 cells and trastuzumab-resistant SKBR (pool2) cells. *Cells were treated with 10uM ENZ, 20ug/ml Tras, or the combination and apoptosis was assessed using a fluorescent Caspase3/7 reagent imaged on the IncucyteZOOM kinetic live cell imaging system. Apoptotic Index is the number of Caspase-positive cells divided by total cell number. ****p<.0001 by ANOVA.*

Using multiple doses of trastuzumab and Enz, we demonstrated that these two drugs are synergistic using the Calcusyn program in the parental SKBR3 (Figure 20). The dose reduction index shows in both experiments that less of each drug could be use when the two are combined to get the same reduction in proliferation. In contrast, in the trastuzumab resistant SKBR3 lines the two really do not act synergistically, but enzalutamide effectively reduces proliferation while trastuzumab is very ineffective (Figure 21).

Figure 20. Enzalutamide synergizes with trastuzumab in Her2+ SKBR3 BC cells. *SKBR3 cells were treated with the indicated concentrations of Enza and/or Tras, and cell number was measured using the IncucyteZOOM kinetic cell imaging system. Data from 72hrs is shown, all calculations performed in CalcuSyn software.*

Enzalutamide

Enza (uM)	% Inhibition
0.1	0.00%
1	7.93%
10	48.29%

Trastuzumab

Tras (ug/mL)	% Inhibition
0.1	22.24%
1	47.58%
10	47.33%

Tras + Enza

Enza (uM)	Tras (ug/mL)	% Inhibition	Combination Index
0.1	0.1	20.77%	3.12
1	1	53.69%	**0.208** ←
10	10	73.47%	**0.858** ←

CI < 1 indicative of synergistic activity

Enza / Trastuzumab synergy in SKBR3 cells

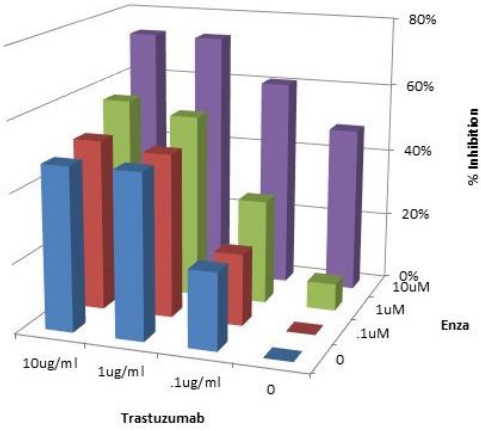

Dose Reduction Index

Combination		Drug alone		Dose Reduction Index (DRI)	
Dose Enza / Tras	% Inhibition	Dose Enza	Dose Tras	Enza	Tras
.1uM / .1nM	20.77%	3.65uM	.03ug/mL	36.53	0.32
1uM / 1nM	53.69%	7.72uM	12.76ug/mL	7.73	12.76
10uM / 10nM	73.47%	11.98uM	423.9ug/mL	1.20	42.38

Figure 21. Enzalutamide effectively inhibits proliferation in trastuzumab resistant SKBR3 (Pool 2) BC cells *Trastuzumab-resistant Pool2 cells were treated with the indicated concentrations of Enza and/or Tras, and cell number was measured using the IncucyteZOOM kinetic cell imaging system. Data from 72hrs is shown, all calculations performed in CalcuSyn* software.

Enzalutamide

Enza (uM)	% Inhibition
0.1	3.51%
1	7.52%
10	51.79%

Trastuzumab

Tras (ug/mL)	% Inhibition
0.1	0.00%
1	3.54%
10	5.94%

Tras + Enza

Enza (uM)	Tras (ug/mL)	% Inhibition	Combination Index
0.1	0.1	2.66%	1.02
1	1	15.18%	**0.88** ←
10	10	54.83%	**0.98** ←

CI < 1 indicative of synergistic activity
(CI=1 indicative of additive activity)

Enza / Trastuzumab synergy in Pool2 cells

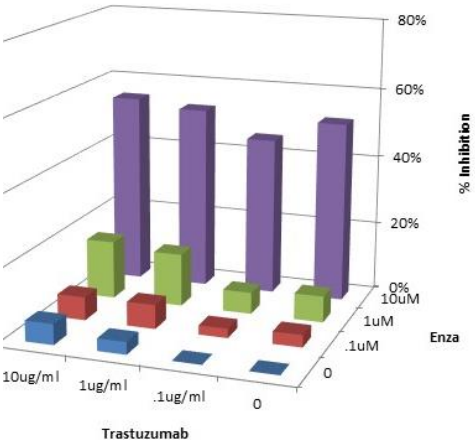

Dose Reduction Index

Combination		Drug alone		Dose Reduction Index (DRI)	
Dose Enza / Tras	% Inhibition	Dose Enza	Dose Tras	Enza	Tras
.1uM / .1nM	2.66%	0.10uM	3.29ug/mL	1.02	32.86
1uM / 1nM	15.18%	1.31uM	8.83ug/mL	1.31	8.83
10uM / 10nM	54.83%	17.67uM	24.19ug/mL	1.77	2.41

Her2 + breast cancer lines are notorious for not growing well *in vivo*. However, our collaborator, Dr. Bolin Liu has shown that the trastuzumab resistant SKBR3 and BT474 grow better in nude mice than their parental counterparts (Figure 22). We have now labeled the trastuzumab resistant SKBR3 pool 2 cells with pLNCX2-EGFP-Luc2, which expresses luciferase for IVIS imaging and will be testing enzalutamide compared to trastuzumab and both drugs together in mice in the next several months.

Figure 22. Trastuzumab-resistant sublines exhibits significant growth advantage in vivo as compared to their sensitive counterparts. *SKBR3, SKBR3-pool2 or BT474, BT474-HR20 breast cancer cells were injected s.c into the flanks of 5-week-old female nude mice. Mice were checked for tumor formation three times per week. Tumor volume was calculated by the formula: volume = (length x width^2)/2, and expressed as cubic millimeters (mean ± SE).*

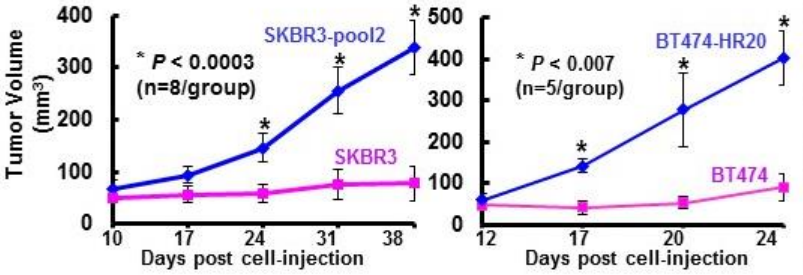

Task 4. Examine enzalutamide in combination with an mTOR inhibitor (Afinitor/everolimus). Months 7-10

Initiation of **Task4,** testing enzalutamide in combination with the mTOR inhibitor Afinitor/everolimus has been underway, primarily driven by postdoctoral fellow Michael Gordon. The PI3K/Akt/mTOR signaling pathway and the androgen receptor (AR) signaling pathway are both important drivers of BC cell growth. mTOR inhibitors such as everolimus have shown promising pre-clinical and clinical effectiveness in BC. However the relationship between these two pathways and the potential benefit of dual inhibition has not yet been explored in BC, particularly with respect to different BC subtypes. We find that the combination of Enz with everolimus inhibits the growth of both parental SKBR3 and the trastuzumab resistant SKBR3 cells in a synergistic manner (Figure 23).

Figure 23. Enza + everolimus inhibits the growth of HER2+/ER- SKBR3 cells and trastuzumab-resistant SKBR3-Pool2 cells. *(A) SKBR3 BC cells and (B) trastuzumab-resistant SKBR3-Pool2 cells engineered to stably express nuclear-RFP were treated with increasing concentrations of enza and/or everolimus at doses indicated. Cells were grown for six days in an IncuCyte live cell imager; images were recorded every four hours, and growth was measured as a function of RFP fluorescence. Percent growth inhibition was calculated by subtracting from vehicle control treated cells. Synergy was calculated using Calcusyn software, and a Combination Index <1 was indicative of synergistic activity between the two drugs (highlighted in bold). Dose reduction index indicates the fold change increase in single-agent drug that would be required to achieve the same amount of inhibition as the combination indicated.*

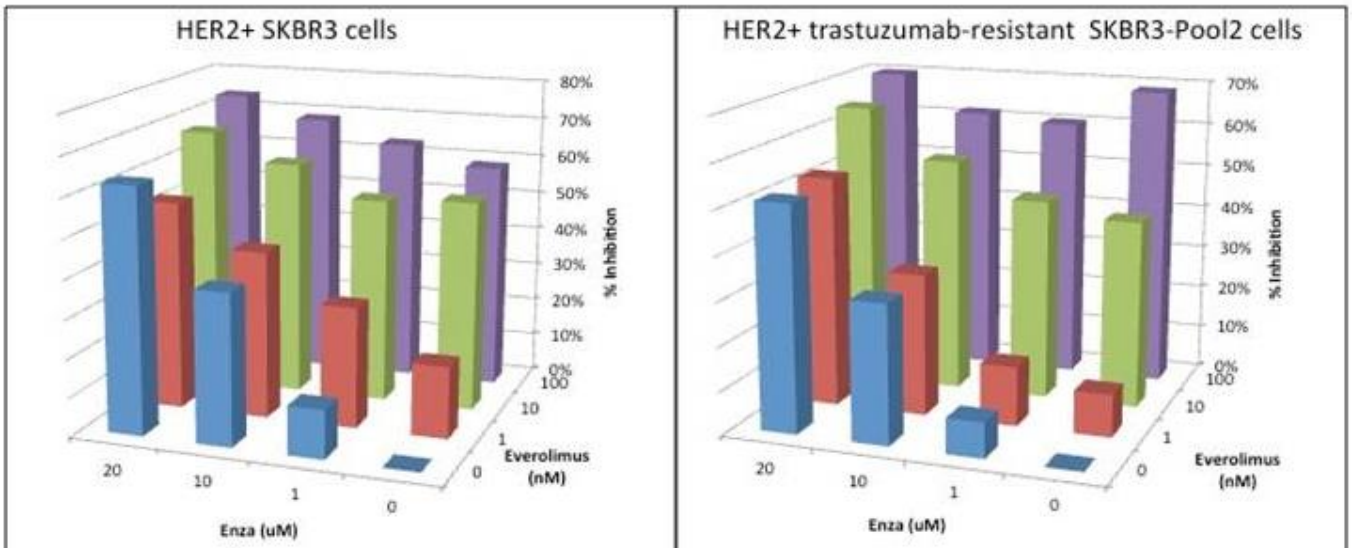

Enza (uM)	Everol (nM)	% Inhibition	Combination Index	Dose Reduction Index (Enza)	Dose Rediction Index (Everol)
1	1	31.03%	**0.545**	4.675	3.021
1	10	52.88%	**0.398**	15.057	3.017
1	100	63.25%	1.168	26.025	0.886
10	1	42.99%	1.195	0.905	11.088
10	10	60.71%	**0.589**	2.267	6.75
10	100	68.65%	**0.898**	3.542	1.624
20	1	53.69%	1.305	0.785	32.748
20	10	67.69%	**0.666**	1.673	14.527
20	100	73.94%	**0.726**	2.467	3.118

Enza (uM)	Everol (nM)	% Inhibition	Combination Index	Dose Reduction Index (Enza)	Dose Reduction Index (Everol)
1	1	0.1358	1.168	2.15	1.423
1	10	0.4601	**0.589**	17.67	1.88
1	100	0.6017	2.248	36.055	0.45
10	1	0.3237	1.289	0.861	7.791
10	10	0.5379	**0.714**	2.606	3.026
10	100	0.6155	2.29	3.875	0.492
20	1	0.5257	**0.851**	1.226	28.075
20	10	0.6495	**0.593**	2.325	6.152
20	100	0.6998	1.468	3.095	0.873

The mTOR pathway integrates numerous signaling events to affect cellular proliferation, and it is a critical driver of BC progression. Upstream of mTOR are proteins such as phosphoinositide 3-kinase (PI3K), protein kinase B (AKT), and the human epidermal growth factor receptor (HER) family including HER2; activating genetic alterations in these genes are among the most common in breast cancer. In turn, mTOR signaling activates many downstream effectors including steroid hormone receptors such as AR. Feedback

loops among these pathways are maintained under normal cellular conditions. However alteration of members of these pathways in cancer affects growth regulation in numerous ways. Importantly, PIK3CA mutations and PTEN loss are associated with increased AR levels. Studies in prostate cancer cells have shown that there is reciprocal regulation of AR and PI3K, whereby inhibition of the PI3K/Akt/mTOR pathway results in activation of AR signaling, and vice versa. In these studies, dual inhibition of PI3K and AR resulted in significantly reduced prostate cancer cell growth; these findings may translate to BC, especially in light of our findings that androgens can drive breast cancer.

Preclinical studies and early clinical trials of the mTOR inhibitor everolimus have shown that therapeutic inhibition of the pathway slows tumor growth and prolongs survival for some BC patients. Notably, the recent BOLERO series of phase III breast cancer clinical trials demonstrated that everolimus provides significant survival benefit, but this is limited to only some patients. For instance, the BOLERO-2 phase III clinical trial demonstrated that everolimus caused an increase in progression-free survival for patients with ER+ breast cancer resistant to anti-estrogen treatment (12, 13). In contrast, the BOLERO-3 phase III trial demonstrated a statistically significant, but clinically insignificant, increase in survival with everolimus in patients with HER2+ breast cancer resistant to the anti-HER2 trastuzumab (14). We therefore hypothesize that adding the anti-androgen Enz to everolimus might improve the efficacy of everolimus.

Interestingly, we find that treatment with everolimus increases the amount of AR protein and this may be why combined inhibition of AR with Enz is beneficial since it abrogates this effect in both Her2 positive breast cancers as well as TNBC (Figure 24). Thus, there is functional overlap and crosstalk between the AR, mTOR, and HER2 pathways, and identifying new ways to exploit these pathways by understanding how they interact and optimizing combinatorial use of their respective targeted therapeutics will be critical for improving survival outcomes. In the next quarter we plan to put the trastuzumab resistant SKBR3 cell *in vivo* and test whether the combination of Enz and everolimus will be effective in this model of Her2+ but trastuzumab resistant disease.

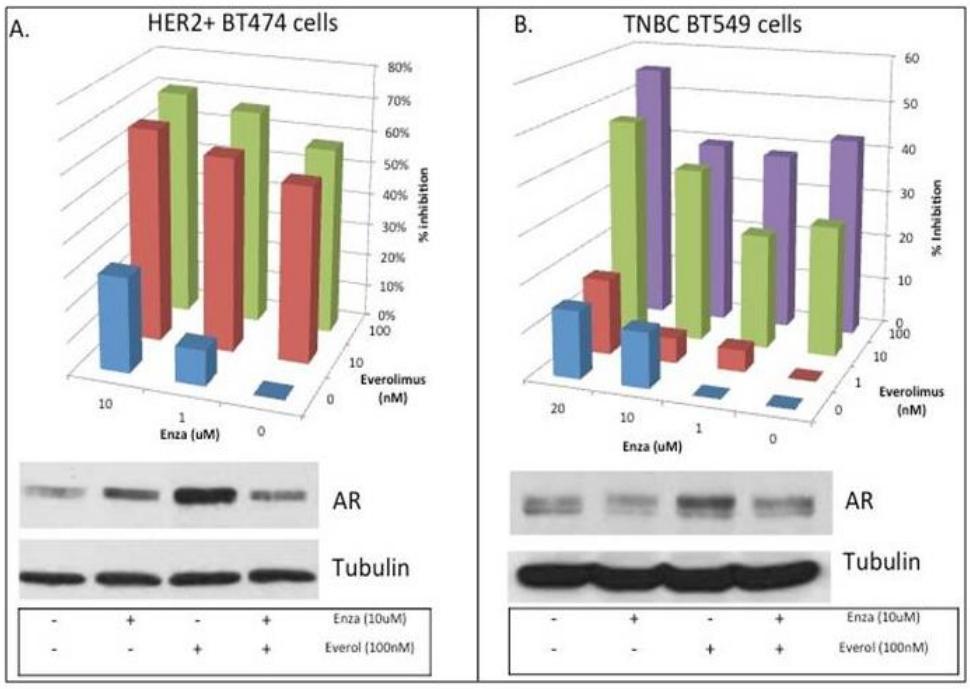

Figure 24. Enza + everolimus inhibits growth of HER2+/ER+ BT474 cells and TNBC BT549 cells. *BT474 (A) and BT549 (B) cells engineered to stably express nuclear-RFP were treated with increasing concentrations of enza and/or everolimus as indicated. Cells were grown as described in Figure 5. Percent growth inhibition was calculated by subtracting from vehicle control treated cells. For western blots, cells were treated with drug concentrations as shown for 48 hours and cell lysate was harvested. AR protein expression was measured by western blot, with tubulin loading control.*

Task 5. In true triple negative breast cancer (TNBC) cell lines and explants that retain AR, enzalutamide will be evaluated alone and in combination with chemotherapy and everolimus, *in vitro* and *in vivo*. Months 12-15 (50% completed ahead of schedule). We are ahead of schedule on this task. This project examining the role of AR in TNBC has been largely conducted by graduate student Valerie Barton, and she has

prepared a manuscript demonstrating that Enz may be able to serve as the first effective targeted therapeutic for TNBC, which has the lowest five-year survival rate of invasive breast carcinomas. Recent studies demonstrate that AR is expressed in up to one third of TNBC. AR is highly expressed in the "luminal AR (LAR)" molecular TNBC subtype and we find a similar percentage of TNBC to be AR positive by immunohistochemistry. We previously demonstrated that the anti-androgen enzalutamide (ENZ) effectively inhibits ER negative MDA-MB-453 cells *in vivo* (2). Because of their high AR protein levels and ER negativity, the MDA-MB-453 cells are considered a good representative of the LAR TNBC subtype. However, AR is also present in the other "true" (non Her2 expressing) TNBC molecular subtypes, albeit at lower level and may present a broader opportunity for targeted therapy. To test the hypothesis that non-LAR TNBC subtypes also critically depend on AR and that AR inhibition would decrease tumor burden in preclinical models of non-LAR TNBC, Valerie Barton utilized ENZ or shRNAs against AR. The results of her manuscript (see Barton et al in the appendix) demonstrate that AR inhibition significantly reduced baseline proliferation, anchorage independent growth (Figure 2), migration and invasion (Figure 5), and increased apoptosis (Figure 3), in SUM159PT, HCC1806, BT549 and MDA-MB-231 cells. *In vivo*, ENZ significantly decreases cellular viability and increases necrosis and apoptosis of SUM159PT (Figure 4) and HCC1806 xenografts (Supplemental Figure 1). Together, our findings suggest that AR+ TNBC of multiple molecular subtypes depend on AR for proliferation and migratory/invasive capacity, and, moreover, that ENZ may be efficacious in non-LAR molecular subtypes of AR+ TNBC in the clinic. We find that the EGFR ligand amphiregulin (AREG) is upregulated by liganded AR and decreased with addition of Enz in TNBC in vitro, and indeed the SUM159 xenografts treated with Enz showed less AREG staining than did vehicle treated controls (Figure 6). We are currently repeating the HCC1806 experiment with more mice (to improve statistics) and fewer cells (because the tumors got too big too fast and even the control had a lot of necrosis (although the enza treated tumors had more). We also collected some tumors early for molecular profiling to further confirm potential mechanisms of action.

References:

1. Collins LC, Cole KS, Marotti JD, Hu R, Schnitt SJ, Tamimi RM. Androgen receptor expression in breast cancer in relation to molecular phenotype: results from the Nurses' Health Study. Mod Pathol 2011; 24: 924-31.
2. Cochrane DR, Bernales S, Jacobsen BM, Cittelly DM, Howe EN, D'Amato NC, Spoelstra NS, Edgerton SM, Jean A, Guerrero J, Gomez F, Medicherla S, Alfaro IE, McCullagh E, Jedlicka P, Torkko KC, Thor AD, Elias AD, Protter AA, Richer JK. Role of the androgen receptor in breast cancer and preclinical analysis of enzalutamide. Breast Cancer Res 2014; 16: R7.
3. Scher HI, Fizazi K, Saad F, Taplin ME, Sternberg CN, Miller K, de Wit R, Mulders P, Chi KN, Shore ND, Armstrong AJ, Flaig TW, Flechon A, Mainwaring P, Fleming M, Hainsworth JD, Hirmand M, Selby B, Seely L, de Bono JS. Increased survival with enzalutamide in prostate cancer after chemotherapy. N Engl J Med 2012; 367: 1187-97.
4. De Leon JT, Iwai A, Feau C, Garcia Y, Balsiger HA, Storer CL, Suro RM, Garza KM, Lee S, Kim YS, Chen Y, Ning YM, Riggs DL, Fletterick RJ, Guy RK, Trepel JB, Neckers LM, Cox MB. Targeting the regulation of androgen receptor signaling by the heat shock protein 90 cochaperone FKBP52 in prostate cancer cells. Proc Natl Acad Sci U S A 2011; 108: 11878-83.
5. Kabos P, Finlay-Schultz J, Li C, Kline E, Finlayson C, Wisell J, Manuel CA, Edgerton SM, Harrell JC, Elias A, Sartorius CA. Patient-derived luminal breast cancer xenografts retain hormone receptor heterogeneity and help define unique estrogen-dependent gene signatures. Breast Cancer Res Treat 2012.
6. Jambal P, Badtke MM, Harrell JC, Borges VF, Post MD, Sollender GE, Spillman MA, Horwitz KB, Jacobsen BM. Estrogen switches pure mucinous breast cancer to invasive lobular carcinoma with mucinous features. Breast Cancer Res Treat 2013; 137: 431-48.
7. Fagan DH, Uselman RR, Sachdev D, Yee D. Acquired Resistance to Tamoxifen Is Associated with Loss of the Type I Insulin-like Growth Factor Receptor: Implications for Breast Cancer Treatment. Cancer Res 2012; 72: 3372-80.
8. Rechoum Y, Rovito D, Iacopetta D, Barone I, Ando S, Weigel NL, O'Malley BW, Brown PH, Fuqua SA. AR collaborates with ERalpha in aromatase inhibitor-resistant breast cancer. Breast Cancer Res Treat 2014.
9. Feng Q, Zhang Z, Shea MJ, Creighton CJ, Coarfa C, Hilsenbeck SG, Lanz R, He B, Wang L, Fu X, Nardone A, Song Y, Bradner J, Mitsiades N, Mitsiades CS, Osborne CK, Schiff R, O'Malley BW. An epigenomic approach to therapy for tamoxifen-resistant breast cancer. Cell Res 2014; 24: 809-19.

10. Buchwalter G, Hickey MM, Cromer A, Selfors LM, Gunawardane RN, Frishman J, Jeselsohn R, Lim E, Chi D, Fu X, Schiff R, Brown M, Brugge JS. PDEF promotes luminal differentiation and acts as a survival factor for ER-positive breast cancer cells. Cancer Cell 2013; 23: 753-67.
11. Ni M, Chen Y, Lim E, Wimberly H, Bailey ST, Imai Y, Rimm DL, Liu XS, Brown M. Targeting androgen receptor in estrogen receptor-negative breast cancer. Cancer Cell 2011; 20: 119-31.
12. Beck JT, Hortobagyi GN, Campone M, Lebrun F, Deleu I, Rugo HS, Pistilli B, Masuda N, Hart L, Melichar B, Dakhil S, Geberth M, Nunzi M, Heng DY, Brechenmacher T, El-Hashimy M, Douma S, Ringeisen F, Piccart M. Everolimus plus exemestane as first-line therapy in HR(+), HER2(-) advanced breast cancer in BOLERO-2. Breast Cancer Res Treat 2014; 143: 459-67.
13. Yardley DA, Noguchi S, Pritchard KI, Burris HA, 3rd, Baselga J, Gnant M, Hortobagyi GN, Campone M, Pistilli B, Piccart M, Melichar B, Petrakova K, Arena FP, Erdkamp F, Harb WA, Feng W, Cahana A, Taran T, Lebwohl D, Rugo HS. Everolimus plus exemestane in postmenopausal patients with HR(+) breast cancer: BOLERO-2 final progression-free survival analysis. Adv Ther 2013; 30: 870-84.
14. Andre F, O'Regan R, Ozguroglu M, Toi M, Xu B, Jerusalem G, Masuda N, Wilks S, Arena F, Isaacs C, Yap YS, Papai Z, Lang I, Armstrong A, Lerzo G, White M, Shen K, Litton J, Chen D, Zhang Y, Ali S, Taran T, Gianni L. Everolimus for women with trastuzumab-resistant, HER2-positive, advanced breast cancer (BOLERO-3): a randomised, double-blind, placebo-controlled phase 3 trial. Lancet Oncol 2014; 15: 580-91.

What opportunities for training and professional development has the project provided?

Cancer Biology Graduate Program doctoral candidate Valerie Barton and postdoctoral fellow Nicholas D'Amato have presented the following oral and poster presentations on this project at various national and local meetings:

Nicholas D'Amato Oral presentations:
Invited oral symposium presentation: Targeting Androgen Receptor in Her2-Driven Breast Cancer. Endocrine Society Annual Meeting, June 2013, San Francisco, CA.

Invited short talk: Targeting Androgen Receptor to Inhibit ER+ Breast Cancer Growth. Keystone Nuclear Receptors Meeting, January 2014, Taos, NM.

The Role of Androgen Receptor in Estrogen Receptor Activity in ER+ Breast Cancer. Functional Development of the Mammary Gland Program Project Grant Retreat, February 2014, Aurora, CO.

Targeting Androgen Receptor to Inhibit ER+ Breast Cancer Growth. UC Denver Anschutz Medical Campus Hormone Related Malignancies Retreat, March 2014, Aurora, CO.

Nicholas D'Amato Poster presentations:
D'Amato, NC, D Cochrane, N Spoelstra, A Chitrakar, B Babbs, A Protter, A Elias, and J Richer. (Mar 2014) Inhibiting Androgen Receptor Nuclear Localization Decreases ER Activity and Tumor Growth in ER+ Breast Cancer. University of Colorado Postdoctoral Research Day, Aurora, CO. * won best overall poster award.

Valerie Barton Oral presentations:

Barton VN, D'Amato N, Richer JK. Targeting androgen receptor decreases proliferation and invasion in preclinical models of triple negative breast cancer. Oral presentation at International Conference of Endocrinology and The Endocrine Society, Chicago, June 2014

Barton VN, D'Amato N, Richer JK. Inhibition of androgen receptor reduces proliferation and invasion through amphiregulin in triple negative breast cancer. Oral presentation at Functional Development of the Mammary

Gland Program Project Retreat, February 2014.

Valerie Barton Poster presentations:

BartonVN, D'Amato N, Richer JK. Targeting androgen receptor decreases proliferation of triple negative breast cancer. Presented at American Association for Cancer Research: Advances in Breast Cancer Research: Genetics, Biology, and Clinical Applications, October 2013.

Barton VN, D'Amato N, Richer JK. Targeting androgen receptor decreases proliferation and invasion of triple negative breast cancer. Presented at ICE/ENDO, Chicago June 2014.

Barton VN, D'Amato N, Gordon M, Elias, A, and JK Richer. Targeting androgen receptor decreases proliferation and invasion in preclinical models of triple negative breast cancer. Presented at University of Colorado Cancer Center Annual Retreat "Novel Experimental Models for Cancer Research," September 2014. * Won outstanding poster award.

- **How were the results disseminated to communities of interest?**

June 2013 Nicholas D'Amato gave a presentation to a group of donors for the Colorado Springs, Colorado Chapter of the American Cancer Society regarding the AR in breast cancer project.

July 2014 Nicholas D'Amato was invited to Anchorage, AK as the keynote speaker for an event for a new local chapter of the American Cancer Society - Making Strides kickoff event. I presented my work in lay terms to an audience of 150+ people, and also had separate meetings with physicians, caregivers, and local ACS staff to discuss

Feb 2014 Dr. Richer was an Invited speaker for student Leading Edge Lecture Series. "Androgen Receptor in Breast Cancer" City of Hope Duarte, California

- **What do you plan to do during the next reporting period to accomplish the goals?**

During the next reporting period we plan to utilize either the BCK4 cells or the PT12 PDX to perform an experiment testing enzalutamide, tamoxifen or the combination in E2 stimulated tumors. This will achieve the goal of determining if Enz will be effective alone or in combination with an anti-estrogen in ER+AR+ breast cancer in breast cancer model recently isolated from a patient since MCF7 cells have been in culture now for many years. We will also put the tamoxifen resistant MCF7 cells *in vivo* and determine if they are responsive to Enz in order to determine if Enz alone would be a viable therapy for breast cancers resistant to tamoxifen.

We will continue to analyze the profiling data from the MCF7 xenograft experiment and perform IHC for SPDEF, TFF3 and CXCR4 on these tumors to confirm the gene expression profiling data at the protein level to determine if decreasing these genes and their protein products is the way that Enz works to inhibit E2/ER driven proliferation.

We will analyze data from the Chromatin Precipitation Experiment that we have performed to determine if keeping AR from the nucleus with Enz will change where ER binds to chromatin.

We will also perform an in vivo experiment with trastuzumab and enzalutamide in the trastuzumab resistant Her2+SKBR3 cells. We will also use these cells to test the combination of enzalutamide plus everolimus. We will make RNA from these experiments and also paraffin enbedded some of the tumors for analysis.

2. **IMPACT:**

- **What was the impact on the development of the principal discipline(s) of the project?**

  These studies are helping to determine the role of androgen receptors in breast cancer and whether new anti-androgens might be utilized as therapy for breast cancers that fail to respond or reoccur while women are on current therapies such as anti-estrogens or trastuzumab. These studies have also provided preclinical evidence that the anti-androgen enzalutamide could serve as the first effective targeted therapy for a subset of triple negative breast cancers (TNBC). TNBC is the most aggressive type of breast cancer and there is currently no effective treatment for TNBCs with de novo or acquired resistance to chemotherapy.

- **What was the impact on other disciplines?** Nothing to Report.

- **What was the impact on technology transfer?**
  - Transfer of results to entities in government or industry: The results of this project are also reported to our clinical industry partners Medivation Inc and Astellas Pharma who are running the clinical trials of enzalutamide in prostate and breast cancer. They are very interested in our preclinical results combining enzalutamide with other therapeutics currently being utilized in breast cancer since these results will guide the design of further industry or investigator initiated clinical trials.

  - **What was the impact on society beyond science and technology?**
  - Since we have given reports of our research to several lay audiences in various community settings, we believe we are improving public knowledge regarding how hormones typically thought of as male hormones (such as androgens) are made by women and do affect women's health.

CHANGES/PROBLEMS: Nothing to Report

Changes in approach and reasons for change .

- **Actual or anticipated problems or delays and actions or plans to resolve them**
  - The delay caused by the mycoplasma contamination of the tamoxifen resistant cell line was reported above, but now we have resolved this issue.
- **Changes that had a significant impact on expenditures**. Nothing to report.
- **Significant changes in use or care of human subjects, vertebrate animals, biohazards, and/or select agents** No significant changes, but we had to do a three year re-write of the protocol and that was approved by the local IACUC and the DOD. IACUC approval 2/12/2014 and protocol expiry date 1/15/2017. Approval of this rewrite was received 1/22 2014.
- **Significant changes in use or care of human subjects. None**
- **Significant changes in use or care of vertebrate animals. None**
- **Significant changes in use of biohazards and/or select agents. None**

PRODUCTS:

Journal publications.

Published:

Dawn R. Cochrane, Sebastian Bernales, Britta M. Jacobsen, Diana M. Cittelly, Erin N. Howe, Nicholas C. D'Amato, Nicole S. Spoelstra, Annie Jean, Paul Jedlicka, Kathleen C. Torkko, Andy Protter, Anthony D. Elias and **J. K. Richer**. Role of the Androgen Receptor in Breast Cancer and Preclinical Analysis of Enzalutamide. BREAST CANCER RESEARCH 2014 Jan 22;16(1). PMID: 24451109

Designated as Highly Cited by the journal Breast Cancer Research.

Submitted:

Barton VN, D'Amato NC, Gordon MA, Lind HT, Spoelstra NS, Babbs B, Heinz RE, Elias A, Jedlicka P, Jacobsen BM**, Richer JK**. Multiple molecular subtypes of triple negative breast cancer depend on androgen receptor for proliferation and invasion. Submitted, September 2014.

- **Books or other non-periodical, one-time publications.** Nothing to report.
- **Other publications, conference papers, and presentations.**

Dr.Richer presented the following seminars/lectures/posters:

National meetings:

Richer, JK. Invited Symposia Lecture "Targeting the Androgen Receptor in Breast Cancer" **AACR Advances in Breast Cancer Research** conference, Targeted Therapies I session. October 3-6, 2013 in San Diego, CA. * published (Cochrane DR et al **Breast Cancer Research** 2014)

Richer, JK. Invited short talk: Role of Androgen Receptors in Estrogen Receptor Negative Breast Cancer. **Keystone Symposia on Nuclear Receptors:** Biological Networks, Genome Dynamics and Disease., Taos, NM. Jan 10-15 2014

Richer, JK. "Targeting Androgen Receptors in a Subset of Triple Negative Breast Cancers." One of two invited keynote presentations for the **MD Anderson Breast Cancer Research Program Retreat** organized by Naoto Ueno, M.D. May 2014 *Barton VN submitted for publication see pdf in appendix

And abstract

Nicholas D'Amato, Nicole Spoelstra, Anthony Elias, Jennifer Richer. Androgen Receptors in Estrogen Receptor Positive Breast Cancer**.** Poster presentation at International Conference of Endocrinology and The Endocrine Society, Chicago, June 2014

Local (Colorado)

2013 April 24 University of Colorado Endocrine Grand Rounds "Targeting Androgen Receptor Activity in Breast Cancer"
2013 Sept 20 University of Colorado Cancer Biology Graduate Program Retreat-Targeting the Androgen Receptor in Breast Cancer"
2013 Dec 12 University of Colorado Cancer Center Developmental Therapeutics Program Retreat- "Targeting the Androgen Receptor in Breast Cancer - Preclinical Studies to Clinical Trials

- **Website(s) or other Internet site(s)**:

  Expert Opinion piece in Oncology PracticeUpdate http://www.practiceupdate.com/journalscan/9370 or http://prac.co/j/5960d32c-988b-423e-ba24-14ca5c8cc39a?elsca1=soc_share-this acknowledgement of federal support –no

  Highlight of Cochrane DR et al **Breast Cancer Research** 2014 in Feb issue of 2014 NATURE REVIEWS CLIICAL ONCOLOGY. acknowledgement of federal support –yes

- **Technologies or techniques**.

We performed gene expression profiling using the Affymetrix exopression array platform. After we have fully analyzed this data we will add it to a publication and deposit the raw data in one of the public databases for gene expression data such as GEO or whatever data base is requested by the journal.

- **Inventions, patent applications, and/or licenses**

  Richer *et. al*., PCT Patent Application WO 2014/031164 filed March 15, 2013, "Methods for Determining Breast Cancer Treatment."

  Protter and JK Richer, PCT Patent Application PCT/US2012/48471 Serial No. 14/236,036 filed on January 29, 2014 "Treatment of Breast Cancer."

- **Other Products**

data or databases- we now have databases of genes expression data from the following experiments:

ER+ MCF7 breast cancer cells treated in vitro with vehicle, enzalutamide alone, estradiol alone (E2), E2 plus enzalutamide for 48 hrs.

ER+ MCF7 breast cancer cells grown as xenografts in nude mice treated with E2, E2 plus tamoxifen, or E2 plus enzalutamide**.**

HCC1806 TNBC breast cancer line treated in vitro with either vehicle, DHT, enzalutamide alone, DHT plus enzalutamide.

- **biospecimen collections**;

formalin fixed paraffin embedded xenograft tumors from the following experiments:

MCF7 tumors grown in nude mice and treated with either E2, E2 plus tamoxifen, E2 plus enzalutamide or in a separate experment, the same treatments plus the combination of E2 plus enzalutamide and tamoxifen.

Triple negative breast cancer (TNBC) cell line SUM159PT grown as xenograft tumors in mice treated with control rodent chow or enzalutamide containing chow.

TNBC cell line HCC1806 grown as xenograft tumors in mice treated with control rodent chow or enzalutamide containing chow.

- research material (e.g., Germplasm; cell lines, DNA probes, animal models); The following cell lines have been made in order to use the Incucyte machine to count the number of red or green nuclei to do real time proliferation assays with enzalutamide alone or in combination with standard therapies for breast cancer.
-

- **What individuals have worked on the project?**
  - Provide the following information for: (1) PDs/PIs; and (2) each person who has worked at least one person month per year on the project during the reporting period, regardless of the source of compensation (a person month equals approximately 160 hours of effort). If information is unchanged from a previous submission, provide the name only and indicate "no change."

Personnel	Role	Percent Effort	Nearest Person Month Worked	Contribution to Project	Funding Support: DOD Contract W81XWH-13-0090
Jennifer Richer, PhD	Partner Principal Investigator	40%	5	Oversees all experiments – helps with animal experiments, writes reports and edits manuscripts	X
Britta Jacobsen, PhD	Collaborator	50%	6	Povides daily oversight and helps with in vitro and in vivo experiments and; helped with animal protocol 3 year rewrite	X
Carol Sartorius, PhD	Collaborator	3%	.4	Provided PT14 PDX	X
Tzu Phang, PhD	Collaborator	5%	.6	Provides bioinformatic s	X
Ann Thor, MD	Collaborator	2%	.2	pathologist	X
Susan Edgerton	Instructor	2%	.2	Pulls pathlogy samples, analyzes results of IHC	X
Haihua Gu, PhD	Collaborator	50%	4	Helps to oversee	X

				experiments, especially for Her2+ disease and everolimus signaling experiments	
Nicole Spoelstra	Technician	66%	8	Performs IHC on FFPE samples	X
Valerie Barton	Graduate Student	100%	12	Directing TNBC experiments	X
Michael Gordon, PhD	PostDoc	100%	12	Performing everolimus studies	X
Beatrice Babbs	Animal Technician	100%	12	Ms. Babbs has provided mouse related care, caliper measuring xenograft tumors in mice and IVIS imaging.*	X
Ann Jean	Technician	50%	4	Ms. Jean provided support for the mouse experiments until she left the department in December, 2013*	X

Has there been a change in the active other support of the PD/PI(s) or senior/key personnel since the last reporting period? Nothing to Report."

No changes in active support for the PD/PI(s) or senior/key personnel.

- **What other organizations were involved as partners?** Medivation Inc. and Astellas Pharma are the Industry partners.

SPECIAL REPORTING REQUIREMENTS

- **COLLABORATIVE AWARDS:** Partnering PI, Dr. Anthony Elias has sent a separate report on the clinical progress.

- **APPENDICES:**

The attached appendix contains Abstracts and Publications

Appendix

Abstracts presented by

Dr. Richer

graduate student Valerie Barton

postdoctoral fellow Dr. D'Amato,

Journal publications.

Published:

Dawn R. Cochrane, Sebastian Bernales, Britta M. Jacobsen, Diana M. Cittelly, Erin N. Howe, Nicholas C. D'Amato, Nicole S. Spoelstra, Annie Jean, Paul Jedlicka, Kathleen C. Torkko, Andy Protter, Anthony D. Elias and **J. K. Richer**. Role of the Androgen Receptor in Breast Cancer and Preclinical Analysis of Enzalutamide. BREAST CANCER RESEARCH 2014 Jan 22;16(1). PMID: 24451109

Designated as Highly Cited by the journal Breast Cancer Research.

Submitted:

Barton VN, D'Amato NC, Gordon MA, Lind HT, Spoelstra NS, Babbs B, Heinz RE, Elias A, Jedlicka P, Jacobsen BM**, Richer JK**. Multiple molecular subtypes of triple negative breast cancer depend on androgen receptor for proliferation and invasion. Submitted, September 2014.

Nicholas D'Amato, Nicole Spoelstra, Anthony Elias, Jennifer Richer. Androgen Receptors in Estrogen Receptor Positive Breast Cancer**.** Poster presentation at International Conference of Endocrinology and The Endocrine Society, Chicago, June 2014

Androgen Receptors in Estrogen Receptor Positive Breast Cancer

Nicholas D'Amato[1], Nicole Spoelstra[1], Anthony Elias[2], Jennifer Richer[1]
[1]Department of Pathology and [2]Department of Medicine, Division of Oncology, University of Colorado Anschutz Medical Campus, Aurora, CO, USA

Background: Androgen receptor (AR) is widely expressed in breast tumors, but the role of AR in estrogen receptor positive (ER+) tumors is not fully understood. In a cohort of 192 women with ER+ breast cancers, we find that a high ratio (≥2.0) of AR to ER percent cells positive by IHC indicated an over four fold increased risk for failure while on tamoxifen (HR=4.43). In preclinical cell line models DHT is proliferative in ER+/AR+ *in vitro* and *in vivo*, and anti-androgens such as bicalutamide (bic) and enzalutamide (enza) inhibit DHT-mediated proliferation. Surprisingly enza, a new generation AR inhibitor, which impairs nuclear localization of liganded AR, uniquely inhibits E2-mediated proliferation of ER+ breast cancer cells, while bic does not. **Hypothesis**: We hypothesize that nuclear localization of AR is necessary for maximal E2-mediated ER activity and proliferation, and targeting AR with Enz or other agents that impede AR nuclear entry will inhibit growth of ER+/AR+ human breast cancer cell lines and decrease tumor burden in preclinical models. We also postulated that if tamoxifen and enza tested Enza inhibit E2-mediated proliferation by different means, the combination would result in additive or synergistic tumor shrinkage *in vivo*. **Results:** Enz and MJC13 blocked E2-induced proliferation of ER+AR+ breast cancer cell lines, but Bic did not. E2-induced expression of ER target genes including PR and SDF1 was inhibited by Enz, but not by Bic. Both DHT and to a lesser extent, E2 treatment, induced nuclear translocation of AR, and Enz inhibits AR nuclear localization in both instances, while Bic does not. *In vivo*, ENZ inhibited growth of MCF7 xenografts as effectively as Tamoxifen, and the combination of the two agents gives an additive effect. **Conclusions:** Our results suggest that nuclear localization of AR plays a previously-unrecognized role in E2-mediated ER activity in ER+/AR+ breast cancer cells. Because of its ability to inhibit nuclear localization of AR, Enz or other agents that inhibit AR nuclear localization, may serve as an effective therapeutic in ER+/AR+ breast cancers. Furthermore, Enz may be useful when combined with traditional anti-estrogens.

Funded by DOD BCRP Clinical Translational Award BC120183 to JKR

Richer, JK. Invited short talk: Role of Androgen Receptors in Estrogen Receptor Negative Breast Cancer. **Keystone Symposia on Nuclear Receptors:** Biological Networks, Genome Dynamics and Disease., Taos, NM. Jan 10-15 2014

Role of Androgen Receptors in Triple Negative Breast Cancer

Valerie Barton[1] Nicholas D'Amato,[1] Andrew Protter[3], Anthony Elias[2] and Jennifer Richer. [1]Department of Pathology and [2]Division of Oncology, Department of Medicine, University of Colorado Anschutz Medical Campus, Aurora, CO, USA, and [3]Medivation Inc., San Francisco, CA, USA.

Recent studies demonstrate that the androgen receptor (AR) is expressed in up to a third of triple negative breast cancer (TNBC) and AR associated genes define a subtype of TNBC with a "luminal AR" gene signature. However, the exact role of AR in TNBC, the extent to which AR+ TNBC are dependent on AR, and how well this subset will respond to new generation anti-androgens remains unknown. **Hypothesis:** We postulate that a subset of TNBCs are critically dependent on AR and that inhibition of AR with new generation anti-androgens that inhibit AR DNA binding will decrease tumor burden in preclinical models of breast cancer. **Results:** Knock down of AR expression using a lentiviral shRNA significantly reduced proliferation in TNBC cells (MDA-231, SUM159, BT549 and HCC1806) compared to those transduced with a non-targeting control (~2-fold reduction, $p<0.001$). Propidium iodide cell cycle analysis demonstrated that TNBC cells with reduced AR had a 22% increase in percentage of cells in S-phase ($p<0.001$). Knockdown of AR also significantly increased apoptosis *in vitro* and significantly inhibited migration and invasion. Enzalutamide (ENZ), an AR inhibitor, prevented ligand-mediated nuclear translocation as assessed by cell fractionation. In MDA-MB-453 xenografts, ENZ significantly decreased tumor volume and weight by up to 85% and increased apoptosis as measured by cleaved caspase-3 by 60% compared to mice that received DHT alone. In addition, a 50% reduction in nuclear AR was observed in tumors of mice treated with enzalutamide. We are now comparing ENZ to bicalutamide in additional preclinical models of TNBC and analyzing gene expression array data to identify AR regulated genes affected by ENZ in TNBC. **Conclusion:** AR may play an important role in a subset of TNBC and presents an opportunity for targeted therapy in this aggressive breast cancer subtype.
Funded by DOD BCRP Clinical Translational Award BC120183 to JKR

Richer, JK. Invited Symposia Lecture "Targeting the Androgen Receptor in Breast Cancer" **AACR Advances in Breast Cancer Research** conference, Targeted Therapies I session. October 3-6, 2013 in San Diego, CA.

Nicholas D'Amato[1], Dawn Cochrane[1], Nicole Spoelstra[1], Annie Jean[1], Andrew Protter[3], Anthony Elias[2], Jennifer Richer[1]
[1]Department of Pathology and [2]Department of Medicine, University of Colorado Anschutz Medical Campus, Aurora, CO, USA, and [3]Medivation Inc., San Francisco, CA, USA.

The androgen receptor (AR) is even more widely expressed in breast cancer (BC) than estrogen receptor alpha (ER) or progesterone receptor (PR), and recently AR has emerged as a useful marker to refine classification of breast cancer (BC). However, we still understand relatively little about the specific effects of AR or its potential as a therapeutic target in the different subtypes of BC. Our data from clinical samples suggests that some ER+ tumors can switch from growth driven by estrogens to growth driven by adrenal androgens, particularly when the estradiol (E2)/ER pathway is inhibited by standard ER-directed endocrine treatments. Indeed, we have evidence showing that a high ratio of AR to ER (≥2.0) leads to a > 4 fold increased risk for relapse while on tamoxifen (HR=4.43, P<0.0001) and is a strong independent predictor of disease-free survival (HR=4.04, P=0.002). Since approximately 30% of metastatic ER+ tumors exhibit *de novo* resistance to standard endocrine therapy and all patients with metastatic disease ultimately progress with acquired resistance, targeting AR in ER^+ BC may be clinically useful. Thus, clinical trials evaluating the role of androgen receptor inhibition in BC are underway.

Importantly, we find that new generation anti-androgens that block AR DNA binding affect BC differently than older generation anti-androgens (which allow DNA binding), leading to new insights into the role of AR. When AR is excluded from the nucleus, both androgen- and estradiol (E2)-stimulated proliferation is inhibited in ER^+ breast cancers, suggesting that AR plays a previously-unknown role in E2-mediated ER activity. Both enzalutamide (ENZ) and bicalutamide inhibited androgen-mediated proliferation of breast cancer lines *in vitro*. Interestingly, ENZ uniquely inhibited E2-mediated proliferation of $ER.^+/AR^+$ breast cancer cells *in vitro,* and also inhibited E2-driven tumor growth as effectively as tamoxifen *in vivo*. When opposing androgen-stimulated tumor growth in ER^+ BC *in vivo* models, ENZ inhibited proliferation and increased apoptosis, while in ER^- models it increased apoptosis but did not alter proliferation. When opposing E2-stimulated tumor growth *in vivo* ENZ decreased proliferation but did not increase apoptosis.

In $Her2^+$ but non-amplified, BC models the AR inhibitor ENZ, inhibited proliferation as well or better than trastuzumab (TRAS), whereas TRAS showed a greater inhibitory effect than ENZ in Her2 amplified lines. In all models tested, the combination of ENZ and TRAS inhibited proliferation more effectively than either agent alone. In TRAS resistant lines, addition of ENZ to TRAS significantly inhibited proliferation. Liganded AR upregulates Her3 in some $Her2^+$ BC lines; however, in other $Her2^+$ lines, Her3 is not increased by androgen stimulation, yet anti-androgens still inhibit proliferation. Our data suggest that the AR and Her2 pathways are linked in ways not previously understood and that there are novel Her3-independent mechanisms whereby AR impacts $Her2^+$BC.

A subset of TNBC express AR and knock down of AR using lentiviral shRNAs significantly reduced proliferation in multiple TNBC lines. Propidium iodide cell cycle analysis demonstrated

that knockdown of AR in TNBC decreased the percentage of cells in G2/M. Lastly, inhibition of AR with ENZ, blocked ligand-mediated nuclear translocation of AR as assessed by nuclear and cytosolic fractionation and significantly decreased proliferation of TNBC *in vitro*.

In summary, our studies demonstrate that AR plays varying roles in the different BC subtypes and will serve to guide appropriate combinations with AR inhibitor and existing therapeutic strategies. Further, we find that assessment of the amount of AR relative to ER may be informative.

Funded by DOD BCRP Clinical Translational Award BC120183 to JKR

Title: Targeting Androgen Receptor Decreases Proliferation and Invasion in Preclinical Models of Triple Negative Breast Cancer

Authors: Valerie Barton, Nicholas D'Amato, Michael Gordon and Jennifer Richer

Program: Hormone Related Malignancies

Background: Triple negative breast cancer (TNBC) constitutes 10-20% of invasive breast carcinomas and has the lowest five-year survival rate compared to other breast cancer subtypes. TNBC lacks estrogen receptor (ER), progesterone receptor (PR) and HER2 amplification and is thus unresponsive to endocrine or HER2-targeted therapies that improve the prognosis of other breast cancer subtypes and currently there are no targeted therapies for this subtype. Although TNBC lacks hormone receptors traditionally associated with breast cancer, recent studies demonstrated that 12-36% of TNBC express androgen receptor (AR). AR is highly expressed in the "luminal AR" (LAR) molecular subtype of TNBC, which has a molecular profile similar to ER+ breast cancer, but it is also present in other TNBC molecular subtypes and may present an opportunity for targeted therapy for this aggressive type of breast cancer. ***We hypothesized that AR+ TNBC critically depend on AR and that AR inhibition will decrease tumor burden in preclinical models of breast cancer.***

Material and Methods: To determine the extent to which AR+ TNBC depend on AR, we inhibited AR activity with the AR antagonist enzalutamide (ENZ) and shRNAs against AR in cell lines representing multiple molecular subtypes of TNBC *in vitro* and evaluated the efficacy of ENZ in two nude mice xenograft models *in vivo*. Expression profiling was used to determine potential mechanisms by which AR+ TNBC critically depend on AR.

Results: *In vitro***,** treatment with ENZ significantly reduced baseline proliferation ($P<0.05$), decreased anchorage-independent growth ($P<0.01$), increased apoptosis ($P<0.001$) and prevented AR nuclear localization in response to DHT in multiple TNBC cell line models. Likewise, AR knockdown significantly reduced proliferation ($P<0.001$) and increased apoptosis ($P<0.001$) compared to cells transduced with a non-targeting control. In addition to reduced proliferation, AR knockdown or treatment with ENZ altered cellular morphology from stellate to round in 3D culture and significantly decreased migration ($P<0.05$) and invasion ($P<0.001$) of TNBC cell lines spanning multiple subtypes. Microarray profiling and ELISA of TNBC lines treated with the AR ligand dihydrotestosterone (DHT) and ENZ suggested that AR regulation of the epidermal growth factor receptor (EGFR) ligand amphiregulin (AREG) is one mechanism by which AR influences proliferation, migration, and invasion in TNBC. Indeed, treatment with exogenous AREG rescued decreased proliferation, migration, invasion and EGFR-MAPK signaling of AR knockdown cells lines. *In vivo*, ENZ significantly decreased tumor viability and increased apoptosis ($P<0.05$) and necrosis ($P<0.01$) of SUM159PT (mesenchymal stem-like) and HCC1806 (basal-like 2) xenografts.

Conclusions: Our findings suggest that AR+ TNBC of multiple molecular subtypes depend on AR for proliferation and invasion and provide promising preclinical data on the efficacy of ENZ in AR+ TNBC. Importantly, we find that non-LAR TNBC subtypes were critically dependent on AR, indicating that patients with relatively low AR expression may also benefit from AR-targeted therapy.

Acknowledgements: Funded by DOD BCRP Clinical Translational Award BC120183 to JKR.

Presented at the University of Colorado Cancer Center Retreat 2014.

Targeting androgen receptor decreases proliferation of triple negative breast cancer

Valerie Barton, Nicholas D'Amato and Jennifer Richer

Recent studies demonstrate that the androgen receptor (AR) is expressed in up to a third of triple negative breast cancer (TNBC) and define a subtype of TNBC with a "luminal AR" gene signature. We hypothesized that AR+TNBC are dependent on AR for growth and that inhibiting AR activity by preventing nuclear localization and DNA binding will decrease proliferation and tumor burden in preclinical models of breast cancer. Indeed, knock down of AR expression using a lentiviral shRNA significantly reduced proliferation in cell line models of TNBC compared to cells transduced with a non-targeting control (2-fold reduction, $p<0.001$). Propidium iodide cell cycle analysis demonstrated that TNBC cells with reduced AR expression had a 22% increase in the percentage of cells in S-phase ($p<0.001$). In TNBC cells that exhibit androgen-stimulated growth, reduced AR expression inhibited response to ligand. Enzalutamide, an AR inhibitor, inhibited ligand mediated nuclear translocation of AR as assessed by nuclear cytosolic fractionation and significantly decreased baseline proliferation of TNBC *in vitro* ($p<0.001$). In MDA453 xenografts, enzalutamide significantly decreased tumor volume and weight by up to 85% and increased apoptosis as measured by cleaved caspase-3 by 60% compared to mice that received DHT alone. In addition, a 50% reduction in nuclear AR was observed in the tumors of mice treated with enzalutamide. Thus AR may play an important role in a subset of TNBC and presents an opportunity for targeted therapy.

Funded by DOD BCRP Clinical Translational Award BC120183 to JKR.

Presented at American Association for Cancer Research: Advances in Breast Cancer Research: Genetics, Biology, and Clinical Applications, October 2013.

Targeting Androgen Receptor Decreases Proliferation and Invasion in Preclinical Models of Triple Negative Breast Cancer

Valerie Barton, Nicholas D'Amato and Jennifer Richer

Triple negative breast cancer (TNBC) constitutes 15-20% of invasive breast carcinomas and has the lowest five-year survival rate. Currently, there are no targeted therapies for TNBC. Recent studies demonstrate that the androgen receptor (AR) is expressed in up to a third of TNBC. AR is highly expressed in the luminal AR (LAR) TNBC subtype but is also present in other TNBC subtypes and may present an opportunity for targeted therapy. We hypothesized that AR+ TNBC critically depend on AR and that AR inhibition will decrease tumor burden in preclinical models of breast cancer. To determine the extent to which AR+ TNBC depend on AR, we inhibited AR activity with enzalutamide (enza) and shRNAs in multiple TNBC subtypes. Treatment with enza significantly reduced baseline proliferation ($p<0.05$) and prevented AR nuclear localization in response to DHT in multiple TNBC cell lines. Likewise, AR knockdown significantly reduced proliferation ($p<0.001$) and increased apoptosis ($p<0.001$) compared to cells transduced with a non-targeting control. Microarray profiling and ELISA of TNBC lines treated with DHT and enza suggested that AR regulation of amphiregulin ($p<0.05$) is a mechanism by which AR influences proliferation in TNBC. In addition to reduced proliferation, AR knockdown or treatment with enza altered cellular morphology from stellate to round and significantly decreased migration ($p<0.05$) and invasion ($p<0.001$) of TNBC cell lines spanning multiple subtypes. *In vivo*, enza significantly decreased tumor volume (85%), increased apoptosis (60%), and reduced AR nuclear localization (50%) in a MDA-MB-453 xenograft model. Our findings suggest that AR influences both proliferation and invasion of AR+ TNBC cells regardless of TNBC subtype and provide promising preclinical data on the efficacy of enza in AR+ TNBC. Inhibition of AR by anti-androgens such as enza may represent an effective new opportunity for targeted therapy in TNBC.

Funded by DOD BCRP Clinical Translational Award BC120183 to JKR.

Oral presentation and poster at International Conference of Endocrinology and The Endocrine Society, Chicago, June 2014

Targeting Androgen Receptor in Her2-Driven Breast Cancer

Nicholas D'Amato[1], Hui Lyu[1], Bolin Liu[1], Haihua Gu[1], Andrew Protter[3], Anthony Elias[2], Jennifer Richer[1]

[1]Department of Pathology and [2]Department of Medicine, Division of Medical Oncology, University of Colorado Anschutz Medical Campus, Aurora, Colorado, USA, and [3]Medivation Inc., San Francisco, California, USA.

The androgen receptor (AR) is expressed in approximately 60% of Her2+ breast cancers. Activated AR elicits transcriptional upregulation of Her3. Her3 can heterodimerize with Her2, is essential for growth of Her2+ tumors, and has been implicated in therapeutic resistance to tamoxifen, paclitaxel and trastuzumab. Enzalutamide (ENZ) is an anti-androgen that impairs nuclear entry of liganded AR, binds to AR with higher affinity than bicalutamide, and was recently approved for treatment of castrate-resistant prostate cancer. **Hypothesis**: ENZ will enhance the efficacy of trastuzumab in Her2+ breast cancer lines by inhibiting Her3 expression. **Methods:** We tested both estrogen receptor positive and negative Her2+ (amplified or overexpressing without amplification) breast cancer cell lines for androgen-induced upregulation of Her3 protein and inhibition of proliferation with trastuzumab or ENZ alone as compared to the two drugs combined. Resistance to trastuzumab was generated in two Her2+ breast cancer cell lines (SKBR3 and BT474) and these lines were also tested. **Results:** Dihydrotestosterone (DHT) induced an increase in total Her3 and phospho-Her3 in some Her2+ BC cell lines and this effect was inhibited by the addition of ENZ. The combination of ENZ and trastuzumab inhibited proliferation more effectively than either agent alone in the ER-/Her2+ MDA-MB-453, SUM185E, and SKBR3 cell lines. Interestingly, ENZ inhibited proliferation in MDA-MB-453 and SUM185PE cells (Her2 overexpression without amplification) as well or better than trastuzumab, whereas trastuzumab showed a greater inhibitory effect than ENZ in SKBR3 cells (Her2 amplified). In the ER+/AR+/Her2 amplified BT474 cell line, the combination of ENZ and trastuzumab inhibited proliferation significantly more than either drug alone. In the trastuzumab resistant lines, where trastuzumab alone is ineffective, ENZ combined with trastuzumab significantly inhibited proliferation. **Conclusions:** Our results suggest that ENZ may serve as an effective therapeutic in Her2+ breast cancer when combined with Her2-directed therapies such as trastuzumab, pertuzumab, or T-DM1. Furthermore, in tumors resistant to Her2 directed therapy, ENZ may be useful alone or in combination with anti-Her3 therapy. Targeting AR with ENZ in patients with Her2+ disease may result in therapeutic benefit and warrants clinical investigation.

Funding: DOD BCRP Clinical Translational Award BC120183

Targeting Androgen Receptor to Inhibit ER+ Breast Cancer Growth

Nicholas D'Amato[1], Dawn Cochrane[1], Nicole Spoelstra[1], Annie Jean[1], Andrew Protter[3], Anthony Elias[2], Jennifer Richer[1]

[1]Department of Pathology and [2]Department of Medicine, Division of Medical Oncology, University of Colorado Anschutz Medical Campus, Aurora, Colorado, USA, and [3]Medivation Inc., San Francisco, California, USA.

Androgen receptor (AR) is widely expressed in breast cancers and has been proposed as a therapeutic target in estrogen receptor alpha (ER) negative breast cancers that retain AR. However, controversy exists regarding the role of AR in ER+ tumors. When the androgen dihydrotestosterone (DHT) is added with estradiol (E2) to ER+/AR+ breast cancer cell lines, E2-mediated proliferation is diminished. However, in the absence of E2, DHT is proliferative in breast cancer cell lines such as MCF7. Anti-androgens such as bicalutamide (Bic) and enzalutamide (ENZ) inhibit this DHT-mediated proliferation. Surprisingly we have found that ENZ, which impairs nuclear entry of liganded AR, also inhibits E2-mediated proliferation of ER+ breast cancer cells, while Bic does not. **Hypothesis**: We hypothesize that nuclear localization of AR is necessary for maximal E2-mediated ER activity and proliferation of ER+/AR+ breast cancer cells, and targeting AR with ENZ will inhibit growth of ER+/AR+ human breast cancer cell lines and decrease tumor burden in preclinical models. **Methods:** We tested ER+ breast cancer cell lines for estrogen- and androgen-induced proliferation and transcription of known ER- and AR-regulated targets following treatment with E2 or DHT in the presence or absence of several anti-androgens. We also tested the efficacy of ENZ, Tamoxifen (Tam), or the combination of ENZ plus Tam in a preclinical model of ER+ breast cancer. **Results:** DHT treatment increased proliferation in MCF7 and BCK4 cells and this was inhibited by the addition of Bic or ENZ. ENZ was also able to block E2-induced proliferation, but Bic did not. E2-induced expression of ER target genes including PR and SDF1 is also inhibited by ENZ, but not Bic. Both DHT and E2 treatment induces nuclear translocation of AR, which is decreased by ENZ. *In vivo*, ENZ inhibits growth of MCF7 tumors as well as Tamoxifen. **Conclusions:** Our results suggest that nuclear localization of AR plays an important and previously-unrealized role in E2-mediated ER activity in ER+ breast cancer cells. Because of its ability to block nuclear entry of liganded AR, ENZ may serve as an effective therapeutic in ER+/AR+ breast cancers. Furthermore, ENZ may be useful in tumors resistant to traditional endocrine therapy.

Funding: DOD BCRP Clinical Translational Award BC120183 to JKR, American Cancer Society Postdoctoral Fellowship PF-13-314-01 – CDD to NCD

TARGETING ANDROGEN RECEPTOR TO INHIBIT ER+ BREAST CANCER GROWTH

NC D'Amato, D Cochrane, N Spoelstra, A Jean, A Elias, J Richer, Department of Pathology, University of Colorado Anschutz Medical Campus, Aurora, CO

Androgen receptor (AR) is widely expressed in breast cancers and has been proposed as a therapeutic target in estrogen receptor alpha (ER) negative breast cancers that retain AR. However, the role of AR in ER+ tumors is controversial. In the absence of E2, DHT is proliferative in breast cancer cell lines such as MCF7, and anti-androgens such as bicalutamide (Bic) and enzalutamide (ENZ) inhibit this DHT-mediated proliferation. Surprisingly we have found that ENZ, which impairs nuclear entry of liganded AR, also inhibits E2-mediated proliferation of ER+ breast cancer cells, while Bic does not. We therefore hypothesized that nuclear localization of AR is necessary for maximal E2-mediated ER activity and proliferation of ER+/AR+ breast cancer cells, and targeting AR with ENZ will inhibit growth of ER+/AR+ human breast cancer cell lines and decrease tumor burden in preclinical models. *In vitro*, DHT treatment increased proliferation in MCF7 and BCK4 cells, and this was inhibited by Bic or ENZ. ENZ was also able to block E2-induced proliferation, but Bic did not. E2-induced expression of ER target genes including PR and SDF1 was also inhibited by ENZ, but not Bic. Both DHT and E2 treatment induced nuclear translocation of AR, which was decreased by ENZ. *In vivo*, ENZ inhibited growth of MCF7 tumors as well as Tamoxifen. Our results suggest that nuclear localization of AR plays an important and previously-unrealized role in E2-mediated ER activity in ER+ breast cancer cells. Because of its ability to block nuclear entry of AR, ENZ may be an effective therapeutic in ER+/AR+ breast cancers. Furthermore, ENZ may be useful in tumors resistant to traditional endocrine therapy.

Funding: DOD BCRP Clinical Translational Award BC120183 to JKR, American Cancer Society Postdoctoral Fellowship PF-13-314-01 – CDD to NCD

Breast Cancer RESEARCH

RESEARCH ARTICLE Open Access

Role of the androgen receptor in breast cancer and preclinical analysis of enzalutamide

Dawn R Cochrane[1†], Sebastián Bernales[2,3†], Britta M Jacobsen[1], Diana M Cittelly[1], Erin N Howe[1], Nicholas C D'Amato[1], Nicole S Spoelstra[1], Susan M Edgerton[1], Annie Jean[1], Javier Guerrero[3], Francisco Gómez[3], Satyanarayana Medicherla[2], Iván E Alfaro[3], Emma McCullagh[2,3], Paul Jedlicka[1], Kathleen C Torkko[1], Ann D Thor[1], Anthony D Elias[4], Andrew A Protter[2] and Jennifer K Richer[1*]

Abstract

Introduction: The androgen receptor (AR) is widely expressed in breast cancers and has been proposed as a therapeutic target in estrogen receptor alpha (ER) negative breast cancers that retain AR. However, controversy exists regarding the role of AR, particularly in ER + tumors. Enzalutamide, an AR inhibitor that impairs nuclear localization of AR, was used to elucidate the role of AR in preclinical models of ER positive and negative breast cancer.

Methods: We examined nuclear AR to ER protein ratios in primary breast cancers in relation to response to endocrine therapy. The effects of AR inhibition with enzalutamide were examined *in vitro* and in preclinical models of ER positive and negative breast cancer that express AR.

Results: In a cohort of 192 women with ER + breast cancers, a high ratio of AR:ER (≥2.0) indicated an over four fold increased risk for failure while on tamoxifen (HR = 4.43). The AR:ER ratio had an independent effect on risk for failure above ER % staining alone. AR:ER ratio is also an independent predictor of disease-free survival (HR = 4.04, 95% CI: 1.68, 9.69; p = 0.002) and disease specific survival (HR = 2.75, 95% CI: 1.11, 6.86; p = 0.03). Both enzalutamide and bicalutamide inhibited 5-alpha-dihydrotestosterone (DHT)-mediated proliferation of breast cancer lines *in vitro*; however, enzalutamide uniquely inhibited estradiol (E2)-mediated proliferation of ER+/AR + breast cancer cells. In MCF7 xenografts (ER+/AR+) enzalutamide inhibited E2-driven tumor growth as effectively as tamoxifen by decreasing proliferation. Enzalutamide also inhibited DHT- driven tumor growth in both ER positive (MCF7) and negative (MDA-MB-453) xenografts, but did so by increasing apoptosis.

Conclusions: AR to ER ratio may influence breast cancer response to traditional endocrine therapy. Enzalutamide elicits different effects on E2-mediated breast cancer cell proliferation than bicalutamide. This preclinical study supports the initiation of clinical studies evaluating enzalutamide for treatment of AR^+ tumors regardless of ER status, since it blocks both androgen- and estrogen- mediated tumor growth.

Introduction

In breast cancers, androgen receptor (AR) is more widely expressed than estrogen receptor alpha (ER) or progesterone receptor (PR), and AR has recently emerged as a useful marker for the further refinement of breast cancer subtype classification [1,2]. Of all 2,171 invasive breast cancers in women enrolled in the Nurses' Health Study, 77% were positive for AR by immunohistochemistry [3]. Among the subtypes, 88% of ER+, 59% of HER2+, and 32% of triple-negative breast cancers (ER−/PR−/HER2−) were positive for AR expression by immunohistochemistry [3]. Similar to ER and PR, AR expression is associated with a well-differentiated state [4] and with more indolent breast cancers [5].

In ER + breast cancers, adjuvant treatment with the competitive antagonist tamoxifen or aromatase inhibitors (AIs), which block conversion of androgens to estrogens, is generally effective for inhibiting disease progression. However, 30 to 50% of all ER + tumors display *de novo* resistance to traditional endocrine therapies and ultimately

* Correspondence: Jennifer.Richer@ucdenver.edu
†Equal contributors
[1]Department of Pathology, University of Colorado Anschutz Medical Campus, RC1 North 5th Floor P18-5127 12800 E. 19th Ave, Aurora, CO 80045, USA
Full list of author information is available at the end of the article

all metastatic ER + breast cancers acquire resistance [6,7]. In ER + tumors that respond to neoadjuvant endocrine therapy, we previously observed that AR mRNA and protein expression decrease, while in tumors that fail to respond AR mRNA does not decrease [8,9]. AR overexpression increases tamoxifen resistance in breast cancer models *in vitro* and *in vivo* [10]. Thus, *de novo* or acquired resistance to anti-estrogen therapies could result from tumor cell adaptation from estrogen dependence to androgen dependence. In mice, treatment with an AI markedly elevated intratumoral testosterone concentrations in dimethylbenz(*a*)anthracene-induced rat mammary tumors [11]. In postmenopausal women with ER + breast cancer, particularly those being treated with AIs, circulating levels of estradiol (E2) are extremely low, while circulating androgen levels are increased [12] since AIs block the conversion of androgens to estrogen. Indeed, circulating levels of testosterone, androstenedione, and dehydroepiandrosterone sulfate (DHEA-S) increase in women on AI therapy [13] as compared with pretreatment levels. Furthermore, high levels of the adrenal androgen DHEA-S before treatment are predictive of failure on AIs, and circulating DHEA-S increased during treatment in patients with tumors that failed to respond to AI treatment [14].

A subset of ER– breast cancers (molecular apocrine or luminal androgen receptor) retain AR [15-18] and have a gene expression pattern that closely resembles that of ER + breast cancers [2,19]. The anti-androgen bicalutamide inhibits the growth of molecular apocrine cell lines *in vitro* and *in vivo*, supporting the hypothesis that anti-androgens may be useful targeted therapies for such tumors [2,17,18,20]. Indeed, a phase II clinical trial testing bicalutamide as treatment for ER–/AR + breast cancers (NCT00468715) showed some efficacy [21]. Bicalutamide is a competitive antagonist that does allow AR to bind DNA [22]; however, in the setting of castrate-resistant prostate cancer, bicalutamide can exhibit an antagonist-to-agonist shift as demonstrated clinically by a decline in prostate-specific antigen following bicalutamide (Casodex) withdrawal [23].

Enzalutamide (formerly MDV3100) is an AR signaling inhibitor that binds AR with fivefold higher affinity than bicalutamide, impairs AR nuclear translocation, and lacks agonist activity at effective doses [20-23]. Enzalutamide significantly improved overall survival in patients with castrate-resistant prostate cancer and is an approved agent for the treatment of patients with metastatic castration-resistant prostate cancer [24]. In this study, we examined the effect of enzalutamide in AR + breast cancer models (ER + and ER–) and present the first preclinical evidence that inhibition of AR with enzalutamide may be an effective therapeutic strategy not only for ER–/AR + breast cancers, but also for ER+/AR + tumors. We also present clinical data which suggest that a high amount of AR relative to ER may be indicative of tumors that will have a less than optimal response to traditional endocrine therapy.

Methods

Cell culture

The identities of all cell lines were authenticated by DNA fingerprinting (Identifier Kit; Applied Biosystems, Grand Island, NY, USA) within 6 months of use. The BCK4 line is an ER+/AR + breast cancer line derived recently from a pleural effusion and has a nearly normal karyotype [25]. For the BCK4 cell line, the patient sample was acquired under a University of Colorado Institutional Review Board-approved tissue-acquisition protocol and patient-informed consent was obtained to acquire blood and tissue for research purposes. All other cell lines were obtained from the American Type Culture Collection; Manassas, Virginia, USA. BCK4 and MCF7 cells were grown in minimum essential media, 5% fetal bovine serum, non-essential amino acids, insulin and penicillin/streptomycin, and ZR75 cells in the same media with the addition of HEPES and L-glutamine. MCF7 cells express a wild-type AR, albeit with a shortened CAG repeat [26] that is often indicative of a more active receptor [27]. T47D cells were grown in Dulbecco's modified Eagle's medium supplemented with 10% fetal bovine serum, L-glutamine penicillin/streptomycin. LNCaP cells were grown in RPMI, 5% fetal bovine serum and penicillin/streptomycin. All cells were grown in a 37°C incubator with 5% carbon dioxide. MDA-MB-453 and MDA-kb2 (a derivative of MDA-MB-453 stably expressing the AR-dependent MMTV-luciferase reporter gene construct; American Type Culture Collection) were cultured in Leibovitz's L-15 media (Invitrogen, Carlsbad, CA, USA) containing 10% fetal bovine serum (Invitrogen) and penicillin/streptomycin. MCF7-TGL cells were generated by stable infection with retroviral SFG-NES-TGL vector, encoding a triple fusion of thymidine kinase, green fluorescent protein and luciferase and sorted for green fluorescent protein.

Tumor studies

MCF7 experiments with enzalutamide delivered in rodent chow were performed at the University of Colorado Anschutz Medical Campus and approved by the University of Colorado Institutional Animal Care and Use Committee (IACUC protocol 83611(03)1E). The MDA-MB-453 xenograft experiment in which enzalutamide was delivered by oral gavage was performed by AntiCancer Inc., San Diego, CA, USA and was approved by the Institutional Animal Care and Use Committee of AntiCancer Inc. All animal experiments were conducted in accordance with the National Institutes of Health Guidelines of Care and Use of Laboratory Animals.

For MCF7 xenograft experiments, 10^6 MCF7-TGL cells that stably express a triple fusion of thymidine kinase, green fluorescent protein and luciferase (SFG-NES-TGL retroviral vector) for *in vivo* imaging purposes were mixed with Matrigel (BD Biosciences, Franklin Lakes, New Jersey, USA) and injected into the fourth inguinal mammary fat pad of female, ovariectomized athymic nu/nu or nonobese diabetic (NOD)/SCID mice (Taconic, Germantown, NY USA). At time of tumor injection, E2 pellets (60-day release, 1.5 mg/pellet; Innovative Research of America, Sarasota, Florida USA) or the nonaromatizable androgen 5-alpha-dihydrotestosterone (DHT) (8 mg/pellet, packed and sealed in silastic tubing) were implanted subcutaneously at the back of the neck. Tumor burden was assessed using an *in vivo* imaging system or caliper measurements (tumor volume was calculated as: length × width × depth/2). Once tumors were established, mice were matched into groups based on the total tumor burden as measured by *in vivo* imaging system or caliper. Groups receiving tamoxifen had a 90-day release, 5 mg/pellet (Innovative Research of America) implanted subcutaneously. Mice were administered enzalutamide in their chow (approximately a 50 mg/kg daily dose) or by oral gavage (10 or 25 mg/kg/day). Enzalutamide was mixed with ground mouse chow (catalog number AIN-76; Research Diets Inc., New Brunswick, NJ, USA) at 0.43 mg/g chow. The feed was irradiated and stored at 4°C before use. Mice in the control group received the same ground mouse chow but without enzalutamide. All mice were given free access to enzalutamide formulated chow or control chow during the entire study period and at an average of 3.5 g/day food intake. Feed was changed in the animal cages twice a week. Water and feed were prepared *ad libitum*. Two hours prior to sacrifice, mice were injected intraperitoneally with 50 mg/kg bromodeoxyuridine (BrdU; Sigma-Aldrich, St. Louis, MO, USA). Mice were euthanized by carbon dioxide asphyxiation followed by cervical dislocation, and the blood, tumors, colon, uteri and mammary glands were harvested.

For the MDA-453 tumor study, 6×10^6 cells were injected into the fourth inguinal mammary fat pad of NOD-SCID-IL2Rgc$^{-/-}$ female mice into which a DHT pellet (1.5 mg 60-day release; Innovative Research of America) was implanted subcutaneously. The tumor size was measured using calipers, and when tumors reached 100 mm^3 the mice began receiving 10 mg/kg enzalutamide or vehicle by oral gavage. Once the tumors reached 400 mm^3, another group was started on 25 mg/kg enzalutamide. At the end of the experiment, tumors were weighed and processed for embedding.

Neoadjuvant endocrine therapy study

The inclusion criteria and trial design are described elsewhere [8,9]. Briefly, women with ER + breast cancers were enrolled in a randomized phase II clinical trial to receive exemestane alone (25 mg daily) or exemestane in combination with tamoxifen (20 mg daily) for 4 months prior to surgery. Women included in the trial were postmenopausal with newly diagnosed cancers of stage II/III, T2 to T3. Core needle biopsies were taken prior to treatment and tumor pieces from the final excision surgery were taken for analysis. The protocol was approved by the Colorado Multiple Institutional Review Board and informed consent was provided by all patients. The criteria for responders ranged from minor response to complete response, while nonresponders had stable or progressive disease.

Tamoxifen study

This study included 192 female patients diagnosed with ER + breast cancer at the Massachusetts General Hospital (Partners) between 1977 and 1993, who were offered tamoxifen treatment as part of their adjuvant therapy and were followed at the hospital through 1998. Patients were offered tamoxifen based on estrogen positivity (≥10 pmol/mg protein) determined using either a ligand binding assay or a radioactive enzyme-linked immunosorbent assay, the standard protocol in use during this time period. As part of the present study, archival formalin-fixed paraffin-embedded tumors collected under the Institutional Review Board protocol Molecular and Cellular Predictors of Breast Cancer were stained for AR and ER by immunohistochemistry. All slides were evaluated and the percentage and intensity of both AR and ER were recorded. Each slide was also scored using the Allred scoring method.

Contingency tables were used to study the associations between the AR/ER ratio and clinicopathologic variables. In this analysis, each clinicopathologic variable was divided into two or three categories (lymph node negative vs. lymph node positive; lymph node negative vs. one to three positive vs. four or more positive; patient age <50 years vs. ≥50 years; tumor size ≤2 cm vs. >2 cm; grade 1 vs. grade 2 vs. grade 3; PR negative vs. positive; ErbB2 ≤30% vs. >30%, MIB-1 < median vs. ≥median, mitoses/10 high-powered fields (mitotic index) < median vs. ≥median, epidermal growth factor receptor < median vs. ≥median). Patients were followed from the date of diagnosis to the date of first failure (local recurrence or distant metastasis) as well as the date of death or last follow-up. Patients who died of causes other than breast cancer and patients who were lost to follow-up or whose last encounter was before the end of the study were censored at the date of death or last encounter for survival analyses. The AR:ER ratio was calculated using a manual receiver operator characteristic analysis where we investigated the ratio that produced the best difference between good and poor prognosis in relation to

disease-free survival (DFS) to identify the cutoff point for this variable. The final AR:ER ratio cutoff point was determined to be 2.0. A Fisher's exact test was used for all dichotomized variables and the chi-square test for all trichotomized variables to compare the AR:ER ratio with other predictive markers. Kaplan–Meier curves used the calculated AR:ER ratio. All statistics were calculated using SAS (version 9.3; SAS Institute, Cary, NC, USA). Significance was determined at $P < 0.05$ and all tests were two-sided.

Immunohistochemistry

Slides were deparaffinized in a series of xylenes and ethanols, and antigens were heat retrieved in either 10 mM citrate buffer pH 6.0 (BrdU, Ki67) or 10 mM Tris/1 mM ethylenediamine tetraacetic acid buffer at pH 9.0 (AR, ER, caspase 3). Tissue for BrdU was incubated in 2 N HCl followed by 0.1 M sodium borate following antigen retrieval. Antibodies used were: AR clone 441 and ER clone 1D5 (Dakocytomation, Carpinteria, CA, USA), cleaved caspase 3 (Cell Signaling Technology, Danvers, MA, USA), Ki67 (sc-15402; Santa Cruz, Dallas, TX, USA) and BrdU (BD Biosciences, Franklin Lakes, NJ, USA). Envision horseradish peroxidase (Dakocytomation) was used for antibody detection.

Terminal deoxynucleotidyl transferase dUTP nick end-labeling (TUNEL) staining for apoptosis was performed using the ApopTag Plus Peroxidase *In Situ* Apoptosis Detection Kit (Millipore, Billerica, MA, USA), as per the manufacturer's instructions. AR and ER staining was assessed by a pathologist (PJ or ADT) and the score is reported as intensity multiplied by percent positive cells, or in the case of the tamoxifen-treated cohort the Kaplan–Meier curve is based on percent positive cells, although results are similar and still significant when the intensity is multiplied by the percent positive cells. For ER, BrdU and TUNEL staining in xenograft studies, three separate 200× fields of each xenograft tumor were taken using an Olympus BX40 microscope (Center Valley, PA, USA) with a SPOT Insight Mosaic 4.2 camera and software (Diagnostic Instruments, Inc., Sterling Heights, MI, USA). A color threshold (RGB for positive staining nuclei, and HSB for total nuclei) was adjusted manually using ImageJ (National Institutes of Health, Bethesda, MD, USA) for each image, and particles created by the thresholds were analyzed for total area. The RGB area was divided by the HSB area and multiplied by 100 for each image. For analysis of the nuclear androgen receptor, cleaved caspase 3 and Ki67, slides were scanned at 20× on an Aperio Scan ScanScope XT, Leica Microsystems Inc. Buffalo Grove, IL United States. Mammary tumor tissue was traced separately for each tumor and necrotic areas of the tumor removed using a negative pen tool in Aperio's Scanscope software. A nuclear algorithm was utilized to measure the percent positive cells for the Ki-67-stained and AR-stained slides and the data were exported. Cleaved caspase 3-stained slides were analyzed using a modified positive pixel count algorithm.

Immunoblotting

Whole cell protein extracts (50 μg) were denatured, separated on SDS-PAGE gels and transferred to polyvinylidene fluoride membranes. After blocking in 3% bovine serum albumin in Tris-buffered saline–Tween, membranes were probed overnight at 4°C. Primary antibodies utilized include: ERα (Ab-16, 1:400 dilution; Neomarkers, Fremont, CA USA), AR (PG-21, 1:400 dilution; Millipore (Bedford, Massachusetts USA) or EP6704, 1:10,000; Abcam (San Francisco, CA USA), glyceraldehyde 3-phosphate dehydrogenase (1:20,000 dilution; Sigma, St. Louis, MO USA), Topo 1 (C-21, 1:100 dilution; Santa Cruz) and alpha-tubulin (clone B-5-1-2, 1:30,000 dilution; Sigma). After incubation with appropriate secondary antibody, results were detected using Western Lightning Chemiluminescence Reagent Plus (Perkin Elmer, Waltham Massachusetts USA).

Cellular fractionation

For the MDA-kb2 cellular fractionation, cells were washed with ice-cold Dulbecco's phosphate-buffered saline, pH 7.4, pelleted using centrifugation and resuspended in 2 volumes of ice-cold NSB (10 mM Tris · Cl, pH 7.4, 10 mM NaCl, 2 mM $MgCl_2$, 1× protease inhibitors). The volume was adjusted with ice-cold NSB to 15 times the initial volume and incubated for 30 minutes on ice. The cytoplasmic fraction was obtained by addition of NP-40 to a final concentration of 0.3%. Nuclei and cytoplasm were separated using a 0.4 mm clearance Dounce homogenizer. After centrifugation, the supernatant containing the cytoplasmic fraction was collected. The pellet containing the nuclear fraction was resuspended in a 250 mM sucrose solution containing 10 mM $MgCl_2$ and then 1 volume was added to 880 mM sucrose containing 5 mM $MgCl_2$ under the nuclear fraction. The nuclei were then purified by centrifugation through the sucrose cushion. For the MCF7s cells, cellular fractionation was performed using the NE-PER Nuclear and Cytoplasmic Extraction Kit, Pierce Biotechnology, Rockford, IL USA as per the manufacturer's instructions.

Nuclear translocation assay

MDA-kb2 cells were seeded at 2×10^3 cells/cm^2 in optical microplates in Leibovitz's L-15 medium supplemented with 5% charcoal-stripped serum. After 3 days of cultivation the cells were pretreated with enzalutamide (1 or 10 μM) for 2 hours and then co-treated with 1 nM DHT for 1 hour in the presence of enzalutamide (total 3 hours of treatment with enzalutamide). The cells

were washed with phosphate-buffered saline, fixed with 4% formaldehyde for 30 minutes at room temperature and permeabilized with 0.2% triton X-100. Samples were then blocked with 5% bovine serum albumin for 1 hour and incubated with an antibody against AR (N20, sc-815 1:100; Santa Cruz) in phosphate-buffered saline 0.1% triton overnight. Incubation with the secondary antibody anti-rabbit Alexa Fluor 488 (1:1,000) was performed in 2.5% bovine serum albumin for 2 hours at ambient temperature. The nuclei were stained with 4',6-diamidino-2-phenylindole (1 μg/ml) for 30 minutes. Cells were visualized with a 60× objective and a Qimaging digital camera coupled to an Olympus X71 fluorescence microscope using a yellow fluorescent protein filter (Chroma U-N31040; Center Valley, PA, USA). The nuclear distribution of AR (ratio of nuclear AR signal/total AR signal) was quantified in a minimum of 48 cells using ImageJ software (National Institutes of Health).

Real-time quantitative polymerase chain reaction

cDNA was synthesized from 1 μg total RNA, using M-Mulv reverse transcriptase enzyme (Promega, Fitchburg, WI, USA). For *FASN*, *PRLR* and *GCDFP-15*, SYBR green quantitative gene expression analysis was performed using the following primers: *FASN* forward, 5′-AAGGACCTGTCTGG ATTTGATGC-3′ and *FASN* reverse, 5′-TGGCTTCATAG GTGACTTCCA-3′; *PRLR* forward, 5′-TATTCACTGACT TACCACAGGGA-3′ and *PRLR* reverse, 5′-CCCATCTGG TTAGTGGCATTGA-3′; *GCDFP-15* forward, 5′-TCCCA AGTCAGTACGTCCAAA-3′ and *GCDFP-15* reverse, 5′-CTGTTGGTGTAAAAGTCCCAG-3′; and 18S forward, 5′-TTGACGGAAGGGCACCACCAG-3′ and 18S reverse, 5′-GCACCACCACCCACGGAATCG-3′. For PR and stromal cell-derived factor 1 (SDF-1, also known as CXCL12), Taqman real-time polymerase chain reaction was performed using validated primer/probe sets from Applied Biosystems (assay ID: PR Hs01556702_m1, SDF-1 Hs00171022_m1, 18S Hs99999901_s1). Relative gene expression calculated using the comparative cycle threshold method and values were normalized to 18S.

Luciferase assays

MDA-kb2 cells were plated at 5×10^3 cells/well in 96-well luminescence plates and incubated overnight. Cells were treated with 10-fold serial dilutions of enzalutamide (10, 1, 0.1 μM) and DHT (10, 1, 0.1, 0.01, 0.001 nM) that were prepared in dimethylsulfoxide. Following 24 hours of incubation, the luminescence levels were determined with the luciferase assay system (Promega). Three independent experiments were performed and the luminescence values were determined as relative units and normalized to vehicle. Values are expressed as the mean fold induction ± standard error.

Results

A new method to examine AR relative to ER

To test the significance of AR and ER expression in breast cancer, we examined primary tumors from a group of tamoxifen-treated patients with clinical outcome data. This study included a cohort of 192 female patients diagnosed with breast cancer at the Massachusetts General Hospital (Partners) between 1977 and 1993, treated with adjuvant tamoxifen and followed at the hospital through 1998 under Institutional Review Board approval. The women ranged in age from 20 to 91 years at the time of cancer diagnosis with a median age of 68 years. Forty-eight (25.0%) of the women failed tamoxifen therapy. Women who relapsed while on tamoxifen were generally younger (median 64 years vs. 70 years for nonfailures, $P = 0.007$), had larger tumors (median 2.6 vs. 1.9 cm^3; $P = 0.003$), had a higher proportion of grade 3 tumors (45.8% vs. 29.4%; $P = 0.034$), had more positive lymph nodes (median 2 vs. 1; $P = 0.006$), had a higher mitotic index (median 5 vs. 4; $P = 0.007$), and had lower levels of PR staining (median 5% vs. 45%, $P = 0.048$). There were no differences in MIB-1, HER2, or epidermal growth factor receptor staining percentages between the two groups. Women who failed had a median ER percent cells positive of 62.5%. This was significantly lower than the 92.5% percent cells positive in tumors that did not fail ($P = 0.001$). Although the AR percent cells positive was higher in tumors of women who failed (70% vs. 57.5% for nonfailures), the difference in AR staining percentage did not reach statistical significance.

Since we had previously observed that AR mRNA and protein decrease with treatment in tumors responsive to neoadjuvant endocrine therapy, but did not decrease in nonresponsive tumors [8,9] (Figure S1, left in Additional file 1), we decided to examine nuclear AR as compared with ER. The median AR:ER ratio in pretreatment biopsies of responsive tumors (Figure S1A in Additional file 1) in the neoadjuvant study was 1.00, with a statistically significant positive correlation between AR and ER expression ($P = 0.006$) (Figure S1A in Additional file 1). However, in nonresponsive tumors (Figure S1B in Additional file 1), the median AR:ER ratio was 3.79 with no significant correlation between AR and ER. Interestingly, in adjacent uninvolved epithelium (Figure S1C in Additional file 1), the median ratio of AR to ER expression was 0.94, again with a significant positive correlation between the two receptors ($P = 0.0003$).

Based on these intriguing results in the small neoadjuvant study, we decided to examine the amount of AR relative to ER in the larger cohort of 192 female patients diagnosed with ER + breast cancer that received adjuvant tamoxifen therapy. To identify the best cutoff point for separating patients into good and poor survival, a manual receiver operator characteristic analysis based on time to

first failure (disease-free interval, DFS) was performed for the AR:ER ratio – and the optimal cutoff point of 2.0 was determined. In addition, since the AR:ER ratio was not in a log-linear relationship with the hazard function, it was necessary to use the dichotomized variable in the Cox proportional hazard models. Both AR percent cell staining and ER percent cell staining contribute to the AR:ER ratio. AR showed strong positive correlation ($r = 0.86$, $P < 0.0001$) with the ratio, while ER showed moderate negative correlation ($r = -0.36$, $P < 0.0001$). The AR:ER ratio with a cutoff value of 2.0 was significantly different between the two groups (failed tamoxifen versus nonfailed), with 27.1% of women who failed having an AR:ER ratio >2.0 compared with only 6.3% of nonfailures ($P < 0.0001$).

High AR:ER ratio indicates poor response to traditional endocrine therapy and overall survival

We compared the correlation between AR:ER ratio (<2 or ≥2) with dichotomized study variables (Table 1). Women with the higher AR:ER ratio are more likely to have positive lymph nodes and are more likely to fail on tamoxifen. Tumors from patients with lymph node-negative disease who did not fail tamoxifen therapy (no failure within 60 months of surgery) were significantly more likely to have an AR:ER ratio less than 2.0 ($P < 0.0001$).

We then compared study variables with tamoxifen failure by 5 years, and overall DFS and overall disease-specific survival (DSS). By univariate analyses, the tumor size, ER percent staining and AR:ER ratio were significantly associated with all survival outcomes (Table 2), while nodal positivity was significant only for tamoxifen failure and DFS. Notably, the AR:ER ratio was the most significant marker of poor survival (hazard ratio (HR) = 4.43 for tamoxifen failure, $P < 0.0001$; HR = 4.40 for DFS, $P < 0.0001$; and HR = 3.66 for DSS, $P < 0.0001$). In contrast, the ER percent cell staining was associated with reduced risk (HR = 0.98 for tamoxifen failure $P < 0.0002$; HR = 0.99 for DFS, $P < 0.0004$; and HR = 0.99 for DSS, $P < 0.0001$) (see Table 2 for 95% confidence intervals and Figure 1A,B for Kaplan–Meier curves). A number of factors were independently predictive of survival in a Cox proportional hazards model. For tamoxifen failure these variables include tumor size (HR = 1.92 for tumors >2 cm, $P = 0.03$), lymph node positivity (HR = 3.41, $P = 0.01$), and ER percent staining (HR = 0.98, $P = 0.0002$) (Table 2).

Table 1 Comparison of AR:ER ratio to clinical and pathologic variables

	AR:ER <2		AR:ER ≥2		Chi-square
Variable	***n***	**%**	***n***	**%**	***P* value**
Age <50	170	7.6	22	13.6	0.34
Tumor size >2 cm	170	42.9	22	59.1	0.15
Tumor grade 2 + 3	169	91.1	22	100	0.15
Lymph node-positive	133	54.1	14	85.7	**0.02**
Failed tamoxifen treatment	170	20.6	22	59.1	**<0.0001**
AR-positive	170	88.2	22	100	0.09
Progesterone receptor-positive	123	83.7	8	75.0	0.52
MIB-1 ≥21.3	168	53.0	21	23.8	**0.01**
Mitotic index number >4	165	50.3	22	45.5	0.67
erbB2 >30%	149	8.1	20	20.0	0.09
EGFR-positive	147	16.3	19	10.5	0.51

AR, androgen receptor; EGFR, epidermal growth factor receptor; ER, estrogen receptor. Bold data are significant.

Figure 1 shows Kaplan–Meier curves with survival separated into two groups: AR:ER ratios <2.0 (blue squares) and those with ratios ≥2.0 (red circles). By the end of 10 years, the observed DFS was 10% for patients with a higher AR:ER ratio compared with approximately 70% for women with a lower ratio (Figure 1A; log-rank $P < 0.0001$). Overall, 27% (6/22) of women with high ratios remained disease free by the end of the study or at the time they were censored compared with 72% (47/169) of women with low ratios. The DSS by the end of the study was about 30% for women with higher AR:ER ratios compared with about 60% for those with lower ratios (Figure 1B; $P < 0.0001$). The majority of women with high ratios (59%; 13/22) died from their breast cancer during the study period; only 21% (36/167) of women with low ratios died (Figure 1B). As shown in Figure 1C, there is a significant difference in the time to recurrence, with patients having tumors with high AR:ER ratio failing approximately 11 months earlier than those with a low (<2) ratio. The significance does not hold up for DSS; however, patients with high AR:ER ratios died from their breast cancer on average 10 months earlier than patients with low ratios (Figure 1D). The number of patients at risk at each time point is reflective of the number of patients censored due to no further follow-up data at each time point (underneath Figure 1A,B,C,D). Representative AR/ER staining in the <2 or ≥2 categories is shown (Figure 1E).

To determine whether the AR:ER ratio was an independent predictor of poor survival, a multivariate model was used that took into account other factors known to influence outcome. Variables included in a multivariate analysis were age, grade, tumor size, ER percent staining, and the dichotomized AR:ER ratio. AR percent staining was not included in the model because it was not a significant independent predictor of failure and it was highly correlated with the AR:ER ratio (Spearman correlation coefficient, $r = 0.86$, $P < 0.0001$). Collinearity was tested for the predictor variables, particularly for ER percent staining and the AR:ER ratio. The ratio as a continuous variable was moderately negatively correlated

Table 2 Univariate analysis for associations of variables with tamoxifen failure at 5 years, disease-free survival and disease-specific survival for entire study period

	Tamoxifen failure 5 years			DFS overall		DSS overall	
Variable	***n***	**HR (95% CI)**	***P* value**	**HR (95% CI)**	***P* value**	**HR (95% CI)**	***P* value**
Age <50	16	1.00		1.00		1.00	
Age ≥50	175	0.49 (0.22, 1.08)	0.08	0.69 (0.33, 1.46)	0.33	0.79 (0.33, 1.87)	0.58
Tumor size ≤2 cm	105	1.00		1.00		1.00	
Tumor size >2 cm	86	1.92 (1.08, 3.42)	**0.03**	1.95 (1.18, 3.24)	**0.01**	2.39 (1.32, 4.31)	**0.004**
Tumor grade 1	15	1.00		1.00		1.00	
Tumor grade 2	112	1.78 (0.42, 7.54)	0.43	1.33 (0.47, 3.74)	0.59	1.05 (0.37, 3.02)	0.92
Tumor grade 3	63	3.33 (0.78, 14.2)	0.10	2.05 (0.71, 5.90)	0.18	1.52 (0.51, 4.51)	0.45
LN-negative	63	1.00		1.00		1.00	
LN-positive	83	3.41 (1.40, 8.31)	**0.01**	2.42 (1.19, 4.94)	**0.02**	2.12 (0.95, 4.75)	0.07
%ER, continuous	192	0.98 (0.98, 0.99)	**0.0002**	0.99 (0.98, 0.99)	**0.0004**	0.99 (0.98, 0.99)	**0.001**
AR = 0%	20	1.00		1.00		1.00	
AR >0%	171	0.61 (0.27, 1.36)	0.23	0.91 (0.42, 2.01)	0.82	1.20 (0.43, 3.33)	0.73
AR/ER < 2	169	1.00		1.00		1.00	
AR/ER ≥ 2	22	4.43 (2.33, 8.42)	**<0.0001**	4.40 (2.47, 7.83)	**<0.0001**	3.66 (1.94, 6.93)	**<0.0001**
PR-negative	22	1.00		1.00		1.00	
PR-positive	108	0.43 (0.18, 1.04)	0.06	0.62 (0.27, 1.43)	0.26	0.69 (0.26, 1.84)	0.46
MIB-1 <21.3	93	1.00		1.00		1.00	
MIB-1 ≥21.3	95	1.17 (0.66, 2.07)	0.59	0.98 (0.59, 1.61)	0.93	0.98 (0.55, 1.73)	0.94
Mitotic index number ≤4	94	1.00		1.00		1.00	
Mitotic index number >4	92	1.64 (0.92, 2.94)	0.10	1.54 (0.93, 2.55)	0.10	1.34 (0.77, 2.37)	0.30
erbB2 ≤30%	152	1.00		1.00		1.00	
erbB2 >30%	16	1.02 (0.36, 2.84)	0.98	0.71 (0.26, 1.96)	0.51	0.69 (0.22, 2.24)	0.54
EGFR = 0%	139	1.00		1.00		1.00	
EGFR >0%	26	1.31 (0.60, 2.83)	0.50	1.01 (0.50, 2.07)	0.97	1.17 (0.54, 2.51)	0.70

AR, androgen receptor; CI, confidence interval; DFS, disease-free survival; DSS, disease-specific survival; EGFR, epidermal growth factor receptor; ER, estrogen receptor; LN, lymph node; PR, progesterone receptor. Bold data are significant.

with ER percent staining ($r = -0.36$, $P < 0.0001$) but there was no evidence of collinearity based on variance inflation analysis from linear regression models. Based on the lack of evidence for collinearity, both variables were included in the Cox models. Using a step-wise modeling strategy, the final model for tamoxifen failure consisted of the AR:ER ratio, ER percent staining and grade. Women with AR:ER ratio ≥2.0 are nearly three times more likely to fail tamoxifen therapy as compared with women with a lower ratio (HR = 2.87, $P = 0.04$; Table 3). This reflects the additional risk from the ratio above the independent effects of ER percent staining, as in this analysis the results are adjusted by the percent of ER staining and by grade. The AR:ER ratio continued to be an independent predictor of failure for DFS and DSS. The hazard ratio for the dichotomized AR:ER ratio was higher for DFS (HR = 4.04, $P = 0.002$). For DSS, the measure of effect was slightly lower (HR = 2.75, $P = 0.03$). Both DFS and DSS models were adjusted for ER percent staining and tumor size.

To investigate whether the AR:ER ratio was merely a reflection of the level of ER positivity, we tested various cutoff points for ER% cell staining. Using 20% cell staining positive for the ER cutoff point, we determined that although those patients with little ER were of course more likely to have a high AR:ER ratio (10/15), there were 12/165 tumors with high ER levels that also had a high AR:ER ratio (>2.0). A high AR:ER ratio is therefore not merely a consequence of low ER. In the multivariate setting, while the dichotomization of ER at <20% versus ≥20% was significant alone, when the AR:ER ratio was added ER percent cell staining lost its significance.

Androgens are proliferative in ER+/AR + breast cancer lines and the AR signaling inhibitor enzalutamide inhibits androgen-mediated proliferation and tumor growth *in vivo*

Lysates from four luminal ER + breast cancer cell lines were probed for AR and ER (Figure 2A). The prostate

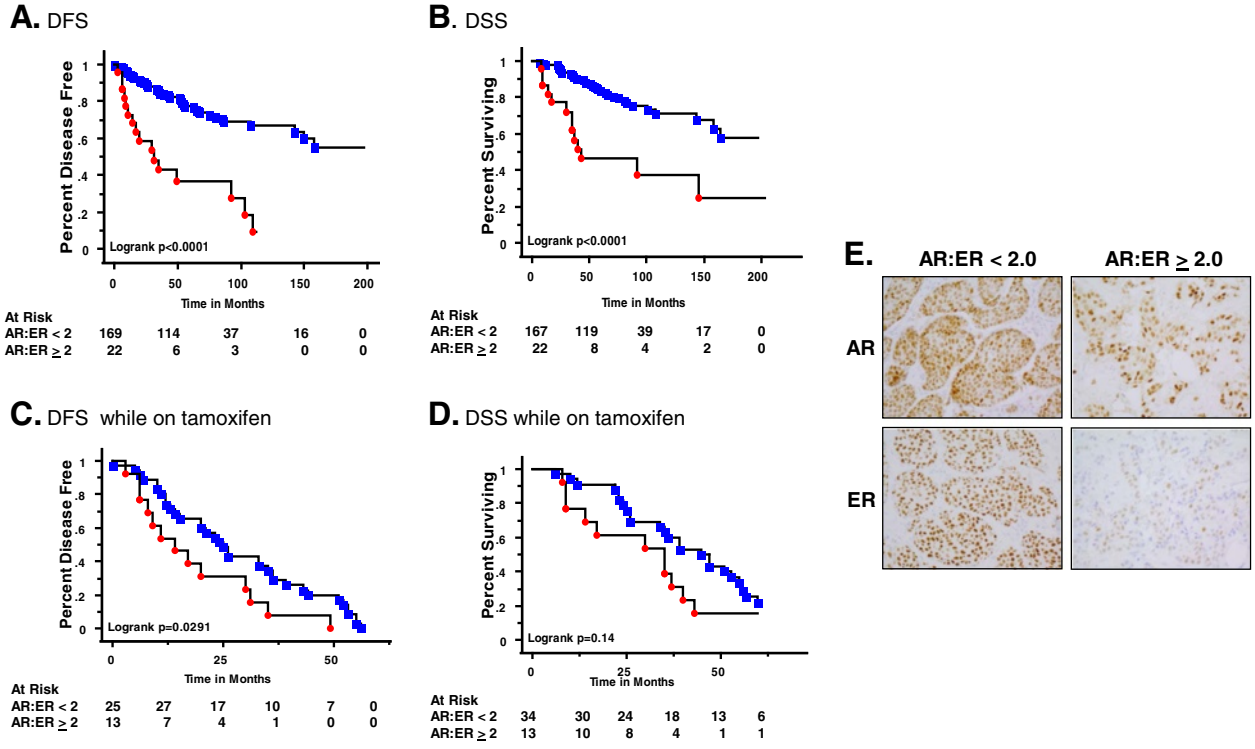

Figure 1 Women with tumors having a higher AR:ER ratio have a shorter disease-free and disease-specific overall survival as compared with patients with lower AR:ER ratio. Immunohistochemistry for androgen receptor (AR) and estrogen receptor (ER) were performed on formalin-fixed paraffin-embedded sections of primary breast cancers. Slides were scored for the percent of positive nuclear staining for AR and ER. Ratios were calculated to determine the best cutoff point for analysis. For **(A)** to **(D)** women are divided into two groups: those with AR:ER ratios <2.0 (blue squares) and those with AR:ER ratios ≥2.0 (red circles). The number of patients at risk at each time point is reflective of the number of patients censored due to no further follow-up data at each time point (underneath). Kaplan–Meier survival curve for: **(A)** disease-free survival (DFS) for all patients; **(B)** disease-specific survival (DSS) overall for all patients; **(C)** DFS for patients who failed while on tamoxifen therapy; **(D)** DSS overall for patients who failed while on tamoxifen therapy; and **(E)** representative images of AR and ER staining from the two groups (400× magnification).

cancer cell line LNCaP and the molecular apocrine breast cancer cell line MDA-MB-453, which express high levels of AR [20,28,29], were used as positive controls for AR expression. MCF7 cells and the newly derived BCK4 cell line express both AR and ER (Figure 2A) and the new androgen receptor signaling inhibitor enzalutamide prevents ligand-mediated stabilization of AR protein in MCF7 cells (Figure 2B). Both cell lines proliferate in response to DHT (Figure 2C,D). Unlike androstenedione and testosterone, DHT is not aromatizable to estrone or E2 [30-32]. DHT-stimulated proliferation was blocked by enzalutamide in both the MCF7 and BCK4 lines (Figure 2C,D). Enzalutamide inhibited DHT-mediated nuclear translocation of AR within 3 hours as determined by nuclear and cytosolic fractionation (Figure 2E).

To determine whether enzalutamide inhibits androgen-mediated growth *in vivo*, MCF7 cells constitutively expressing luciferase (MCF7-TGL) were injected into the mammary fat pad of ovariectomized mice implanted with DHT pellets and the tumor burden was measured using

Table 3 Multivariate Cox proportional hazards models for tamoxifen failure at 5 years, disease-free survival and disease-specific survival for entire study period

	AR:ER ratio ≥ 2					
	n	**Events**	**HR**	**95% CI**	***P* value**	**Model adjusted by**
Tamoxifen failure at 5 years	191*	48	2.87	1.08, 7.67	**0.04**	ER%, tumor grade
DFS overall	191**	63	4.04	1.68, 9.69	**0.002**	ER%, tumor size
DSS overall	190**	49	2.75	1.11, 6.86	**0.03**	ER%, tumor size

AR, androgen receptor; CI, confidence interval; DFS, disease-free survival; DSS, disease-specific survival; ER, estrogen receptor. Bold data are significant.
*One case was missing tumor grade.
**Missing outcome data.

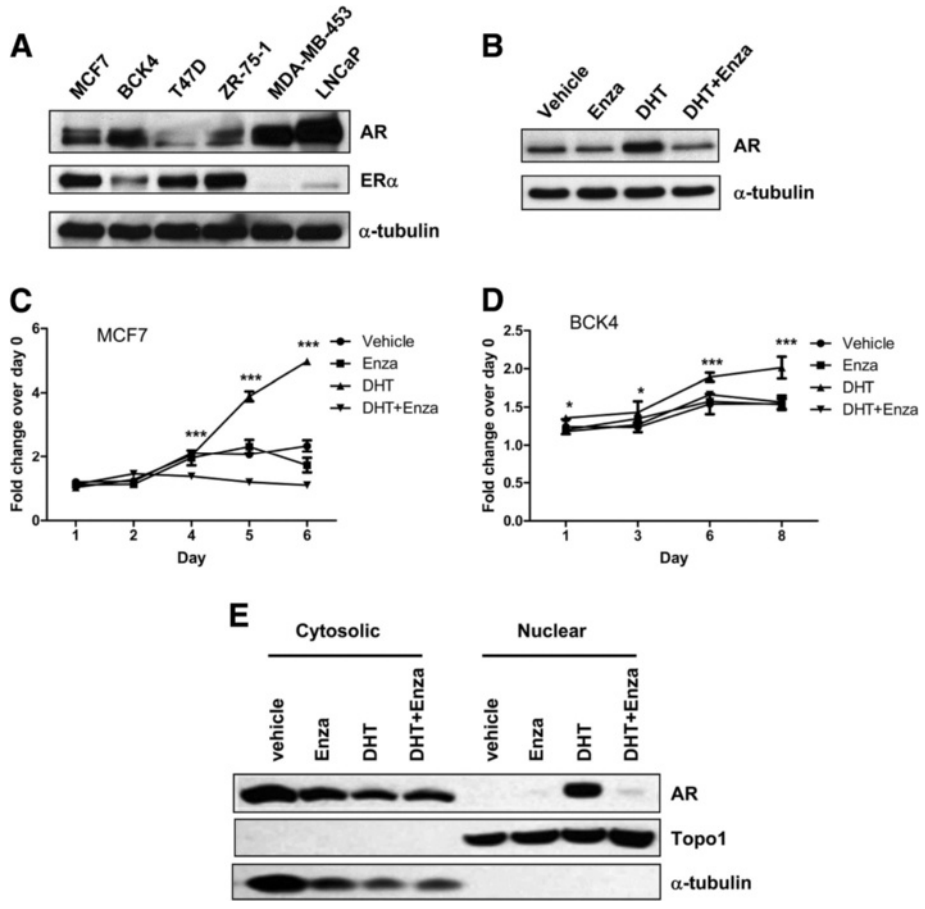

Figure 2 Enzalutamide abrogates androgen mediated proliferation in estrogen receptor-positive breast cancer cells. (A) Baseline levels of androgen receptor (AR) and estrogen receptor (ER) alpha protein in whole cell lysates from ER-positive (MCF7, BCK4, T47D and ZR-75-1) and ER-negative (MDA-MB-453) breast cancer and prostate (LNCaP) cancer cell lines. **(B)** AR protein levels in MCF7 cells plated in charcoal-stripped serum-containing media for 48 hours prior to treatment with vehicle control, 10 nM 5-alpha-dihydrotestosterone (DHT), 10 μM enzalutamide (Enza) or a combination of DHT and Enza for 48 hours. **(C)** MCF7 and **(D)** BCK4 breast cancer cells, both ER + AR+, were treated with vehicle control, 10 nM DHT, 10 μM Enza or a combination of DHT and Enza, and MTS proliferation assays were performed. Error bars represent standard error of the mean. *$P < 0.05$, ***$P < 0.001$ for DHT versus DHT + Enza, analysis of variance with Bonferroni's multiple comparison test correction. **(E)** AR levels in cytosolic and nuclear fractions of MCF7 cells treated with vehicle, 10 nM DHT, 10 μM enzalutamide or DHT + Enza for 3 hours.

luminescent imaging and caliper measurements. Once tumors were established, mice were matched based upon tumor imaging (day −2) into two treatment groups, one receiving control chow and the other receiving chow containing 50 mg/kg enzalutamide on day 0. Tumors in the DHT-treated mice on control chow continued to grow, while mice receiving DHT plus enzalutamide showed regression of tumors by the *in vivo* imaging system (Figure 3A) and caliper measurement (data not shown). On the final day of imaging (day 19), tumors had regressed to near undetectable levels, with an 83.2% decrease in luminescence in mice receiving DHT plus enzalutamide as compared with the DHT group (Figure 3A,B). As determined by BrdU incorporation and immunostaining, proliferation in the enzalutamide-treated tumors was 31.3% lower than in tumors treated with DHT alone (Figure 3C). TUNEL staining indicated a 50% increase in apoptotic cells in enzalutamide-treated tumors (Figure 3D). A dramatic (92.5%) decrease in AR nuclear localization was observed in the tumors treated with enzalutamide (Figure 3E), consistent with the ability of enzalutamide to impair nuclear entry of AR in prostate cancer [33]. Similar results to the above with MCF7 xenografts were obtained in mice administered enzalutamide by oral gavage, where tumor burden decreased in a dose-dependent manner (data not shown).

Enzalutamide inhibits androgen-mediated growth in ER– breast cancer cells *in vitro* and *in vivo*

The MDA-MB-453 breast cancer cell line represents the ER– molecular apocrine or luminal androgen receptor subtype of breast cancer with high levels of AR [17,18,20,34]. In this line, AR contains a point mutation (Q865H) reported to decrease sensitivity to

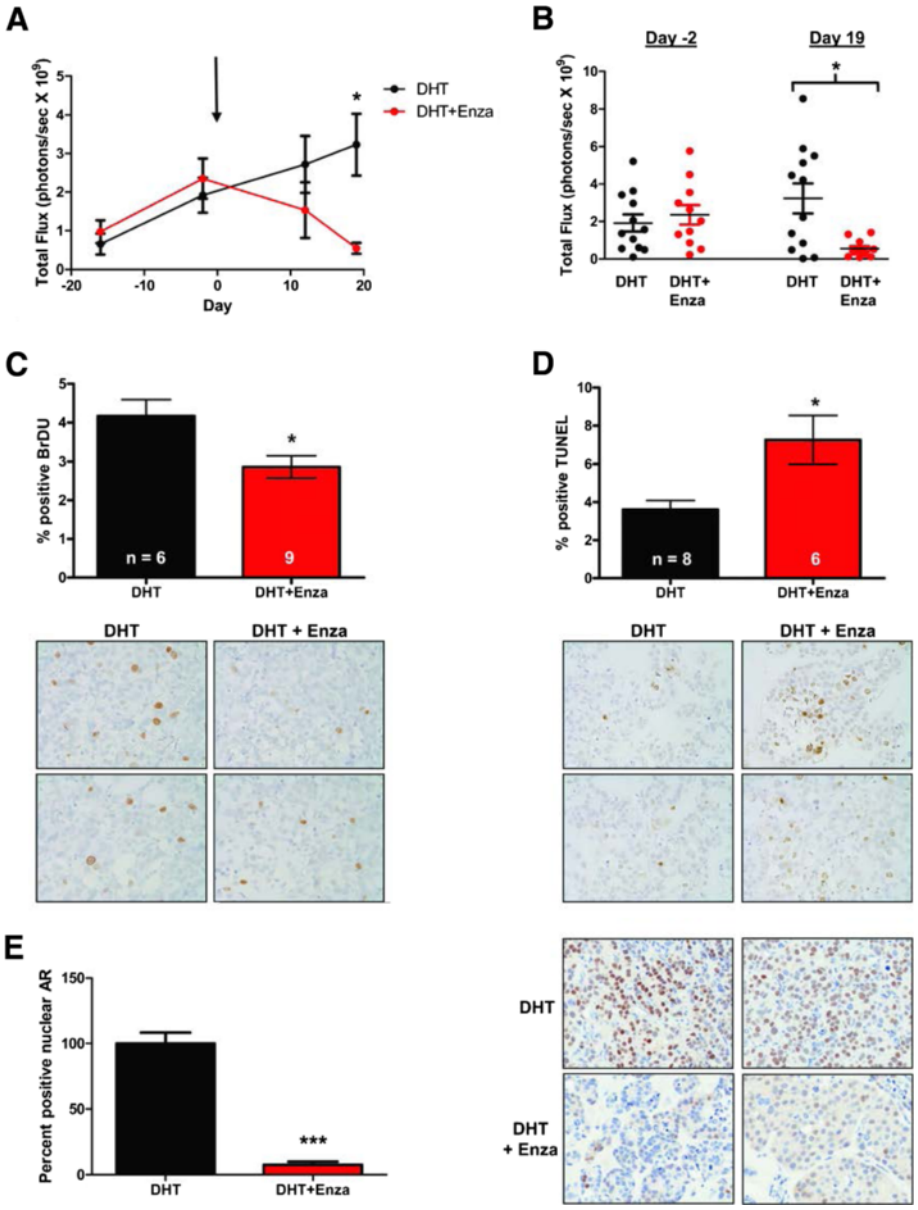

Figure 3 Enzalutamide inhibits androgen-stimulated growth of MCF7 tumors *in vivo*. MCF7-TGL cells stably expressing luciferase were implanted orthotopically in the mammary gland of NOD/SCID ovariectomized female mice with a 5-alpha-dihydrotestosterone (DHT) pellet implanted subcutaneously. Mice were matched into two groups based on tumor volume (day −2) and treatment with either control chow (DHT) or chow containing 50 mg/kg enzalutamide (DHT + Enza) begun (day 0, indicated by arrow), and the tumor burden was measured by whole-body luminescence. **(A)** Mean total flux of all mice in each of the treatment groups. Error bar represents standard error of the mean. *$P < 0.05$, Wilcoxon rank sum. **(B)** Total luminescent flux is shown for all individual mice at the day of matching (day −2) and at the final imaging day (day 19). *$P < 0.05$, Wilcoxon rank sum. **(C)** Mice were injected with bromodeoxyuridine (BrdU) 2 hours prior to sacrifice and BrdU immunohistochemistry was performed on formalin-fixed paraffin-embedded tumor sections and quantified. *$P < 0.05$, Student's *t* test. Representative images of BrdU staining (400× magnification) and quantification. **(D)** Quantification of apoptotic cells as measured by terminal deoxynucleotidyl transferase dUTP nick end-labeling (TUNEL) staining with representative images below (400× magnification). *$P < 0.05$, Student's *t* test. **(E)** Quantification of nuclear AR staining and representative images (400× magnification). ***$P < 0.001$, Wilcoxon rank sum.

DHT [35]. Nonetheless, these cells proliferate in response to androgens [28,29] and we therefore sought to determine whether enzalutamide could block DHT-mediated effects on proliferation and gene expression. Indeed, enzalutamide completely abrogated proliferation induced by DHT (Figure S2A in Additional file 2) and expression of known AR-regulated genes [29], such as fatty acid synthase, gross cystic disease fluid protein (also called prolactin inducible protein) and prolactin receptor, was reduced by enzalutamide (Figure S2B in Additional file 2).

Further, in MDA-MB-453 cells that stably express an androgen responsive luciferase reporter (MDA-kb2) [36], enzalutamide inhibited luciferase reporter activity in a dose-dependent manner (Figure S2C in Additional file 2). Enzalutamide impairs ligand-mediated nuclear import of AR in prostate cells [33], and in MDA-kb2 cells it reduced the ratio of nuclear to total AR (Figure S2D in Additional file 2). Immunoblotting for AR in nuclear and cytoplasmic lysates demonstrates that the same is true in wild-type MDA-MB-453 cells (Figure S3 in Additional file 3).

To determine whether enzalutamide inhibits androgen-induced tumor growth of ER– breast cancer cells, MDA-MB-453 xenografts were grown at the orthotopic site in mice implanted with a DHT pellet and the tumor size was measured by caliper. Once tumors reached 100 mm^3, mice were treated with 10 mg/kg/day enzalutamide or vehicle by oral gavage (Figure 4A, green arrow). DHT stimulates tumor growth as previously reported [20], but in mice treated with DHT plus enzalutamide (10 mg/kg by oral gavage) tumors did not significantly differ from mice that received vehicle control (Figure 4A). Another group of mice received a higher dose of enzalutamide (25 mg/kg/day) starting when tumors reached an average of 400 mm^3 (Figure 4A, blue arrow). At this higher dose, there was a trend towards decreased tumor size, although this did not reach statistical significance (Figure 4A). Tumor weights in either the low-dose or high-dose enzalutamide treatments were significantly lower than mice treated with DHT only, an 85.2% and 65.0% decrease respectively (Figure 4B), indicating that the caliper measurements for a high dose of enzalutamide underestimates the decreased tumor burden in this group. Interestingly, there was a statistically significant increase in apoptosis in both enzalutamide treatment groups versus DHT (60.0% and 54.3% increase in low-dose and high-dose groups respectively), as measured by cleaved caspase 3 (Figure 4C, quantification on left and representative images on right), but there was no difference in the proliferation rate of any of the groups, as measured by Ki67 staining (not shown). Thus, in MDA-MB-453 tumors, DHT protects cells against apoptosis and enzalutamide impairs this anti-apoptotic effect. Consistent with the *in vitro* data, enzalutamide decreased ligand-mediated nuclear entry of AR such that there is a significant decrease (50.0% in low dose and 44.3% in high dose) in the number of AR-positive nuclei in the enzalutamide-treated tumors (Figure 4D, quantification on left and representative images on right). Similarly, when an MDA-MB-453 xenograft study was performed with low-dose and high-dose enzalutamide treatments initiated when the tumors reached 100 mm^3 (Figure S4A in Additional file 4), tumor growth was decreased in a dose-dependent manner (Figure S4B in Additional file 4) and was associated with significantly reduced nuclear AR staining in enzalutamide-treated tumors (Figure S4C in Additional file 4). Steady-state concentrations of enzalutamide, including the pharmacologically active metabolite *N*-desmethyl-MDV3100, in the MDA-MB-453 xenograft studies were only moderately lower than what has been reported in patients receiving 160 mg/day enzalutamide (Cmax values for enzalutamide and the pharmacologically active metabolite, *N*-desmethyl enzalutamide, were 16.6 μg/ml and 12.7 μg/ml, respectively).

Enzalutamide inhibits estrogen mediated growth *in vitro* and *in vivo*

While enzalutamide has high affinity binding for AR, it does not significantly bind to either ERα or ERβ as determined by ligand binding assays (Table S1 in Additional file 5). However, originally as a negative control in experiments where we were antagonizing DHT with enzalutamide, we combined enzalutamide with E2 in ER+/AR + breast cancer cells. Surprisingly, enzalutamide significantly inhibited E2-induced proliferation of both MCF7 and BCK4 cells *in vitro* (Figure 5A,B). Enzalutamide also inhibited E2-induced upregulation of PR and SDF-1, two estrogen-responsive genes (Figure 5C). In stark contrast, although bicalutamide effectively inhibited DHT-mediated proliferation in MCF7 cells (Figure 5D), it had the opposite effect on E2 signaling, as it significantly increased E2-mediated proliferation (Figure 5E) and increased the E2-mediated induction of PR and SDF-1 mRNA (Figure 5F).

To determine the effect of enzalutamide on E2-stimulated breast tumor growth *in vivo*, a xenograft study was performed injecting MCF7-TGL cells in ovariectomized mice implanted with an E2 pellet. Cells were injected orthotopically and once tumors were established (arrow, average size of 100 mm^3), mice were matched into three groups: control chow; control chow and a tamoxifen pellet; and chow containing 50 mg/kg enzalutamide (Figure 6A). Enzalutamide significantly inhibited E2-mediated MCF7 tumor growth as effectively as tamoxifen, with a decrease in tumor luminescence of 59.9% for the tamoxifen group and 70.3% in the enzalutamide group at day 11. Day 11 was the final day of imaging for the E2-only group since these mice had to be euthanized due to tumor burden. Luminescence flux for individual animals (Figure 6B) and images of mice (Figure 6C) are shown for the day of matching (day –3) and the last imaging day when all mice were alive (day 11). Both drugs significantly decreased cell proliferation, with a 46.4% decrease in the E2 plus tamoxifen group and a 54.2% decrease in the E2 plus enzalutamide group compared with the E2 group, as measured by BrdU incorporation (Figure 6D). In contrast to what was observed in DHT-mediated tumor growth, enzalutamide did not

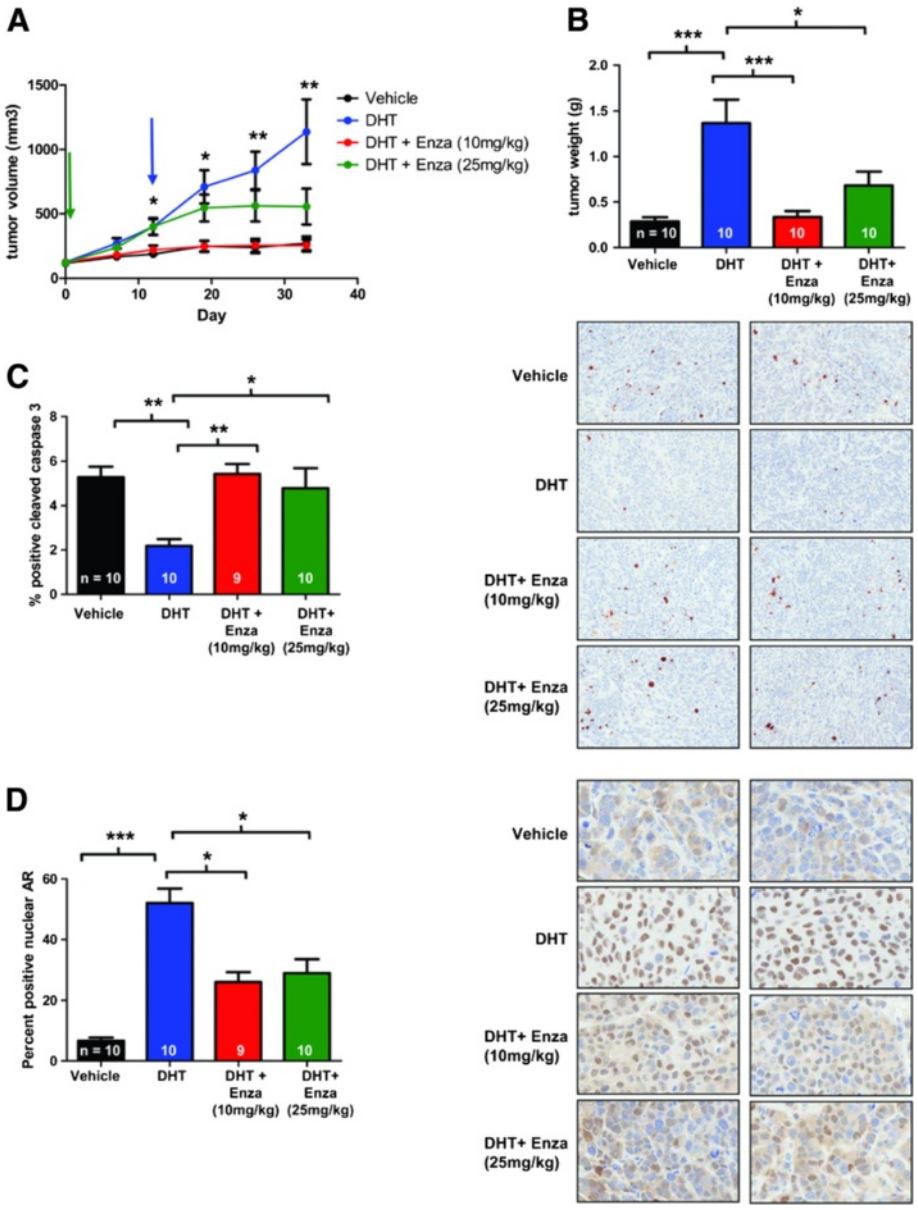

Figure 4 Enzalutamide inhibits androgen-stimulated growth of MDA-MB-453 tumors. MDA-MB-453 cells were injected orthotopically in the mammary gland of female NOD-SCID-IL2Rgc$^{-/-}$ mice. Three groups had a 5-alpha-dihydrotestosterone (DHT) pellet implanted subcutaneously and one group had no pellet (Vehicle). Once tumors reached an average size of 100 mm^3 (green arrow), mice were given either enzalutamide (Enza, 10 mg/kg) or vehicle (Vehicle and DHT groups) by daily oral gavage. Another group was given a higher dose of Enza (25 mg/kg) by oral gavage when tumors reached an average size of 400 mm^3 (blue arrow). **(A)** Tumor volume was measured weekly by caliper. Error bars represent standard error of the mean. *$P < 0.05$, **$P < 0.01$ for DHT versus DHT + Enza (10 mg/kg), Wilcoxon rank sum. **(B)** Tumors were excised and weighed at the end of the experiment. **(C)** Tumor sections stained for cleaved caspase 3 were quantified (left) and representative images shown (right) (200× magnification). *$P < 0.05$, **$P < 0.01$, ***$P < 0.001$, analysis of variance with Bonferroni's multiple comparison test correction. **(D)** Nuclear androgen receptor staining was quantified (left) and representative images (400× magnification) are shown (right). *$P < 0.05$, ***$P < 0.001$, Kruskal–Wallis with Dunn's multiple comparison test correction.

increase apoptosis when opposing E2-stimulated growth (data not shown). Interestingly, ER protein levels in the MCF7 xenograft tumors were affected differently by tamoxifen versus enzalutamide (Figure S5 in Additional file 6). ER immunostaining was quantified with ImageJ and by pathologist (PJ) scoring in a blinded manner for percent cells positive for nuclear ER. By both methods, ER was extremely low in the E2-alone group, but significantly increased with the addition of tamoxifen. However, in the E2 plus enzalutamide group, ER levels are not significantly different from E2 alone, indicating that enzalutamide does not elicit upregulation of ER

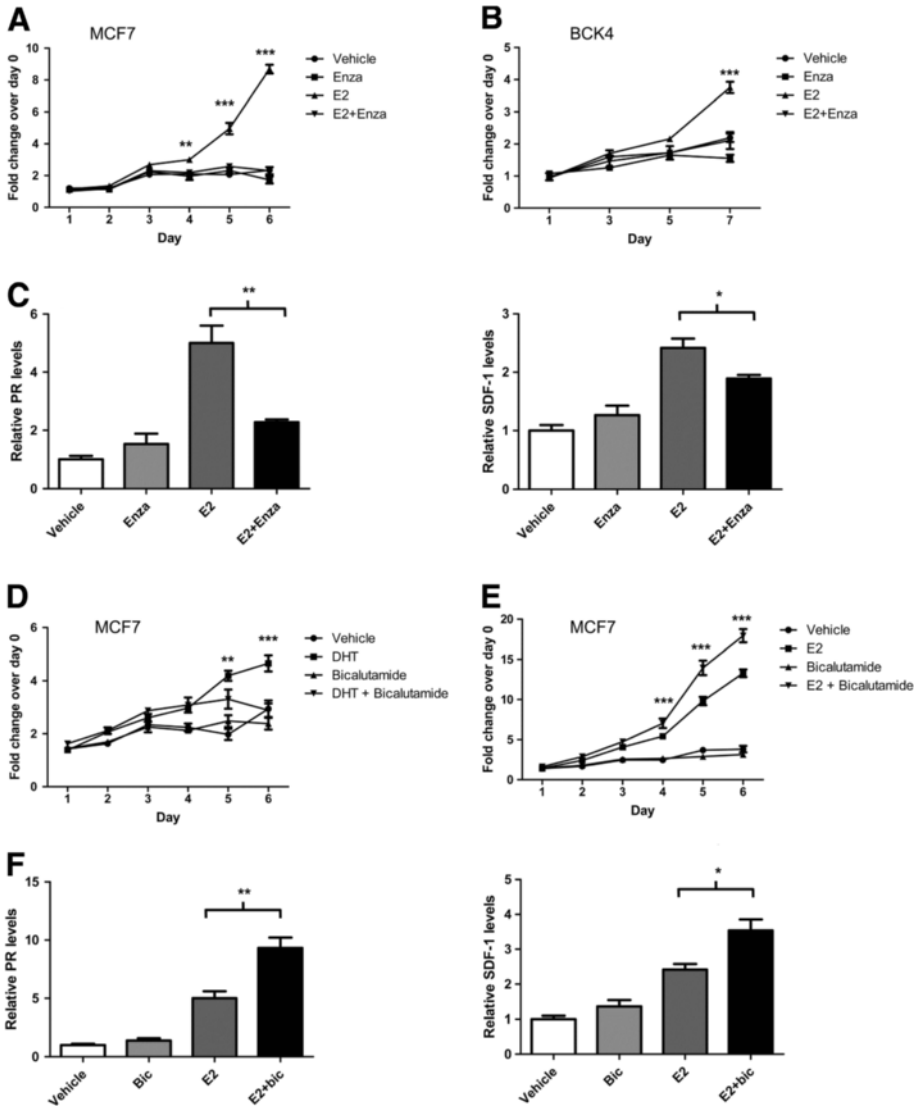

Figure 5 Enzalutamide inhibits estradiol-mediated proliferation of breast cancer cells, while bicalutamide does not. MTS proliferation assays were performed on **(A)** MCF7s cells and **(B)** BCK4 cells treated with vehicle control, 10 nM estradiol (E2), 10 μM enzalutamide (Enza) or a combination of E2 and Enza. Error bars represent standard error of the mean (SEM). $^{**}P < 0.01$, $^{***}P < 0.001$ for E2 versus E2 + Enza, analysis of variance (ANOVA) with Bonferroni's multiple comparison test correction. **(C)** MCF7 cells were treated for 48 hours with treatments as above and real-time polymerase chain reaction (PCR) was performed for estrogen-responsive genes, progesterone receptor (PR) and stromal cell-derived factor 1 (SDF-1, also known as CXCL12). Each gene is normalized to 18S and shown relative to vehicle. $^{*}P < 0.05$, $^{***}P < 0.001$, Student's *t* test. MCF7 cells were treated with vehicle control, **(D)** 1 μM bicalutamide, 10 nM 5-alpha-dihydrotestosterone (DHT) and DHT + bicalutamide or **(E)** with 10 nM E2 and E2 + bicalutamide. $^{**}P < 0.01$, $^{***}P < 0.001$ for DHT versus DHT + bicalutamide, or E2 versus E2 + bicalutamide, ANOVA with Bonferroni's multiple comparison test correction. **(F)** MCF7 cells treated for 48 hours with vehicle, 1 μM bicalutamide, 10 nM E2 and E2 + bicalutamide and real-time PCR performed for PR and SDF-1. $^{*}P < 0.05$, $^{***}P < 0.001$, Student's *t* test. Error bars represent SEM, Student's *t* test (all analyses).

like tamoxifen (Figure S5 in Additional file 6) and suggests that enzalutamide affects ER by a different mechanism than the competitive antagonist tamoxifen. This intriguing finding will be the focus of a subsequent study.

Importantly, mean animal weights during and at the end of all *in vivo* studies showed no differences across treatment groups, indicating no adverse effects on the general health of the mice (Figure S6 in Additional file 7).

Discussion

The vast majority of ER + breast cancers are clearly also AR + (84 to 91%) [5,37,38] and patients with tumors that co-express AR with ER and PR have a longer DFS than those with tumors negative for all three receptors [37], probably reflecting a more well-differentiated state than that of receptor-negative tumors . However, the question of whether androgens and ARs are harmful or beneficial for patients with breast cancer is complex [39-41] and

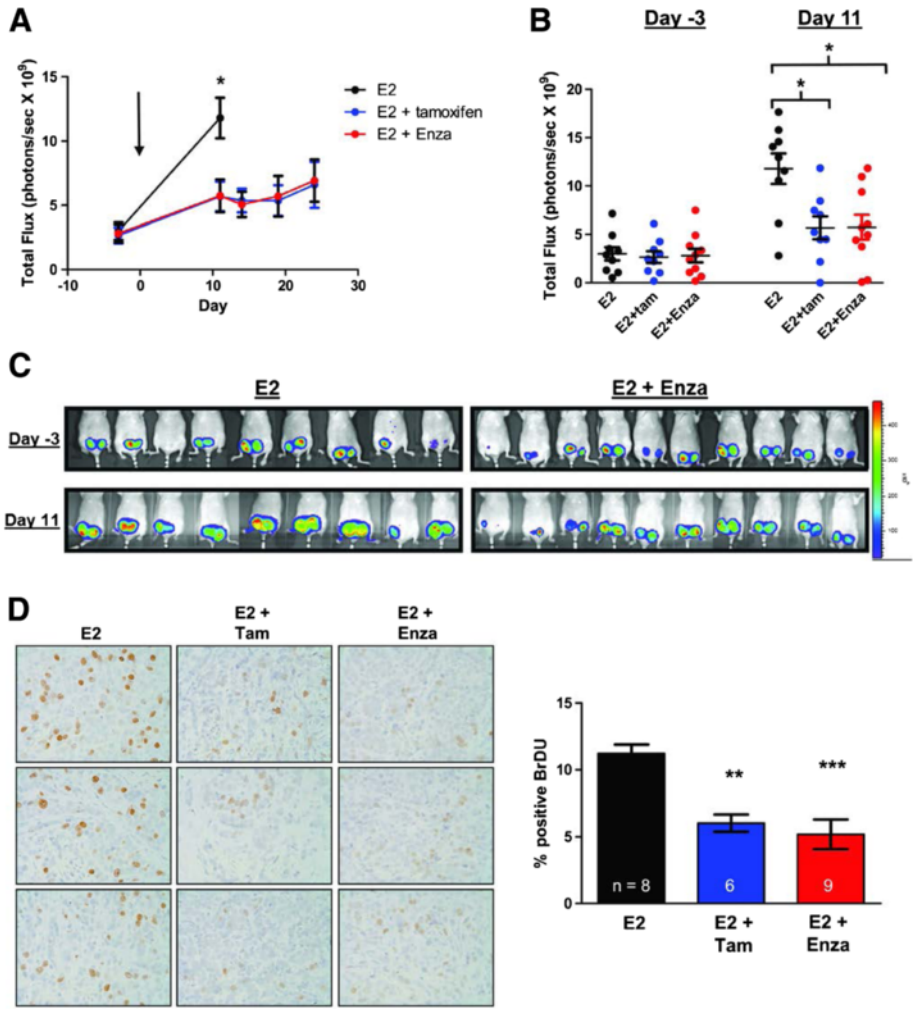

Figure 6 Enzalutamide inhibits estrogen-stimulated growth of MCF7 tumors as effectively as tamoxifen. MCF7-TGL cells stably expressing luciferase were implanted orthotopically in the mammary gland of ovariectomized female nude mice. All mice had an estradiol (E2) pellet implanted subcutaneously and were given either control chow (E2), control chow plus a tamoxifen pellet implanted subcutaneously (E2 + Tam) or chow containing 50 mg/kg enzalutamide (E2 + Enza). The tumor burden was measured by whole-body luminescence. **(A)** Mean total flux. Mice were matched on day −3 and treatment began on day 0 (arrow). $^{*}P < 0.05$, analysis of variance (ANOVA) with Bonferroni's multiple comparison test correction. **(B)** The total luminescent flux is shown for individual mice on the day of matching (day −3) and of final imaging (day 11). $^{*}P < 0.05$, ANOVA with Bonferroni's multiple comparison test correction. **(C)** Images of luminescent signal in the two treatment groups at time of matching (day −3) and the final day of imaging (day 11). **(D)** Mice were injected with bromodeoxyuridine (BrdU) 2 hours prior to sacrifice and immunohistochemistry for BrdU was performed on tumor sections and quantified using imageJ (National Institutes of Health, Bethesda, MD, USA). Representative images of BrdU staining (left, 400× magnification) and quantification (right). $^{**}P < 0.01$ for E2 versus E2 + Tam, $^{***}P < 0.001$ for E2 versus E2 + Enza, ANOVA with Bonferroni's multiple comparison test correction.

probably differs with menopausal status, treatment and breast cancer subtype.

Our analysis of 192 women with ER + breast cancers treated with tamoxifen revealed that rather than the level of AR expression, the AR:ER ratio may play a role in disease progression and response to treatment. In our cohort, women with tumors expressing a high ratio of AR:ER (≥2.0) had over four times the risk for failure while on tamoxifen (HR = 4.43) compared with women with a low ratio (<2.0). When ER percent cell staining was added to the model, the risk dropped to 2.87-fold, showing that although ER percent staining explained some of the increase in risk from a higher ratio, the AR:ER ratio actually has an independent effect on risk for failure above ER percent staining. In summary, the data indicate that a high ratio of nuclear AR to ER protein is indicative of shorter time to relapse in patients treated with tamoxifen, and may also be indicative of a lack of response to neoadjuvant AI treatment. Although they need to be tested in additional cohorts, these provocative findings suggest that the AR:ER ratio may be a new, independent predictor of response to traditional E2/ER-directed endocrine

therapies. The finding may also indicate that patients that relapse while on tamoxifen or AIs might be good candidates for AR-directed therapy. Lastly, AR:ER ratio is also an independent predictor of DFS (HR = 4.04, 95% confidence interval: 1.68, 9.69; $P = 0.002$) and DSS (HR = 2.75, 95% confidence interval: 1.11, 6.86; $P = 0.03$).

Our *in vitro* and preclinical results demonstrate that enzalutamide inhibits androgen-stimulated growth of both ER+/AR + and ER−/AR + breast tumors. Surprisingly, with regard to E2-mediated proliferation, enzalutamide, which works by impairing androgen-mediated AR nuclear entry, gives a completely different result than the traditional anti-androgen, bicalutamide. Although DHT is clearly proliferative in MCF7 and BCK4 cells, in some breast cancer cell lines DHT decreased E2-induced proliferation [28,42-44]; however, the antagonist bicalutamide consistently increased E2-mediated proliferation. This bicalutamide-mediated increase in E2-stimulated proliferation was interpreted as indicating that AR is protective against E2-mediated breast cancer cell proliferation. However, we now present contrasting results demonstrating that inhibition of AR with enzalutamide decreases ER-mediated proliferation. A critical difference between the two drugs is that while bicalutamide permits AR nuclear entry, enzalutamide greatly impairs AR localization and ligand-mediated stabilization, as indicated in studies in prostate cancer and our nuclear and cytosolic fractionation and immunohistochemistry in xenograft tumors presented in this study. Our results with enzalutamide thus shed new light on the role of AR in breast cancer, since *in vitro* and *in vivo* preclinical studies demonstrate that inhibiting AR nuclear localization decreases both androgen and estrogen-stimulated tumor growth.

We propose an explanation that reconciles conflicting reports regarding the role of AR in breast cancer by recognizing that hormonal influences on the breast are quite different in premenopausal versus postmenopausal women. Data suggesting a protective effect of androgens studied androgen in the presence of estrogen, thereby more closely modeling the premenopausal state [45] where androgens and AR may be protective against E2-mediated proliferation. AR can bind to the ER cofactor FOXA1 and to estrogen response elements, albeit as a weaker transcriptional activator than ER at these loci; therefore, the net effect of liganded AR competing with liganded ER may be decreased E2-mediated proliferation [42]. Additionally, in ER−/AR + tumors such as the MDA-MB-453 cell line, global AR binding events largely overlap that of ER in ER + luminal A tumors [19]. In contrast, in postmenopausal women with ER + breast cancer (which represent the majority of cases), and particularly in those being treated with AIs, circulating levels of E2 are extremely low, while circulating androgen levels are slightly elevated since AIs block the conversion of androgens to estrogen [12]. Importantly, circulating levels of testosterone, androstenedione, and DHEA-S increase in women on AI therapy [13] as compared with pretreatment levels. Furthermore, high levels of the adrenal androgen DHEA-S before treatment are predictive of failure on AIs and circulating DHEA-S increased during treatment in patients with tumors that failed to respond to AI treatment [14]. In the context of a postmenopausal woman on AI therapy (in the absence of estrogen), it is possible that activated AR could mediate protumorigenic pathways in breast cancers. As recently reviewed [40,46], the data in cell lines regarding whether DHT is proliferative are very conflicting; however, a study with seven lines derived from ductal carcinomas demonstrated that the majority were growth stimulated by physiologic levels of testosterone [47]. Interestingly, local production of sex steroids can occur, and DHT levels have been found to be significantly higher in carcinomatous breast tissues than in the blood of postmenopausal breast cancer patients [48].

DHT is not aromatizable [31,32,49], indicating that conversion to estrogens is not causing breast tumor growth in our study. Furthermore, we observe that enzalutamide acts differently when it opposes DHT versus E2-driven tumor growth. Enzalutamide very effectively blocks DHT-mediated protection against apoptosis in both ER + and ER− tumors, but it inhibits proliferation but does not affect apoptosis when opposing E2-stimulated tumor growth in ER+/AR + models. Although enzalutamide does not bind ER, it appears to affect ER in MCF7 xenograft tumors, but in a different manner than tamoxifen. Furthermore, we find that enzalutamide blocks the E2-mediated induction of ER-regulated genes such as the chemokine SDF-1 (also known as CXCL12). SDF-1 mediates the mitogenic effects of E2 in breast cancer cells [50]. The SDF-1/CXCR4 pathway can activate ER via phosphorylation, and E2-driven proliferation is blocked by inhibition of this pathway [51]. SDF-1 promotes the growth of prostate epithelial cells by promoting the nuclear localization of AR, binding of AR to DNA and increased PSA protein in a ligand independent manner [52]. In contrast to enzalutamide, bicalutamide enhances upregulation of SDF-1 and other E2-regulated genes, and enhances E2-mediated breast cancer cell proliferation. This difference in how enzalutamide and bicalutamide affect ER activity may provide insight into the role of AR in breast cancer. When bound to bicalutamide, AR can still translocate to the nucleus and bind to DNA [22]. In contrast, enzalutamide has been reported to impair liganded AR nuclear entry in prostate cancer cells [33,53], as we see in this study in breast cancer cell lines in culture and xenografts. Our observation that enzalutamide blocks E2-induced proliferation and inhibits liganded ER activity on classical ER-regulated

genes thus suggests that nuclear AR is critical for ER function. Indeed, AR and ER can directly interact in breast cancer cells [54,55].

Conclusion

While AR has been considered a potential therapeutic target in ER−/AR + breast cancers [2,17,18,20], it has not previously been suggested as a target in ER + breast cancers. Our data in clinical specimens suggest that the ratio of nuclear AR to ER may critically influence tumor biology and response to endocrine therapy. A high AR:ER ratio may be predictive of suboptimal response to ER-directed endocrine therapy. Furthermore, higher nuclear expression of AR relative to ER may also be indicative of active AR, since AR translocates to the nucleus and is stabilized upon ligand binding. AR and ER are expressed at roughly equivalent amounts in tumors that respond to neoadjuvant endocrine therapy and in adjacent uninvolved epithelium, suggesting that similar levels of AR and ER reflect a more normal state. In addition to being a predictor of poorer response to traditional endocrine therapy and overall DFS, high levels of AR relative to ER may also identify a subset of breast cancers that would respond more favorably to enzalutamide alone or combined with tamoxifen or AIs. Targeting AR may prove useful in patients with recurrent ER + disease. If the long-term selective pressure of drugs targeting the E2/ER pathway leads to tumors switching to dependence on androgens, initial treatment with both AI and enzalutamide may be beneficial. In summary, our preclinical data support the initiation of clinical studies evaluating enzalutamide for treatment of AR + tumors regardless of ER status, since enzalutamide uniquely blocks both androgen-mediated and estrogen-mediated tumor growth. Recently, a mutation was discovered in AR that confers resistance to enzalutamide and another new generation anti-androgen, ARN-509, [56,57]. Whether such mutations will also arise in breast cancer patients treated with anti-androgens remains to be seen.

Additional files

Additional file 1: Figure S1. Showing breast tumors that respond to endocrine therapy tend to have decreased AR expression while nonresponders tend to maintain AR expression. There is a positive correlation between AR and ER in responsive tumors and uninvolved adjacent epithelium. Patients received 4 months of neoadjuvant endocrine therapy (exemestane or exemestane + tamoxifen). Core biopsies taken prior to treatment (pre) and a tumor sample at the time of surgery (post) were stained for AR expression. Graph depicts the AR score (percent cells positive for nuclear AR staining versus intensity) in the pre and post treatment samples for those who responded to the endocrine therapy versus nonresponders. $P = 0.064$, Wilcoxon matched-pair test (left top). Staining of AR in representative responsive and nonresponsive tumors pre versus post treatment is shown below (400× magnification) (left, bottom). In the same tumors, staining score (percent positive staining × intensity) for nuclear AR was plotted on the *y* axis and ER on the *x* axis for patients who responded (A, graph) versus those who did not (B, graph). Normal uninvolved glands adjacent to tumors were scored for AR and ER (C, graph). The slope of the line (β) is indicated, as well as the *P* value, Spearman correlation. Representative images of AR and ER staining (400× magnification) in responders (A, right), nonresponders (B, right) and normal adjacent (C, right) (1,000× magnification).

Additional file 2: Figure S2. Showing that enzalutamide (Enza) abrogates DHT-mediated proliferation in ER-negative breast cancer cells. (A) MTS proliferation assays were performed in MDA-MB-453 cells treated with vehicle, 10 nM DHT, 10 μM Enza or DHT + Enza. Error bars = standard error of the mean (SEM). (B) Real-time polymerase chain reaction for androgen responsive genes fatty acid synthase (FASN), gross cystic disease fluid protein (GCDFP-15, also called prolactin inducible protein) and prolactin receptor (PRLR) was performed from RNA harvested from MDA-MB-453 breast cancer cells treated with vehicle, 10 μM Enza, 10 nM DHT or DHT + Enza for 24 hours. Genes normalized to 18S and relative to vehicle. $^{*}P < 0.05$, $^{**}P < 0.01$ for Student's *t* test. (C) MDA-k2b cells, which contain an androgen responsive luciferase construct, were treated for 24 hours with various concentrations of DHT alone or in combination with 1 or 10 μM Enza prior to luciferase assay, and luciferase units relative to the 0.001 nM DHT are shown. Error bars = SEM. (D) MDA-kb2 cells were treated as indicated for 3 hours. Nuclear and total AR staining was quantified with graph indicating the ratio of nuclear to total AR (each triangle represents one cell). Representative images (600× magnification). For proliferation and luciferase assays and the quantification of nuclear/total AR ratio, $^{*}P < 0.05$, $^{**}P < 0.01$, $^{***}P < 0.001$ for DHT versus DHT + Enza, analysis of variance with Bonferroni's multiple comparison test correction.

Additional file 3: Figure S3. Showing that enzalutamide (Enza) impairs DHT-mediated nuclear entry of AR in apocrine breast cancer cells. MDA-453 cells were treated with vehicle, 10 nM DHT, 10 μM enzalutamide or DHT + Enza for 3 hours. After nuclear and cytoplasmic fractionation, lysates were immunoblotted for AR, Topo I (control for nuclear fraction) and glyceraldehyde 3-phosphate dehydrogenase (GAPDH; control for cytoplasmic fraction).

Additional file 4: Figure S4. Showing that enzalutamide (Enza) inhibits androgen-mediated growth of MDA-MB-453 tumors. MDA-MB-453 cells were injected orthotopically in the mammary gland of female NOD-SCID-IL2Rgc$^{-/-}$ mice. Three groups had a DHT pellet implanted subcutaneously and one group had no pellet (Vehicle). Once the tumors reached 100 mm^3, the mice were given vehicle (Vehicle and DHT groups) or Enza at 10 mg/kg or 25 mg/kg, by daily oral gavage. (A) Tumor volume was measured weekly by caliper. Error bars represent standard error of the mean. $^{*}P < 0.05$, $^{**}P < 0.01$, $^{***}P < 0.001$ for DHT versus DHT + Enza (10 mg/kg) and DHT + (25 mg/kg), Wilcoxon rank sum. (B) Tumors were excised and weighed at the end of the experiment. $^{***}P < 0.001$, analysis of variance with Bonferroni's multiple comparison test correction. (C) Tumor sections stained for AR. Nuclear AR staining was quantified and representative images (200× magnification) are shown below. $^{*}P < 0.05$, Kruskal–Wallis with Dunn's multiple comparison test correction.

Additional file 5: Table S1. Presenting the competitive radioligand binding assay with enzalutamide competing with 0.5 nM [3H] estradiol for binding to ERα and ERβ. The competing reference ligand was 1 μM diethylstilbestrol, which gave 50% inhibition at 0.5 nM on ERα and 0.9 nM on ERβ, while enzalutamide at concentrations up to 100 mM only gave between 1 and 4% inhibition on ERα and between 1 and 6% on ERβ.

Additional file 6: Figure S5. Showing that enzalutamide (Enza) affects ER protein differently than tamoxifen *in vivo* in MCF7 xenografts. Immunohistochemical staining of ER performed on formalin-fixed paraffin-embedded MCF7 tumor sections ($n = 8$ E2 and E2 + TAM, and $n = 9$ E2 + Enza) scored by pathologist for (A) percent positive nuclear staining ($^{**}P < 0.005$) and (B) intensity. (C) Overall percent positive signal quantified by ImageJ. $^{*}P < 0.05$. (D) Representative images at 1,000 ×.

Additional file 7: Figure S6. Showing that treatments did not affect mouse body weights in any of the three xenograft experiments. Average mouse weights in grams for (A) mice with MCF7 xenografts in the E2, E2 + enzalutamide (Enza), and E2+ tamoxifen (Tam) treatment groups at the end of the study (day 11); (B) mice with MCF7 xenografts in the DHT versus DHT + Enza treatment groups at the end of the study (day 19); and (C) mice with MDA-MB-453 xenografts treated with vehicle, DHT alone, DHT + 25 mg/kg MDV3100 (Enza), or DHT + 10 mg/kg MDV3100 (Enza) throughout the experiment.

Abbreviations

AI: aromatase inhibitor; AR: androgen receptor; BrdU: bromodeoxyuridine; DFS: disease-free survival; DHEA-S: dehydroepiandrosterone sulfate; DHT: 5-alpha-dihydrotestosterone; DSS: disease-specific survival; E2: estradiol; ER: estrogen receptor; HR: hazard ratio; NOD-SCID: nonobese diabetic, severe combined immunodeficiency; PR: progesterone receptor; SDF-1: stromal cell-derived factor 1; TUNEL: terminal deoxynucleotidyl transferase dUTP nick end-labeling.

Competing interests

AAP, SB, and SM are full-time employees of Medivation. JG, FG, IEA, and EMcC are employed by Fundacion Ciencia & Vida in Santiago, Chile and receive partial funding from Medivation. The remaining authors declare that they have no competing interests. Enzalutamide is being co-developed by Medivation, Inc. and Astellas.

Authors' contributions

DRC performed proliferation assays, reverse transcriptase-polymerase chain reaction, tumor imaging, necropsies, statistical analysis of xenograft experiments and drafted the manuscript. SB directed the work at FCV in Chile, and contributed to study conception and design. BMJ performed BCK4 proliferation assays, assisted with xenograft surgeries, experimental design of in *vitro* and *in vivo* assays at Universit of Colorado (UC) and revised the manuscript. DMC conducted imaging and assisted with statistical analysis of xenograft experiments at UC. ENH assisted with xenograft studies (imaging and necropsies) at UC. NCD performed westerns and nuclear and cytosolic fractionations. NSS performed all tissue processing for preclinical histology, immunohistochemistry, TUNEL assays, and ImageJ analysis for xenograft studies at UC. SME identified tamoxifen treatment patient clinical specimens, collected clinical follow-up data, calculated AR:ER percent cell positive ratios, and performed statistics for the archival tamoxifen AR study. AJ performed proliferation assays, western assays, cellular fractionation, imaging and measurements of xenograft assays. JG carried out *in vitro* experiments including cell proliferation, cell imaging and fractionation. FG conducted molecular biology experiments and quantitative reverse transcriptase-polymerase chain reaction of MDA-MB-453 experiments. SM assisted in the design of dose selection and interpretation of *in vivo* data. IEA and EMcC contributed to the design of *in vivo* MDA-MB-231 xenografts, analysis and interpretation of *in vitro* and *in vivo* data performed in Chile. Pathologist PJ performed pathological examination of preclinical tissue samples. KCT performed or reviewed all statistical analysis of clinical data. ADT, breast pathologist, was principal investigator for the archival tamoxifen dataset used and retains overall responsibility for the database, reviewed immunohistochemistry for this study and all of the original tissue sections for diagnosis and tumor characteristics from over 1,200 patients to identify tissue sections usable for research. Oncologist ADE was the principal investigator of the AI clinical trial and also made substantial intellectual contributions to conception and design of preclinical studies. AAP contributed to the design of tissue culture and preclinical studies and assisted in the interpretation of data. JKR was principal investigator of laboratory studies conducted at UC, was responsible for overall conception and design of studies, collection, review, and interpretation of data and writing of the manuscript. All authors read and revised the manuscript critically for intellectual content and approved the final manuscript.

Acknowledgements

The study was supported by DOD Breast Cancer Program Idea Award W8IXWM-08-1-0311, Avon Foundation for Women, and AMC Cancer Fund to JKR, by DOD Breast Cancer Program Clinical Translational Award BC120183 W81XWH-13-1-0090 and UC Center Pilot Project Funds to JKR and ADE, and by Conicyt PFB-16 (SB, JG and FG). The authors thank Lisa Litzenberger, Department of Pathology, UC for graphic assistance. They acknowledge Claudia Acuña for providing technical assistance for analysis of the effects of enzalutamide on DHT-mediated nuclear entry of AR in apocrine breast cancer cells. The authors acknowledge the UC Cancer Center Shared Resource Facilities for DNA Sequencing, Animal Imaging, and Tissue Biobanking & Processing, supported by National Institutes of Health NCI Grant P30CA046934. Editorial assistance was provided by Kathryn Whitfield from Complete HealthVizion and was supported by Medivation Inc. and Astellas.

Author details

[1]Department of Pathology, University of Colorado Anschutz Medical Campus, RC1 North 5th Floor P18-5127 12800 E. 19th Ave, Aurora, CO 80045, USA. [2]Medivation Inc., 525 Market Street, 36th Floor, San Francisco, CA 94105, USA. [3]Fundación Ciencia & Vida, Avda. Zañartu 1482 - Ñuñoa, Santiago 7780272, Chile. [4]Department of Medicine, Division of Oncology, University of Colorado Anschutz Medical Campus, Aurora, CO, USA.

Received: 12 July 2013 Accepted: 8 January 2014
Published: 22 January 2014

References

1. Guedj M, Marisa L, de Reynies A, Orsetti B, Schiappa R, Bibeau F, MacGrogan G, Lerebours F, Finetti P, Longy M, Bertheau P, Bertrand F, Bonnet F, Martin AL, Feugeas JP, Bieche I, Lehmann-Che J, Lidereau R, Birnbaum D, Bertucci F, de The H, Theillet C: **A refined molecular taxonomy of breast cancer.** *Oncogene* 2012, **31:**1196–1206.
2. Lehmann BD, Bauer JA, Chen X, Sanders ME, Chakravarthy AB, Shyr Y, Pietenpol JA: **Identification of human triple-negative breast cancer subtypes and preclinical models for selection of targeted therapies.** *J Clin Invest* 2011, **121:**2750–2767.
3. Collins LC, Cole KS, Marotti JD, Hu R, Schnitt SJ, Tamimi RM: **Androgen receptor expression in breast cancer in relation to molecular phenotype: results from the Nurses' Health Study.** *Mod Pathol* 2011, **24:**924–931.
4. Park S, Koo J, Park HS, Kim JH, Choi SY, Lee JH, Park BW, Lee KS: **Expression of androgen receptors in primary breast cancer.** *Ann Oncol* 2010, **21:**488–492.
5. Hu R, Dawood S, Holmes MD, Collins LC, Schnitt SJ, Cole K, Marotti JD, Hankinson SE, Colditz GA, Tamimi RM: **Androgen receptor expression and breast cancer survival in postmenopausal women.** *Clin Cancer Res* 2011, **17:**1867–1874.
6. Bergh J, Jonsson PE, Lidbrink EK, Trudeau M, Eiermann W, Brattstrom D, Lindemann JP, Wiklund F, Henriksson R: **FACT: an open-label randomized phase III study of fulvestrant and anastrozole in combination compared with anastrozole alone as first-line therapy for patients with receptor-positive postmenopausal breast cancer.** *J Clin Oncol* 2012, **30:**1919–1925.
7. Mouridsen H, Gershanovich M, Sun Y, Perez-Carrion R, Boni C, Monnier A, Apffelstaedt J, Smith R, Sleeboom HP, Jaenicke F, Pluzanska A, Dank M, Becquart D, Bapsy PP, Salminen E, Snyder R, Chaudri-Ross H, Lang R, Wyld P, Bhatnagar A: **Phase III study of letrozole versus tamoxifen as first-line therapy of advanced breast cancer in postmenopausal women: analysis of survival and update of efficacy from the International Letrozole Breast Cancer Group.** *J Clin Oncol* 2003, **21:**2101–2109.
8. Harvell DM, Richer JK, Singh M, Spoelstra N, Finlayson C, Borges VF, Elias AD, Horwitz KB: **Estrogen regulated gene expression in response to neoadjuvant endocrine therapy of breast cancers: tamoxifen agonist effects dominate in the presence of an aromatase inhibitor.** *Breast Cancer Res Treat* 2008, **112:**489–501.
9. Harvell DM, Spoelstra NS, Singh M, McManaman JL, Finlayson C, Phang T, Trapp S, Hunter L, Dye WW, Borges VF, Elias A, Horwitz KB, Richer JK: **Molecular signatures of neoadjuvant endocrine therapy for breast cancer: characteristics of response or intrinsic resistance.** *Breast Cancer Res Treat* 2008, **112:**475–488.
10. De Amicis F, Thirugnansampanthan J, Cui Y, Selever J, Beyer A, Parra I, Weigel NL, Herynk MH, Tsimelzon A, Lewis MT, Chamness GC, Hilsenbeck SG, Ando S, Fuqua SA: **Androgen receptor overexpression induces tamoxifen resistance in human breast cancer cells.** *Breast Cancer Res Treat* 2010, **121:**1–11.
11. Spinola PG, Marchetti B, Merand Y, Belanger A, Labrie F: **Effects of the aromatase inhibitor 4-hydroxyandrostenedione and the antiandrogen flutamide on growth and steroid levels in DMBA-induced rat mammary tumors.** *Breast Cancer Res Treat* 1988, **12:**287–296.
12. Dimitrakakis C, Bondy C: **Androgens and the breast.** *Breast Cancer Res* 2009, **11:**212.
13. Gallicchio L, Macdonald R, Wood B, Rushovich E, Helzlsouer KJ: **Androgens and musculoskeletal symptoms among breast cancer patients on aromatase inhibitor therapy.** *Breast Cancer Res Treat* 2011, **130:**569–577.
14. Morris KT, Toth-Fejel S, Schmidt J, Fletcher WS, Pommier RF: **High dehydroepiandrosterone-sulfate predicts breast cancer progression during new aromatase inhibitor therapy and stimulates breast cancer cell growth in tissue culture: a renewed role for adrenalectomy.** *Surgery* 2001, **130:**947–953.

15. Niemeier LA, Dabbs DJ, Beriwal S, Striebel JM, Bhargava R: **Androgen receptor in breast cancer: expression in estrogen receptor-positive tumors and in estrogen receptor-negative tumors with apocrine differentiation.** *Mod Pathol* 2010, **23:**205–212.
16. Tsutsumi Y: **Apocrine Carcinoma as Triple-negative Breast Cancer: Novel Definition of Apocrine-type Carcinoma as Estrogen/Progesterone Receptor-negative and Androgen Receptor-positive Invasive Ductal Carcinoma.** *Jpn J Clin Oncol* 2012, **42:**375–386.
17. Doane AS, Danso M, Lal P, Donaton M, Zhang L, Hudis C, Gerald WL: **An estrogen receptor-negative breast cancer subset characterized by a hormonally regulated transcriptional program and response to androgen.** *Oncogene* 2006, **25:**3994–4008.
18. Farmer P, Bonnefoi H, Becette V, Tubiana-Hulin M, Fumoleau P, Larsimont D, Macgrogan G, Bergh J, Cameron D, Goldstein D, Duss S, Nicoulaz AL, Brisken C, Fiche M, Delorenzi M, Iggo R: **Identification of molecular apocrine breast tumours by microarray analysis.** *Oncogene* 2005, **24:**4660–4671.
19. Robinson JL, Macarthur S, Ross-Innes CS, Tilley WD, Neal DE, Mills IG, Carroll JS: **Androgen receptor driven transcription in molecular apocrine breast cancer is mediated by FoxA1.** *Embo J* 2011, **30:**3019–3027.
20. Ni M, Chen Y, Lim E, Wimberly H, Bailey ST, Imai Y, Rimm DL, Liu XS, Brown M: **Targeting androgen receptor in estrogen receptor-negative breast cancer.** *Cancer Cell* 2011, **20:**119–131.
21. Gucalp A, Tolaney S, Isakoff SJ, Ingle JN, Liu MC, Carey LA, Blackwell K, Rugo H, Nabell L, Forero A, Stearns V, Doane AS, Danso M, Moynahan ME, Momen LF, Gonzalez JM, Akhtar A, Giri DD, Patil S, Feigin KN, Hudis CA, Traina TA: **Phase II trial of bicalutamide in patients with androgen receptor-positive, estrogen receptor-negative metastatic Breast Cancer.** *Clin Cancer Res* 2013, **19:**5505–5512.
22. Masiello D, Cheng S, Bubley GJ, Lu ML, Balk SP: **Bicalutamide functions as an androgen receptor antagonist by assembly of a transcriptionally inactive receptor.** *J Biol Chem* 2002, **277:**26321–26326.
23. Small EJ, Carroll PR: **Prostate-specific antigen decline after casodex withdrawal: evidence for an antiandrogen withdrawal syndrome.** *Urology* 1994, **43:**408–410.
24. Scher HI, Fizazi K, Saad F, Taplin ME, Sternberg CN, Miller K, de Wit R, Mulders P, Chi KN, Shore ND, Armstrong AJ, Flaig TW, Flechon A, Mainwaring P, Fleming M, Hainsworth JD, Hirmand M, Selby B, Seely L, de Bono JS: **Increased survival with enzalutamide in prostate cancer after chemotherapy.** *N Engl J Med* 2012, **367:**1187–1197.
25. Jambal P, Badtke MM, Harrell JC, Borges VF, Post MD, Sollender GE, Spillman MA, Horwitz KB, Jacobsen BM: **Estrogen switches pure mucinous breast cancer to invasive lobular carcinoma with mucinous features.** *Breast Cancer Res Treat* 2013, **137:**431–448.
26. Magklara A, Brown TJ, Diamandis EP: **Characterization of androgen receptor and nuclear receptor co-regulator expression in human breast cancer cell lines exhibiting differential regulation of kallikreins 2 and 3.** *Int J Cancer* 2002, **100:**507–514.
27. Chamberlain NL, Driver ED, Miesfeld RL: **The length and location of CAG trinucleotide repeats in the androgen receptor N-terminal domain affect transactivation function.** *Nucleic Acids Res* 1994, **22:**3181–3186.
28. Birrell SN, Bentel JM, Hickey TE, Ricciardelli C, Weger MA, Horsfall DJ, Tilley WD: **Androgens induce divergent proliferative responses in human breast cancer cell lines.** *J Steroid Biochem Mol Biol* 1995, **52:**459–467.
29. Hall RE, Birrell SN, Tilley WD, Sutherland RL: **MDA-MB-453, an androgen-responsive human breast carcinoma cell line with high level androgen receptor expression.** *Eur J Cancer* 1994, **30A:**484–490.
30. Beyer C, McDonald P, Vidal N: **Failure of 5-alpha-dihydrotestosterone to elicit estrous behavior in the ovariectomized rabbit.** *Endocrinology* 1970, **86:**939–941.
31. McDonald P, Beyer C, Newton F, Brien B, Baker R, Tan HS, Sampson C, Kitching P, Greenhill R, Pritchard D: **Failure of 5alpha-dihydrotestosterone to initiate sexual behaviour in the castrated male rat.** *Nature* 1970, **227:**964–965.
32. Ryan KJ: **Biological aromatization of steroids.** *J Biol Chem* 1959, **234:**268–272.
33. Tran C, Ouk S, Clegg NJ, Chen Y, Watson PA, Arora V, Wongvipat J, Smith-Jones PM, Yoo D, Kwon A, Wasielewska T, Welsbie D, Chen CD, Higano CS, Beer TM, Hung DT, Scher HI, Jung ME, Sawyers CL: **Development of a second-generation antiandrogen for treatment of advanced prostate cancer.** *Science* 2009, **324:**787–790.
34. Lehmann BD, Bauer JA, Chen X, Sanders ME, Chakravarthy AB, Shyr Y, Pietenpol JA: **Identification of human triple-negative breast cancer subtypes and preclinical models for selection of targeted therapies.** *J Clin Invest* 2011, **121.**
35. Moore NL, Buchanan G, Harris JM, Selth LA, Bianco-Miotto T, Hanson AR, Birrell SN, Butler LM, Hickey TE, Tilley WD: **An androgen receptor mutation in the MDA-MB-453 cell line model of molecular apocrine breast cancer compromises receptor activity.** *Endocr Relat Cancer* 2012, **19:**599–613.
36. Wilson VS, Bobseine K, Lambright CR, Gray LE Jr: **A novel cell line, MDA-kb2, that stably expresses an androgen- and glucocorticoid-responsive reporter for the detection of hormone receptor agonists and antagonists.** *Toxicol Sci* 2002, **66:**69–81.
37. Kuenen-Boumeester V, Van der Kwast TH, Claassen CC, Look MP, Liem GS, Klijn JG, Henzen-Logmans SC: **The clinical significance of androgen receptors in breast cancer and their relation to histological and cell biological parameters.** *Eur J Cancer* 1996, **32A:**1560–1565.
38. Soreide JA, Lea OA, Varhaug JE, Skarstein A, Kvinnsland S: **Androgen receptors in operable breast cancer: relation to other steroid hormone receptors, correlations to prognostic factors and predictive value for effect of adjuvant tamoxifen treatment.** *Eur J Surg Oncol* 1992, **18:**112–118.
39. Garay JP, Park BH: **Androgen receptor as a targeted therapy for breast cancer.** *Am J Cancer Res* 2012, **2:**434–445.
40. Hickey TE, Robinson JL, Carroll JS, Tilley WD: **Minireview: the androgen receptor in breast tissues: growth inhibitor, tumor suppressor, oncogene?** *Mol Endocrinol* 2012, **26:**1252–1267.
41. Moe RE, Anderson BO: **Androgens and androgen receptors: a clinically neglected sector in breast cancer biology.** *J Surg Oncol* 2007, **95:**437–439.
42. Peters AA, Buchanan G, Ricciardelli C, Bianco-Miotto T, Centenera MM, Harris JM, Jindal S, Segara D, Jia L, Moore NL, Henshall SM, Birrell SN, Coetzee GA, Sutherland RL, Butler LM, Tilley WD: **Androgen receptor inhibits estrogen receptor-alpha activity and is prognostic in breast cancer.** *Cancer Res* 2009, **69:**6131–6140.
43. Poulin R, Baker D, Labrie F: **Androgens inhibit basal and estrogen-induced cell proliferation in the ZR-75-1 human breast cancer cell line.** *Breast Cancer Res Treat* 1988, **12:**213–225.
44. Macedo LF, Guo Z, Tilghman SL, Sabnis GJ, Qiu Y, Brodie A: **Role of androgens on MCF-7 breast cancer cell growth and on the inhibitory effect of letrozole.** *Cancer Res* 2006, **66:**7775–7782.
45. Cops EJ, Bianco-Miotto T, Moore NL, Clarke CL, Birrell SN, Butler LM, Tilley WD: **Antiproliferative actions of the synthetic androgen, mibolerone, in breast cancer cells are mediated by both androgen and progesterone receptors.** *J Steroid Biochem Mol Biol* 2008, **110:**236–243.
46. Garay JP, Karakas B, Abukhdeir AM, Cosgrove DP, Gustin JP, Higgins MJ, Konishi H, Konishi Y, Lauring J, Mohseni M, Wang GM, Jelovac D, Weeraratna A, Sherman Baust CA, Morin PJ, Toubaji A, Meeker A, De Marzo AM, Lewis G, Subhawong A, Argani P, Park BH: **The growth response to androgen receptor signaling in ERalpha-negative human breast cells is dependent on p21 and mediated by MAPK activation.** *Breast Cancer Res* 2012, **14:**R27.
47. Simon WE, Albrecht M, Trams G, Dietel M, Holzel F: **In vitro growth promotion of human mammary carcinoma cells by steroid hormones, tamoxifen, and prolactin.** *J Natl Cancer Inst* 1984, **73:**313–321.
48. Recchione C, Venturelli E, Manzari A, Cavalleri A, Martinetti A, Secreto G: **Testosterone, dihydrotestosterone and oestradiol levels in postmenopausal breast cancer tissues.** *J Steroid Biochem Mol Biol* 1995, **52:**541–546.
49. Swerdloff RS, Wang C: **Dihydrotestosterone: a rationale for its use as a non-aromatizable androgen replacement therapeutic agent.** *Baillieres Clin Endocrinol Metab* 1998, **12:**501–506.
50. Hall JM, Korach KS: **Stromal cell-derived factor 1, a novel target of estrogen receptor action, mediates the mitogenic effects of estradiol in ovarian and breast cancer cells.** *Mol Endocrinol* 2003, **17:**792–803.
51. Sauve K, Lepage J, Sanchez M, Heveker N, Tremblay A: **Positive feedback activation of estrogen receptors by the CXCL12-CXCR4 pathway.** *Cancer Res* 2009, **69:**5793–5800.
52. Kasina S, Macoska JA: **The CXCL12/CXCR4 axis promotes ligand-independent activation of the androgen receptor.** *Mol Cell Endocrinol* 2012, **351:**249–263.
53. Kang Z, Janne OA, Palvimo JJ: **Coregulator recruitment and histone modifications in transcriptional regulation by the androgen receptor.** *Mol Endocrinol* 2004, **18:**2633–2648.
54. Panet-Raymond V, Gottlieb B, Beitel LK, Pinsky L, Trifiro MA: **Interactions between androgen and estrogen receptors and the effects on their transactivational properties.** *Mol Cell Endocrinol* 2000, **167:**139–150.
55. Migliaccio A, Di Domenico M, Castoria G, Nanayakkara M, Lombardi M, de Falco A, Bilancio A, Varricchio L, Ciociola A, Auricchio F: **Steroid receptor**

regulation of epidermal growth factor signaling through Src in breast and prostate cancer cells: steroid antagonist action. *Cancer Res* 2005, **65:**10585–10593.

56. Joseph JD, Lu N, Qian J, Sensintaffar J, Shao G, Brigham D, Moon M, Maneval EC, Chen I, Darimont B, Hager JH: **A clinically relevant androgen receptor mutation confers resistance to second-generation antiandrogens enzalutamide and ARN-509.** *Cancer Discov* 2013, **3:**1020–1029.
57. Korpal M, Korn JM, Gao X, Rakiec DP, Ruddy DA, Doshi S, Yuan J, Kovats SG, Kim S, Cooke VG, Monahan JE, Stegmeier F, Roberts TM, Sellers WR, Zhou W, Zhu P: **An F876L Mutation in Androgen Receptor Confers Genetic and Phenotypic Resistance to MDV3100 (Enzalutamide).** *Cancer Discov* 2013, **3:**1030–1043.

doi:10.1186/bcr3599
Cite this article as: Cochrane *et al.*: Role of the androgen receptor in breast cancer and preclinical analysis of enzalutamide. *Breast Cancer Research* 2014 **16**:R7.

Multiple Molecular Subtypes of Triple Negative Breast Cancer Depend on Androgen Receptor for Proliferation and Invasion

Valerie N. Barton, Nicholas C. D'Amato, Michael A. Gordon, Hanne T. Lind, Nicole S. Spoelstra, Beatrice Babbs, Richard E. Heinz, Anthony Elias, Paul Jedlicka, Britta M. Jacobsen and Jennifer K. Richer

University of Colorado Anschutz Medical Campus, Department of Pathology, Aurora CO

Running title: Targeting Androgen Receptor in Triple Negative Breast Cancer

Keywords: triple negative breast cancer, androgen receptor, amphiregulin, enzalutamide, invasion

Funded by DOD BCRP Clinical Translational Award BC120183 to JKR and AE.

The authors disclose no potential conflicts of interest.

Word count: 4,130/5,000

Number of figures: 6

Number of tables: 0

Number of supplemental figures: 4

Number of supplemental tables: 0

Corresponding author: Jennifer K. Richer
Email: Jennifer.Richer@ucdenver.edu
Phone: 303-724-3735
Fax: 303-724-3712
RC1 North P18-5127 Mail Stop 8104
12800 E. 19th Ave
Aurora, CO 80045
Ph. 303 724-3735

Abstract

Triple negative breast cancer (TNBC) has the lowest five-year survival rate of invasive breast carcinomas. Currently, there are no targeted therapies for TNBC. Recent studies demonstrate that the androgen receptor (AR) is expressed in up to one third of TNBC. AR is highly expressed in the "luminal AR (LAR)" molecular TNBC subtype and we previously demonstrated that the anti-androgen enzalutamide (ENZ) effectively inhibits this TNBC subtype *in vivo*. However, AR is also present in the other TNBC molecular subtypes and may present a broader opportunity for targeted therapy. To test the hypothesis that non-LAR TNBC also critically depend on AR and that AR inhibition would decrease tumor burden in preclinical models of non-LAR TNBC, we utilized ENZ or shRNAs against AR. AR inhibition significantly reduced baseline proliferation, anchorage independent growth, migration and invasion, and increased apoptosis, in SUM159PT, HCC1806, BT549 and MDA-MB-231 cells. In SUM159PT and HCC1806, dihydrotestosterone and ENZ altered expression of the EGFR ligand amphiregulin (AREG), while treatment with exogenous AREG rescued decreased proliferation and migration of AR knockdown cell lines. This suggests that AR regulation of AREG is one mechanism by which AR influences proliferation, migration and invasion. *In vivo*, ENZ significantly decreased the viability of SUM159PT and HCC1806 xenografts. Together, our findings suggest that AR+ TNBC of multiple molecular subtypes depend on AR for proliferation and migratory/invasive capacity, and, moreover, that ENZ may be efficacious in non-LAR molecular subtypes of AR+ TNBC in the clinic.

Introduction

Triple negative breast cancer (TNBC) constitutes 10-20% of invasive breast carcinomas and has the lowest five-year survival rate compared to other breast cancer subtypes (1). In TNBC patients, 12-28% achieve a pathological complete response following neoadjuvant chemotherapy and have a better disease free and overall survival compared to TNBC patients with residual disease (2, 3). Importantly, TNBC patients with residual disease have a significantly worse overall survival than non-TNBC patients (2). The discrepancy in survival between TNBC and non-TNBC patients with residual disease is exacerbated by the absence of effective targeted therapy for TNBC. TNBC lacks estrogen receptor (ER) and progesterone receptor (PR) expression as well as HER2 amplification and thus is unresponsive to traditional endocrine or HER2 therapies that improve overall survival in other breast cancer (BC) subtypes. Although TNBC lacks the hormone receptors traditionally associated with BC, many TNBCs express other hormone receptors, including the glucocorticoid receptor (4) and androgen receptor (AR). AR, a ligand-activated nuclear hormone transcription factor (5), is expressed in 12-36% of TNBC (6-9).

A defining role for AR and AR-regulated genes in the molecular biology and classification of breast cancer was established by microarray profiling studies of invasive breast carcinomas, including TNBC (10-14). Lehmann *et al.* characterized TNBC as a heterogeneous disease with seven molecular subtypes, including unstable, basal-like 1, basal-like 2, mesenchymal-like, mesenchymal stem-like, immunomodulatory, and luminal AR (LAR). The LAR subtype is similar to previously characterized molecular apocrine tumors (12, 13, 15) and its gene expression profile and chromatin binding patterns mimic luminal, ER+ breast cancer despite being ER negative (11, 14). Within the TNBC molecular subtypes, LAR TNBC has the

highest AR expression (16) and thus preclinical research has predominately focused on the efficacy of AR-targeted therapy using LAR cell line models of AR+ TNBC.

Our group and others have demonstrated that the LAR cell line MDA-MB-453 is sensitive to androgens *in vitro* (17, 18) and *in vivo* (17). Xenograft studies with AR antagonists have also demonstrated that LAR SUM185PE, CAL-148 and MDA-MB-453 cell lines are sensitive to bicalutamide (14) or enzalutamide (ENZ) (17). Although there is strong preclinical data to suggest that LAR TNBC subtypes may benefit from AR-targeted therapy, other TNBC molecular subtypes express AR and may also benefit from treatment with AR antagonists.

A phase II trial of bicalutamide in ER-/PR-/AR+ metastatic breast cancer demonstrated a 19% clinical benefit rate (19) indicating that AR antagonists may be an effective targeted therapy for some AR+ TNBC patients. A phase II trial (NCT01889238) of the newer generation AR antagonist enzalutamide (ENZ), which blocks AR nuclear localization and is thus less likely to act as a partial agonist, is underway in TNBC. While the inclusion criteria for the current phase II trial of ENZ is 1% AR+ staining, most *in vitro* studies have focused on AR in LAR TNBC cell line models with very high AR expression and little is known about the role of AR or efficacy of ENZ in TNBC with lower AR expression. We hypothesized that non-LAR, AR+ TNBC may also critically depend on AR and could benefit from treatment with ENZ. Our study indicates that multiple subtypes of AR+ TNBC depend on AR for proliferation, migration and invasion, and tumor growth *in vivo*, and provides promising preclinical data on the efficacy of ENZ in TNBC with low AR expression.

Materials and Methods

Cell culture

All cell lines were authenticated by short tandem repeat analysis and tested negative for mycoplasma in July of 2014. Molecular subtypes of TNBC cell lines used in the present study were previously categorized by Lehmann *et al.* (14). SUM159PT cells were purchased from the University of Colorado Cancer Center Tissue Culture Core in August of 2013 and were grown in Ham's F-12 with 5% fetal bovine serum, penicillin/streptomycin, hydrocortisone, insulin, HEPES and L-glutamine supplementation. MD-MB-231 (MD231) cells were purchased from the ATCC in August of 2008 and were grown in minimum essential media with 5% fetal bovine serum, penicillin/streptomycin, HEPES, L-glutamine, non-essential amino acids and insulin supplementation. HCC1806 cells were obtained from the laboratory of Dr. Haihua Gu in 2011 and propagated in RPMI Medium 1640 with 10% fetal bovine serum and penicillin/streptomycin. BT549 cells, purchased from the ATCC in 2008, were grown in RPMI Medium 1640 with 10% fetal bovine serum, penicillin/streptomycin and insulin. All crystal violet were conducted in 5% charcoal-stripped serum to directly study the effect of DHT on cellular proliferation or transcription respectively. All other experiments were performed in full serum as described above with the exception of migration assays which were performed in serum-free conditions to prevent cellular proliferation.

SUM159PT-TGL and HCC1806-TGL cells were generated by stable retroviral transduction with a SFG-NES-TGL vector, encoding a triple fusion of thymidine kinase, green fluorescent protein and luciferase and sorted for green fluorescent protein. SUM159PT, HCC1806, BT549 and MDA231 AR knockdown cells were generated by lentiviral transduction of shRNAs targeting AR (pMISSION VSV-G, Sigma Aldrich; St Louis, MO), including AR

shRNA 3715 (shAR15) and AR shRNA 3717 (shAR17). Lentiviral transduction of pMISSION shRNA NEG (shNEG) was used as a non-targeting control. Plasmids were purchased from the University of Colorado Functional Genomics Core Facility.

Cellular Assays and Reagents

Cells were treated with 10 μM enzalutamide (ENZ, Medivation; San Francisco, CA), 10 nM dihydrotestosterone (DHT, Sigma Aldrich), and 1μg/ml recombinant human amphiregulin (AREG, R&D Systems; Minneapolis, MN). 10 μM ENZ approximates the IC_{50} of the four cell lines studied (data not shown) and is a clinically achievable, well-tolerated treatment concentration (NCT01889238). Androgen concentrations have been previously examined in breast cancer(20) and intratumoral DHT concentrations (249 pg/g) were significantly higher than in blood. The DHT concentration of the present study is consistent with other *in vitro* studies of DHT in breast cancer (18, 21), and approximates levels of circulating testosterone in obese, postmenopausal women (22) as well as DHT levels in fetal bovine serum used during routine tissue culture propagation (23).

Migration and invasion scratch wound assays were performed with or without BD Matrigel (BD Biosciences), respectively, per the manufacturer's instructions and scanned with the Incucyte ZOOM apparatus (Essen BioSciences; Ann Arbor, MI). When an attractant was required for invasion, trans-well invasion assays were performed with BD BioCoat Matrigel Invasion Chambers (BD Biosciences; Bedford MA) per the manufacturer's protocol. Caspase 3/7 fluorescent reagent (Essen BioSciences) was used at a dilution of 1:1000 and normalized to cell count (apoptotic index), following the manufacturer's protocol, to assess apoptosis *in vitro*. The Amphiregulin Human ELISA Kit (Abcam; Cambridge, MA) was used to measure extracellular AREG concentrations per the manufacturer's protocol.

For crystal violet assays, cells were fixed in 10% formalin, rinsed in PBS and stained with 5% crystal violet. Crystal violet was then dissolved in 10% acetic acid and measured at 540λ. MTS assays were performed with the CellTiter 96 Aqueous One Solution Cell Proliferation Assay (Promega; Madison, WI) according to the manufacturer's protocol. Proliferation assays were also performed using the Incucyte ZOOM imaging system (Essen BioSciences). Soft agar assays were performed in 0.5% bottom and 0.25% top layer agar (Difco Agar Noble, BD Biosciences).

Tumor studies

Xenograft experiments were approved by the University of Colorado Institutional Animal Care and Use Committee (IACUC protocol 83614(01)1E). All animal experiments were conducted in accordance with the National Institutes of Health Guidelines of Care and Use of Laboratory Animals. For both xenograft experiments, 10^6 SUM159PT-TGL or HCC1806-TGL cells were mixed with Matrigel (BD Biosciences; Franklin Lakes, New Jersey) and bilaterally injected into the fourth inguinal mammary fat pad of female, athymic nu/nu mice (Taconic; Germantown, NY). Tumor burden was assessed by luciferase activity and caliper measurements (tumor volume was calculated as volume=(length × width^2)/2). Once tumors were established, mice were randomized into groups based on the total tumor burden as measured by *in vivo* imaging. Mice were administered ENZ in their chow (approximately a 50 mg/kg daily dose). ENZ was mixed with ground mouse chow (Research Diets Inc.; New Brunswick, NJ) at 0.43 mg/g chow. The feed was irradiated and stored at 4°C before use. Mice in the control group received the same ground mouse chow but without ENZ. All mice were given free access to ENZ formulated chow or control chow during the study period. Two hours prior to sacrifice, mice were injected intraperitoneally with 50 mg/kg bromodeoxyuridine (Sigma-Aldrich). Mice

were euthanized by carbon dioxide asphyxiation followed by cervical dislocation, and the tumors, small intestine, and mammary glands were harvested.

Histology

Tissues were fixed in 10% neutral buffered formalin, and tissue processing and paraffin embedding was performed by either the UCDenver Tissue Biobanking and Processing Core or the UCH Anatomic Pathology Laboratory. Hematoxylin and Eosin stains were purchased from Anatech Ltd. (Battle Creek, MI) and used per the manufacturer's instructions.

Archival formalin-fixed paraffin-embedded primary breast tumors designated as hormone receptor negative and HER2 ≤ 10% were collected under the Institutional Review Board protocol Molecular and Cellular Predictors of Breast Cancer (#10-0755) from 125 women diagnosed Massachusetts General Hospital (Partners) between 1977 and 1993. Slides were immunostained for AR as described below and evaluated for the percentage and intensity of AR.

Immunohistochemistry

Slides were deparaffinized in a series of xylenes and ethanols, and antigens were heat retrieved in 10mM citrate buffer, pH 6.0. Tissue for BrdU was incubated in 2N HCl followed by 0.1M sodium borate following antigen retrieval. Antibodies used were AR clone 441 (Dakocytomation; Carpinteria, CA) and BrdU clone B44 (BD Biosciences). Envision horseradish peroxidase (Dakocytomation) was used for detection.

***In Situ* Hybridization**

Terminal deoxynucleotidyl transferase dUTP nick-end labeling (TUNEL) staining for apoptosis was performed using the ApopTag Plus Peroxidase *In Situ* Apoptosis Detection kit (Millipore; Billerica, MA), per the manufacturer's instructions.

Immunoblotting

Whole cell protein extracts (50 μg) were denatured, separated on SDS-PAGE gels and transferred to polyvinylidene fluoride membranes. After blocking in 3% bovine serum albumin in Tris-buffered saline–Tween, membranes were probed overnight at 4°C. Primary antibodies utilized include: AR (PG-21, 1:500 dilution; EMD Millipore, Darmstadt, Germany), TOPO1 (C-21, 1:100 dilution; Santa Cruz Biotechnology, Inc., Dallas, TX), p44/42 MAPK (4695, 1:1000; Cell Signaling Technology), phospho p44/42 MAPK (9101S, 1:500; Cell Signaling Technology) and α-TUBULIN (clone B-5-1-2, 1:30,000 dilution; Sigma Aldrich). Following secondary antibody incubation, results were detected using Western Lighting Chemiluminescence Reagent Plus (Perkin Elmer; Waltham, MA).

Cellular fractionation

Cellular fractionation was performed using the NE-PER Nuclear and Cytoplasmic Extraction Kit (Pierce Biotechnology; Rockford, IL) as per the manufacturer's instructions.

Real-time quantitative polymerase chain reaction

RNA was isolated by Trizol (Invitrogen; Grand Island, NY) and cDNA was synthesized from 1 μg total RNA, using M-Mulv reverse transcriptase enzyme (Promega; Fitchburg, WI). SYBR green quantitative gene expression analysis was performed using the following primers: *AREG* forward, 5-CGAACCACAAATACCTGGCTA-3′ and *AREG* reverse, 5′-TCCATTTTTGCCTCCCTTTT-3′; *βACTIN* forward, 5′-CTGTCCACCTTCCAGCAGATG-3′ and *βACTIN* reverse, 5′-CGCAACTAAGTCATAGTCCGC-3′; and *RPL13A* forward, 5′-CCTGGAGGAGAAGAGGAAAGAGA-3′ and *RPL13A* reverse, 5′-TTGAGGACCTCTGTGTATTTGTCAA-3′. Relative gene expression was calculated using the comparative cycle threshold method and values were normalized to *β-ACTIN* or *RPL13A*.

Statistical significance

Statistical significance was evaluated using a two-tailed student's t-test or ANOVA with GraphPad Prism software. A P-value of less than or equal to 0.05 was considered statistically significant.

Results

Androgen receptor is expressed in 22% of TNBC patient tumors and in multiple molecular subtypes of triple negative breast cancer.

We examined 125 hormone receptor negative, HER2 ≤ 10% positive (negative by College of American Pathology (CAP) and FDA criteria) breast cancers for the presence of androgen receptor (AR). In this group of tumors, 22% showed some nuclear staining (range 1-100%). The presence of AR positive tumor nuclei strongly correlated with older patients using the Pearson Product Moment correlation ($r = 0.383$, $p < 0.0001$). There was a modest correlation between tumors from older patients with lower measures of proliferation (MIB-1 $r = -0.230$, $p = 0.0121$ and mitoses/10hpf $r = -0.204$, $P = 0.0255$). Representative images with a range of AR expression are displayed in Fig. 1A. Nuclear AR expression indicates that AR may be ligand-bound and transcriptionally active in AR+ TNBC. Our findings are consistent with earlier studies which have reported AR protein expression in 12-36% of TNBC (6-9).

Previously, Lehmann *et al.* report that TNBC is a heterogeneous disease with the highest AR mRNA and protein expression within the luminal AR molecular subtype (LAR) of TNBC (14). However, AR is also expressed in cell lines representing the basal-like 1 and 2 (BL1, BL2), mesenchymal-like (ML), and mesenchymal stem-like (MSL) TNBC molecular subtypes (Fig. 1B) and may also present an opportunity for targeted therapy in these subtypes. In two non-LAR TNBC cell lines, treatment with DHT increased AR nuclear localization, while ENZ, which blocks AR nuclear localization, inhibited this effect (Fig. 1C). These findings suggest that AR nuclear localization is blocked by ENZ in non-LAR molecular subtypes and that AR is expressed in cell lines representing multiple molecular subtypes of TNBC in addition to the LAR subtype.

Androgen receptor inhibition decreases baseline proliferation and increases apoptosis in AR+ TNBC.

Androgen receptor inhibition was studied in four cell lines representing non-LAR TNBC subtypes including SUM159PT (MSL), HCC1806 (BL2), BT549 (ML) and MDA231 (MSL). By crystal violet staining, DHT increased baseline proliferation of the SUM159PT cell line and ENZ significantly decreased ligand-mediated and baseline proliferation in charcoal-stripped serum (Fig. 2A, $P<0.01$). Interestingly, ENZ decreased baseline proliferation of HCC1806, BT549 and MDA231, but DHT did not increase baseline proliferation in these cell lines. ENZ also increased caspase 3/7 activity compared to vehicle control (Fig. 2B, $P<0.001$). In soft agar, ENZ significantly decreased colony formation compared to vehicle control in full serum conditions (Fig. 2C), suggesting that ENZ decreases anchorage-independent growth and may decrease tumorigenicity *in vivo*.

To confirm that the effects of ENZ are specific to AR inhibition, we examined the effects of shRNAs specifically targeting AR (shAR15, shAR17) compared to a non-targeting control (shNEG). Transduction of shRNAs targeting AR decreased AR protein expression and significantly reduced proliferation in an MTS assay in four non-LAR TNBC cell lines (Fig. 3A-C). By crystal violet assay, AR knockdown significantly inhibited baseline and ligand-mediated proliferation of SUM159PT cells indicating that the shRNAs are effectively targeting AR (Fig. 3C). The SUM159PT cell line was chosen for this assay because DHT increases its baseline proliferation *in vitro*. AR knockdown also increased apoptosis in all four cell lines as measured by cleaved-caspase 3 activity (Fig. 3D).

Enzalutamide decreases tumor viability *in vivo*.

Luciferase-tagged SUM159PT-TGL cells, representing the MSL TNBC subtype, were bilaterally injected into the mammary fat pads of immune-compromised mice and treated with ENZ or vehicle control (Veh) following randomization when the tumors reached 50 mm^3 (Day -1, Supplementary Fig. S1A and S1B). ENZ significantly decreased luciferase activity on day 35 (P=0.008, Fig. 4A-C). While no significant differences between caliper measurements or tumor weights were found between treatment groups (Supplementary Fig. S2A, S2B, and S2C), hematoxylin and eosin (H&E) staining demonstrated that the median percentage of necrotic tumor was 90% in the ENZ treatment group compared to 10% in Veh xenografts (P=0.009, Fig. 4D). ENZ-treated xenografts also exhibited a four-fold increase in TUNEL staining, compared to vehicle-treated controls (P=0.04, Fig. 4E).

As in the SUM159PT xenograft study, luciferase-tagged HCC1806-TGL cells, which represent the BL2 TNBC subtype, were bilaterally injected into the mammary fat pads of immune compromised mice and treated with ENZ or Veh following randomization (Supplementary Fig. S1C and S1D). ENZ significantly decreased luciferase activity on day 14 (P=0.041, Supplementary Fig. S3A-S3C). HCC1806 xenografts grew at a faster rate than SUM159PT xenografts, resulting in early termination of the study on day 14 and relatively higher necrosis in both treatment groups. However, by H&E staining, ENZ-treated xenografts had a significant increase in percent necrotic tumor (Supplementary Fig. S3D). No significant differences between caliper measurements or tumor weights were found between treatment groups (Supplementary Fig. S2D-S2F). In summary, our results show that ENZ decreases cellular viability while increasing necrosis and apoptosis *in vivo* in multiple non-LAR molecular subtypes of TNBC in addition to the LAR MDA-MB-453 cell line previously reported (17).

Androgen receptor inhibition alters cellular morphology and decreases migration and invasion.

AR knockdown altered cellular morphology of BT549 and MDA231 cells in 3D Matrigel (BD Biosciences) culture from stellate to round (Fig. 5A). In a scratch wound assay, AR knockdown significantly decreased migration compared to a non-targeting control in four AR+ non-LAR cell lines (Fig. 5B). Scratch wound assays were conducted in serum-starved, attractant-free conditions and over a short time course to minimize potential confounding effects of AR knockdown on cell proliferation. MDA231 and BT549 cell lines invade through Matrigel without an attractant and AR knockdown in these cell lines inhibited invasion (Fig. 5C). Changes in cellular morphology and decreased migration and invasion were next examined in BT549 cells treated with ENZ. In 3D Matrigel, cellular morphology was altered from predominately stellate to predominately round (Fig. 5D), and migration (Fig. 5E left) and invasion (Fig. 5E right) were significantly inhibited by ENZ. In identical serum-starved conditions, BT549 control wells treated with ENZ and cleaved-caspase reagent (Essen BioSciences) exhibited no changes in proliferation or apoptosis (Supplementary Fig.S4), demonstrating that AR influences migration independently of proliferation or apoptosis.

Amphiregulin is regulated by androgen receptor in TNBC and rescues decreased proliferation and migration associated with androgen receptor inhibition.

By microarray and AR chromatin immunoprecipitation of an immortalized human prostate epithelial cell line, Bolton *et al.* identified amphiregulin (AREG) as an AR-regulated gene (24). AREG is required for mammary ductal morphogenesis and is the predominant epidermal growth factor receptor (EGFR) ligand during mammary gland development (25). To date, AR is not

known to regulate AREG in breast cancer or normal breast tissue. However, within TNBC, AR expression correlates with activated EGFR (26). We thus hypothesized that AR may regulate AREG in TNBC.

By quantitative real-time PCR (qRTPCR), treatment with ENZ decreased *AREG* mRNA expression in by 2-fold in SUM159PT and 4-fold in HCC1806 ($P<0.001$, Fig. 6A). At the protein level, treatment with DHT significantly increased secreted AREG by ELISA in both SUM159PT and HCC1806 ($P<0.05$, Fig. 6B). EGFR activation by AREG induces multiple downstream signaling pathways including MAPK (16). Compared to non-targeting controls, AR knockdown decreased endogenous phosphorylation of ERK while exogenous AREG rescued this effect in HCC1806 (Fig. 6C). These results were recapitulated in the SUM159PT cell line (data not shown).

Given our data suggesting that AR regulates AREG which activates the MAPK signaling pathway with key roles in proliferation, migration and invasion(27), we next tested whether exogenous AREG would rescue the phenotypes associated with AR inhibition. As in Figure 4B, AR knockdown significantly inhibited proliferation of HCC1806 compared to non-targeting controls, and the addition of exogenous AREG partially rescued this effect ($P<0.0001$, Fig. 6D). Similarly, AR knockdown decreased migration of HCC1806 cells (as in Fig. 5B) and exogenous AREG partially rescued this effect (Fig. 6E, left) without altering proliferation in these serum-free conditions (Fig. 6E, right). Exogenous AREG also partially rescued proliferation and invasion in SUM159PT (data not shown). Together, these data indicate that AR regulation of AREG is one mechanism by which AR effects proliferation, migration and invasion in AR+ TNBC.

Discussion

Compared to non-TNBC patients, TNBC patients with residual disease following chemotherapy have a significantly worse overall survival (2). The poor prognosis of TNBC patients is due, in part, to a lack of effective targeted therapy. However, AR is expressed in up to a third of TNBC patients (6-9) and represents an opportunity for targeted therapy. Indeed, if AR-targeted therapy is effective in AR+ TNBC, it would represent the first effective targeted therapy for this aggressive breast cancer subtype and would greatly benefit this population of women. Previous studies focused on the role of AR in the high AR-expressing, LAR molecular subtype of TNBC and found that they were responsive to bicalutamide, while the non-LAR subtypes were less responsive or non-responsive (14). In contrast, we find that multiple non-LAR subtypes with relatively low AR expression critically depend on AR for proliferation, migration and invasion and that even those previously found to be resistant to bicalutamide are sensitive to the new-generation anti-androgen ENZ *in vitro* and *in vivo*.

In TNBC cell lines representing the "mesenchymal-like," "mesenchymal stem-like," and "basal-like" molecular subtypes (14), pharmacological inhibition of AR with ENZ and AR knockdown decreased proliferation and anchorage-independent growth, and increased apoptosis. Thus, AR may be required for optimal baseline proliferation even though DHT does not increase proliferation in all AR+ TNBC cell lines. The discordance between baseline inhibition and lack of ligand-mediated proliferation in some cell lines may indicate that the mechanism by which AR mediates proliferation in TNBC is non-transcriptional or ligand-independent in some cell lines.

Decreased proliferation and increased apoptosis by AR inhibition *in vitro* was recapitulated in SUM159PT and HCC1806 xenografts in nude mice. Sensitivity of SUM159PT xenografts to ENZ contrasts previous work demonstrating that bicalutamide did not inhibit tumor

volume (14). The discrepancy in results may be due to differences in the mechanisms of action of the two AR antagonists. Bicalutamide permits AR nuclear localization and binding to chromatin, recruiting co-repressors rather than co-activators, while ENZ inhibits nuclear localization and DNA binding (28). Bicalutamide has partial agonist effects in prostate cancer (29), and thus may also have partial agonist effects in TNBC. However, it should be noted that ENZ significantly increased tumor necrosis but did not decrease tumor volume according to caliper measurements. Thus, an increase in necrosis may not have been apparent in the bicalutamide study by measurement of tumor volume alone.

A phase II clinical trial of bicalutamide in AR+/ER-/PR- metastatic breast cancer reported a 19% clinical benefit rate and a 12 week longer median progression free survival (19). Of note, the study included HER2 amplified patients and required 10% AR positive staining for trial eligibility. However, bicalutamide has partial agonist effects (29) and prostate cancer patients who acquire resistance to bicalutamide often respond to ENZ (30), suggesting that ENZ may also be a more effective antagonist in TNBC. The results of the present study are promising and timely as a phase II clinical trial is currently testing the efficacy of ENZ in AR+ TNBC (NCT01889238). Importantly, we find that non-LAR subtypes critically depend on AR, perhaps indicating that patients with relatively low AR expression may also benefit from AR-targeted therapy. The trial has recently expanded patient eligibility to 1% AR+ staining, which may greatly improve the number of patients eligible for treatment.

In vitro, AR inhibition altered cellular morphology and decreased migration and invasion suggesting that AR+ TNBC is also dependent on AR for these functions. Extensive evidence suggests that advanced, metastatic prostate cancer is causally related to continued AR activation (5) and recent prostate and bladder cancer studies demonstrate that AR regulates multiple

metastasis-promoting genes (31-33). In breast cancer, initial surgically resected breast cancer metastases retain nuclear AR expression as in the primary tumor (34). Interestingly, breast cancer metastases, including those in TNBC patients, also have significantly increased AR phosphorylation (35), indicative of active receptors.

Multiple studies have demonstrated that AR expression is associated with an overall favorable prognosis in breast cancer including the TNBC subtype (8, 36-38). However, this is not surprising because like ER, AR is indicative of a more well-differentiated form of the disease, but may still drive tumor growth and therefore serve as a rational therapeutic target. High AR expression may be indicative of a more luminal, well-differentiated, less aggressive tumor, and this confers a good prognosis. Future studies are needed to further characterize the role of AR in breast cancer metastasis and determine if AR-targeted therapy will reduce metastatic burden in preclinical models of TNBC.

Treatment with AREG, an EGFR ligand with critical roles in normal mammary gland development, partially rescued decreased proliferation, migration and invasion resulting from AR knockdown. Thus, AR regulation of AREG may be one mechanism by which AR mediates these critical functions and AR antagonists may also indirectly target EGFR signaling. Recent clinical trials demonstrate that treatment with the anti-EGFR antibody cetuximab in addition to chemotherapy may benefit patients with metastatic breast cancer (39, 40). *In vitro* data suggests that combined AR antagonist and EGFR or ERK1/2 inhibitors may be effective in TNBC (26). Exogenous AREG only partially rescued phenotypes associated with AR inhibition suggesting that additional AR-regulated genes are also involved in these phenotypes.

Although extensive genomic studies to identify novel therapeutic strategies have expanded our knowledge of the diverse molecular biology of TNBC, there are currently no

effective targeted therapies for TNBC patients. The present study demonstrates that multiple molecular subtypes of TNBC depend on AR for critical cancer phenotypes. Despite heterogeneity among tumors, hormone receptor-targeted therapies have greatly improved the prognosis of multiple hormone-related malignancies and exploiting AR dependence with AR-targeted therapies may ultimately improve TNBC patient prognosis.

Disclosure of Potential Conflicts of Interest

The authors declare no conflicts of interest.

Grant Support

This work was supported by Department of Defense BCRP Clinical Translational Award BC120183 to JKR and AE. Enzalutamide was provided by Astellas and Medivation.

Acknowledgments

We wish to acknowledge the Shared Resources at University of Colorado Denver Anschutz Medical Campus and the Cancer Center NCI Support Grant (P30CA046934).

Figure 1. Androgen receptor expression and nuclear localization in triple negative breast cancer patient samples and cell lines. A, Immunohistochemistry (IHC) of androgen receptor (AR) protein expression (brown) in a panel of triple negative breast cancer (TNBC) patient samples. Photomicrographs represent a 400X magnification. B, Western blot for AR expression in a panel of TNBC cell lines representing multiple molecular subtypes of triple negative breast cancer (TNBC) including basal-like 2 (BL2), mesenchymal stem-like (MSL), and mesenchymal-like (ML) (14). The prostate cancer cell line LNCaP is shown as a positive control for AR. C, Nuclear-cytoplasmic fractionation of TNBC cell lines grown in 5% charcoal stripped serum for 48 hours and following a three hour treatment with vehicle control (Veh), enzalutamide (ENZ), and/or dihydrotestosterone (DHT). Topoisomerase I (TOPOI) is a loading control for the nuclear fraction and α-TUBULIN is a loading control for the cytosolic fraction.

Figure 2. Enzalutamide decreases proliferation and anchorage independent growth and increases apoptosis in cell line models of multiple triple negative breast cancer molecular subtypes. A, Crystal violet assay of triple negative breast cancer (TNBC) cell lines treated with vehicle control (Veh), enzalutamide (ENZ), and/or dihydrotestosterone (DHT) in 5% charcoal-stripped serum for 5-10 days. B, Apoptotic index (green count/nuclear red count) of nuclear red SUM159PT and BT549 cell lines treated with Veh (open circle) or ENZ (solid square) and green fluorescent caspase 3/7 reagent and imaged on the Incucyte ZOOM (Essen BioSciences). C, Soft agar assays of TNBC cell lines treated with Veh or ENZ in full serum, stained with nitro blue tetrazolium, and quantified using pixel contrast analysis. *P<0.05, **P<0.01, ***P<0.001 and error bars represent standard deviations.

Figure 3. Androgen receptor knockdown inhibits baseline and ligand-mediated proliferation and increases apoptosis in triple negative breast cancer. A, Western blot of triple negative breast cancer (TNBC) cell lines infected with shRNAs targeting AR (shAR15, shAR17) compared to a non-targeting control (shNEG). B, MTS assays of transduced TNBC cell lines. C, Crystal violet assay of transduced SUM159PT shNEG or shAR15/shAR17 cells treated one week with vehicle control (Veh), enzalutamide (ENZ), and/or dihydrotestosterone (DHT). D, Changes in apoptosis in AR knockdown cells measured with cleaved-caspase reagent (Essen BioSciences) and normalized to cell count (apoptotic index) at 42 hours. Staurosporine (SSP) was used a positive control for apoptosis.* $P<0.05$, ***$P<0.001$ by ANOVA and error bars represent standard deviations.

Figure 4. Enzalutamide decreases cellular viability and increases necrosis and apoptosis in SUM159PT xenografts. A, Total flux growth curve of SUM159PT nude mice xenografts bilaterally injected into the mammary fat pads. Mice were randomized at day -1 and treatment was initiated on day 0. P-value represents a two-tailed t-test comparing total flux between groups on day 35 and error bars represent standard error of the mean. B, Change in total flux between randomization and day 35, by mouse. C, Luminescent overlay of Veh and ENZ treated mice. D, Percent necrotic tissue by hematoxylin and eosin (H&E) staining was scored by a pathologist blinded to sample identity. Horizontal bars represent median percentage necrotic tissue. P-value represents a two-tailed t-test comparing percent necrosis between groups on day 35. Photomicrographs depict examples of tumor xenograft H&E staining showing viable tumor (Veh) and necrotic tumor (ENZ). E, Terminal deoxynucleotidyl transferase dUTP nick-end labeling (TUNEL) staining for apoptosis. Photomicrographs depict examples of TUNEL staining. *$P<0.05$ and error bars represent standard error of the mean.

Figure 5. Androgen receptor inhibition decreases migration and invasion of triple negative breast cancer cells. A, Cellular morphology (200X) of BT549 cells transduced with a non-targeting control (shNEG) compared to a shRNA targeting androgen receptor (AR, shAR15) in 3D Matrigel culture. Arrow exhibits stellate cellular morphology. B, Migration scratch wound assay of triple negative breast cancer (TNBC) cell lines with AR knockdown under serum-starved conditions. C, Scratch wound assay of TNBC AR knockdown cell lines invading through Matrigel. D, Changes in cellular morphology of BT549 cells treated with enzalutamide (ENZ) in 3D Matrigel culture (200X). E, Migration (left) and invasion (right) assays of BT549 cells treated with ENZ. **P<0.01, ***P<0.001 by t-test at the final time point.

Figure 6. AR regulation of amphiregulin mediates baseline proliferation and migration of TNBC. A, Quantitative real-time PCR (qRTPCR) for amphiregulin (AREG) in SUM159PT cells after 24 hours (microarray experiment time point) and 48 hours of treatment with enzalutamide (ENZ) in full serum. qRTPCR for AREG in HCC1806 cells following 4 and 8 hours of treatment with ENZ in full serum. B, ELISA for extracellular AREG in SUM159PT and HCC1806 cell lines treated with dihydrotestosterone (DHT) for 48 and 72 hours respectively. C, Western blot of HCC1806 shNEG and shAR15 cells treated for thirty minutes with exogenous human recombinant AREG and probed for phospho-ERK (pERK), ERK or AR. α-TUBULIN is shown as a loading control. D, Proliferation assay of HCC1806 shNEG and shAR15 cells in the presence of exogenous AREG. E, Migration (left) and proliferation (right) assays of HCC1806 cells treated with exogenous AREG in identical, serum starved conditions. F) AREG protein expression by IHC in SUM159PT xenografts. Photomicrographs depict representative AREG staining (400X). *P<0.05, ***P<0.001 by t-test.

Supplementary Figure S1. Total flux and caliper measurements of SUM159PT and HCC1806 xenografts at randomization. A, SUM159PT caliper measurements at randomization. B, Total flux of SUM159PT xenografts at randomization. C, HCC1806 caliper measurements at randomization. D, Total flux of HCC1806 xenografts at randomization.

Supplementary Figure S2. Enzalutamide does not significantly decrease caliper volume or tumor weight of SUM159PT and HCC1806 xenografts. A, Caliper measurements of SUM159PT xenografts over time. B, Tumor volume of vehicle control and enzalutamide (Enza) treated SUM159PT xenografts at day 35 (P=0.22). C, Weight of extracted SUM159PT xenografts by treatment group. D, Caliper measurements of HCC1806 xenografts over time. E, Tumor volume of vehicle control and enzalutamide (Enza) treated HCC1806 xenografts at day 14 (P=0.12). F, Weight of extracted HCC1806 xenografts by treatment group.

Supplementary Figure S3. Enzalutamide decreases cellular viability in HCC1806 xenografts. A, Total flux growth curve of HCC1806 nude mice xenografts bilaterally injected into the mammary fat pads. Mice were randomized at day 0 and treatment was initiated with 10 mg/kg enzalutamide (ENZ) or vehicle control chow (Veh). P-value represents a two-tailed t-test comparing total flux between groups on day 14. B, Change in total flux between randomization and day 14 by mouse. C, Luminescent overlay of Veh and ENZ treated mice at day 14. D, Percent necrotic tissue by hematoxylin and eosin (H&E) staining. Horizontal bars represent mean percentage necrotic tissue. P-value represents a two-tailed t-test comparing percent necrosis between groups on day 14. Photomicrographs depict examples of tumor xenograft H&E staining showing viable tumor (Veh) and necrotic tissue (ENZ).

Supplementary Figure S4. No change in proliferation or apoptosis between enzalutamide and vehicle control groups during the migration assay. A) Nuclear red counts of BT549 cells on control, non-scratched plate over the duration of the migration assay. B) Apoptosis as measured using a cleaved-caspase reagent and normalized to nuclear red count (apoptotic index).

References

1. Dent R, Trudeau M, Pritchard KI, Hanna WM, Kahn HK, Sawka CA, et al. Triple-negative breast cancer: clinical features and patterns of recurrence. Clinical cancer research : an official journal of the American Association for Cancer Research. 2007;13:4429-34.
2. Liedtke C, Mazouni C, Hess KR, Andre F, Tordai A, Mejia JA, et al. Response to neoadjuvant therapy and long-term survival in patients with triple-negative breast cancer. Journal of clinical oncology : official journal of the American Society of Clinical Oncology. 2008;26:1275-81.
3. Cortazar P, Zhang L, Untch M, Mehta K, Costantino JP, Wolmark N, et al. Pathological complete response and long-term clinical benefit in breast cancer: the CTNeoBC pooled analysis. Lancet. 2014;384:164-72.
4. Skor MN, Wonder EL, Kocherginsky M, Goyal A, Hall BA, Cai Y, et al. Glucocorticoid receptor antagonism as a novel therapy for triple-negative breast cancer. Clinical cancer research : an official journal of the American Association for Cancer Research. 2013;19:6163-72.
5. Lonergan PE, Tindall DJ. Androgen receptor signaling in prostate cancer development and progression. J Carcinog. 2011;10:20.
6. Collins LC, Cole KS, Marotti JD, Hu R, Schnitt SJ, Tamimi RM. Androgen receptor expression in breast cancer in relation to molecular phenotype: results from the Nurses' Health Study. Modern pathology : an official journal of the United States and Canadian Academy of Pathology, Inc. 2011;24:924-31.
7. Mrklic I, Pogorelic Z, Capkun V, Tomic S. Expression of androgen receptors in triple negative breast carcinomas. Acta Histochem. 2013;115:344-8.
8. Thike AA, Yong-Zheng Chong L, Cheok PY, Li HH, Wai-Cheong Yip G, Huat Bay B, et al. Loss of androgen receptor expression predicts early recurrence in triple-negative and basal-like breast cancer. Mod Pathol. 2014;27:352-60.
9. Safarpour D, Pakneshan S, Tavassoli FA. Androgen receptor (AR) expression in 400 breast carcinomas: is routine AR assessment justified? American journal of cancer research. 2014;4:353-68.
10. Guedj M, Marisa L, de Reynies A, Orsetti B, Schiappa R, Bibeau F, et al. A refined molecular taxonomy of breast cancer. Oncogene. 2012;31:1196-206.
11. Robinson JL, Macarthur S, Ross-Innes CS, Tilley WD, Neal DE, Mills IG, et al. Androgen receptor driven transcription in molecular apocrine breast cancer is mediated by FoxA1. The EMBO journal. 2011;30:3019-27.
12. Doane AS, Danso M, Lal P, Donaton M, Zhang L, Hudis C, et al. An estrogen receptor-negative breast cancer subset characterized by a hormonally regulated transcriptional program and response to androgen. Oncogene. 2006;25:3994-4008.
13. Farmer P, Bonnefoi H, Becette V, Tubiana-Hulin M, Fumoleau P, Larsimont D, et al. Identification of molecular apocrine breast tumours by microarray analysis. Oncogene. 2005;24:4660-71.
14. Lehmann BD, Bauer JA, Chen X, Sanders ME, Chakravarthy AB, Shyr Y, et al. Identification of human triple-negative breast cancer subtypes and preclinical models for selection of targeted therapies. The Journal of clinical investigation. 2011;121:2750-67.
15. Teschendorff AE, Miremadi A, Pinder SE, Ellis IO, Caldas C. An immune response gene expression module identifies a good prognosis subtype in estrogen receptor negative breast cancer. Genome Biol. 2007;8:R157.
16. Stern KA, Place TL, Lill NL. EGF and amphiregulin differentially regulate Cbl recruitment to endosomes and EGF receptor fate. The Biochemical journal. 2008;410:585-94.

17. Cochrane DR, Bernales S, Jacobsen BM, Cittelly DM, Howe EN, D'Amato NC, et al. Role of the androgen receptor in breast cancer and preclinical analysis of enzalutamide. Breast cancer research : BCR. 2014;16:R7.
18. Ni M, Chen Y, Lim E, Wimberly H, Bailey ST, Imai Y, et al. Targeting androgen receptor in estrogen receptor-negative breast cancer. Cancer cell. 2011;20:119-31.
19. Gucalp A, Tolaney S, Isakoff SJ, Ingle JN, Liu MC, Carey LA, et al. Phase II trial of bicalutamide in patients with androgen receptor-positive, estrogen receptor-negative metastatic Breast Cancer. Clinical cancer research : an official journal of the American Association for Cancer Research. 2013;19:5505-12.
20. Recchione C, Venturelli E, Manzari A, Cavalleri A, Martinetti A, Secreto G. Testosterone, dihydrotestosterone and oestradiol levels in postmenopausal breast cancer tissues. The Journal of steroid biochemistry and molecular biology. 1995;52:541-6.
21. Peters AA, Ingman WV, Tilley WD, Butler LM. Differential effects of exogenous androgen and an androgen receptor antagonist in the peri- and postpubertal murine mammary gland. Endocrinology. 2011;152:3728-37.
22. Gallicchio L, Macdonald R, Wood B, Rushovich E, Helzlsouer KJ. Androgens and musculoskeletal symptoms among breast cancer patients on aromatase inhibitor therapy. Breast cancer research and treatment. 2011;130:569-77.
23. Sedelaar JP, Isaacs JT. Tissue culture media supplemented with 10% fetal calf serum contains a castrate level of testosterone. The Prostate. 2009;69:1724-9.
24. Bolton EC, So AY, Chaivorapol C, Haqq CM, Li H, Yamamoto KR. Cell- and gene-specific regulation of primary target genes by the androgen receptor. Genes & development. 2007;21:2005-17.
25. Aupperlee MD, Leipprandt JR, Bennett JM, Schwartz RC, Haslam SZ. Amphiregulin mediates progesterone-induced mammary ductal development during puberty. Breast Cancer Res. 2013;15:R44.
26. Cuenca-Lopez MD, Montero JC, Morales JC, Prat A, Pandiella A, Ocana A. Phospho-kinase profile of triple negative breast cancer and androgen receptor signaling. BMC cancer. 2014;14:302.
27. Dhillon AS, Hagan S, Rath O, Kolch W. MAP kinase signalling pathways in cancer. Oncogene. 2007;26:3279-90.
28. Osguthorpe DJ, Hagler AT. Mechanism of androgen receptor antagonism by bicalutamide in the treatment of prostate cancer. Biochemistry. 2011;50:4105-13.
29. Kemppainen JA, Wilson EM. Agonist and antagonist activities of hydroxyflutamide and Casodex relate to androgen receptor stabilization. Urology. 1996;48:157-63.
30. Scher HI, Fizazi K, Saad F, Taplin ME, Sternberg CN, Miller K, et al. Increased survival with enzalutamide in prostate cancer after chemotherapy. The New England journal of medicine. 2012;367:1187-97.
31. Yin JJ, Liu YN, Tillman H, Barrett B, Hewitt S, Ylaya K, et al. AR-regulated TWEAK-FN14 Pathway Promotes Prostate Cancer Bone Metastasis. Cancer Res. 2014.
32. Jacob S, Nayak S, Fernandes G, Barai RS, Menon S, Chaudhari UK, et al. Androgen receptor as a regulator of ZEB2 expression and its implications in epithelial-to-mesenchymal transition in prostate cancer. Endocr Relat Cancer. 2014;21:473-86.
33. Jing Y, Cui D, Guo W, Jiang J, Jiang B, Lu Y, et al. Activated androgen receptor promotes bladder cancer metastasis via Slug mediated epithelial-mesenchymal transition. Cancer Lett. 2014;348:135-45.
34. Cimino-Mathews A, Hicks JL, Illei PB, Halushka MK, Fetting JH, De Marzo AM, et al. Androgen receptor expression is usually maintained in initial surgically resected breast cancer metastases but is often lost in end-stage metastases found at autopsy. Human pathology. 2012;43:1003-11.
35. Ren Q, Zhang L, Ruoff R, Ha S, Wang J, Jain S, et al. Expression of androgen receptor and its phosphorylated forms in breast cancer progression. Cancer. 2013;119:2532-40.

36. Peters KM, Edwards SL, Nair SS, French JD, Bailey PJ, Salkield K, et al. Androgen receptor expression predicts breast cancer survival: the role of genetic and epigenetic events. BMC Cancer. 2012;12:132.
37. Agoff SN, Swanson PE, Linden H, Hawes SE, Lawton TJ. Androgen receptor expression in estrogen receptor-negative breast cancer. Immunohistochemical, clinical, and prognostic associations. Am J Clin Pathol. 2003;120:725-31.
38. Luo X, Shi YX, Li ZM, Jiang WQ. Expression and clinical significance of androgen receptor in triple negative breast cancer. Chin J Cancer. 2010;29:585-90.
39. Baselga J, Gomez P, Greil R, Braga S, Climent MA, Wardley AM, et al. Randomized phase II study of the anti-epidermal growth factor receptor monoclonal antibody cetuximab with cisplatin versus cisplatin alone in patients with metastatic triple-negative breast cancer. Journal of clinical oncology : official journal of the American Society of Clinical Oncology. 2013;31:2586-92.
40. Nechushtan H, Vainer G, Stainberg H, Salmon AY, Hamburger T, Peretz T. A phase 1/2 of a combination of Cetuximab and Taxane for "triple negative" breast cancer patients. Breast. 2014;23:435-8.

A

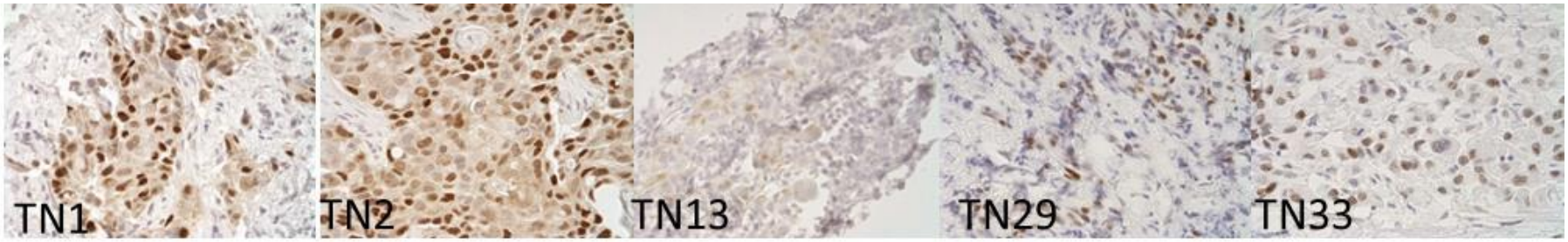
TN1
TN2
TN13
TN29
TN33

B

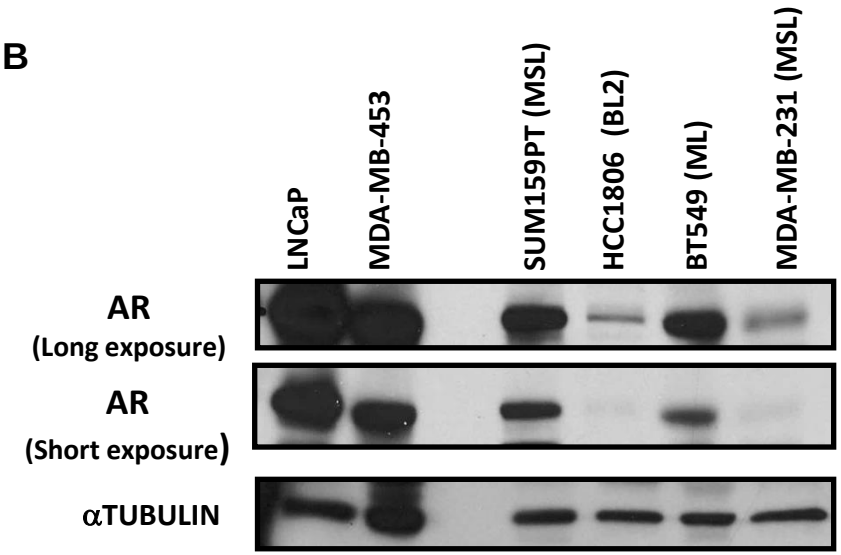
LNCaP
MDA-MB-453
SUM159PT (MSL)
HCC1806 (BL2)
BT549 (ML)
MDA-MB-231 (MSL)
AR
(Long exposure)
AR
(Short exposure)
αTUBULIN

C

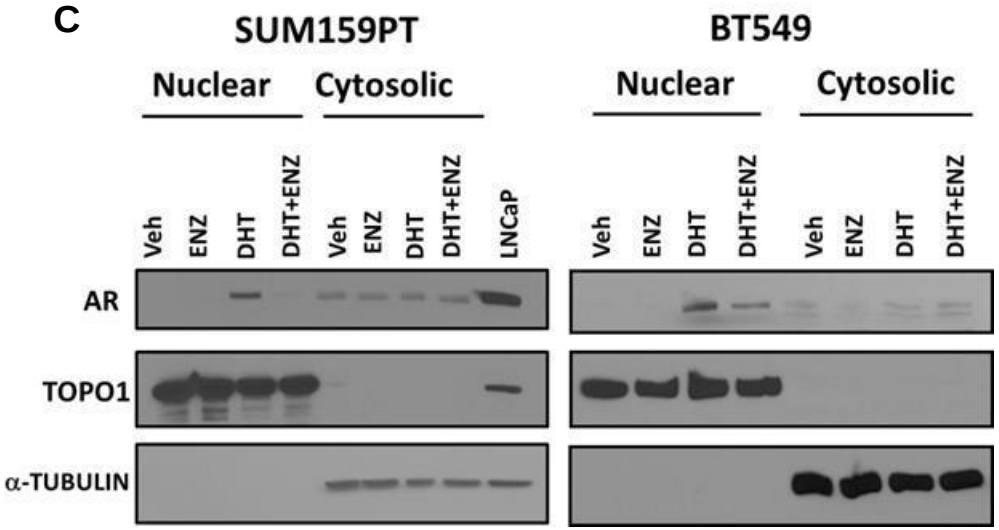
SUM159PT
BT549
Nuclear
Cytosolic
Nuclear
Cytosolic
Veh
ENZ
DHT
DHT+ENZ
Veh
ENZ
DHT
DHT+ENZ
LNCaP
Veh
ENZ
DHT
DHT+ENZ
Veh
ENZ
DHT
DHT+ENZ
AR
TOPO1
α-TUBULIN

Fig 1

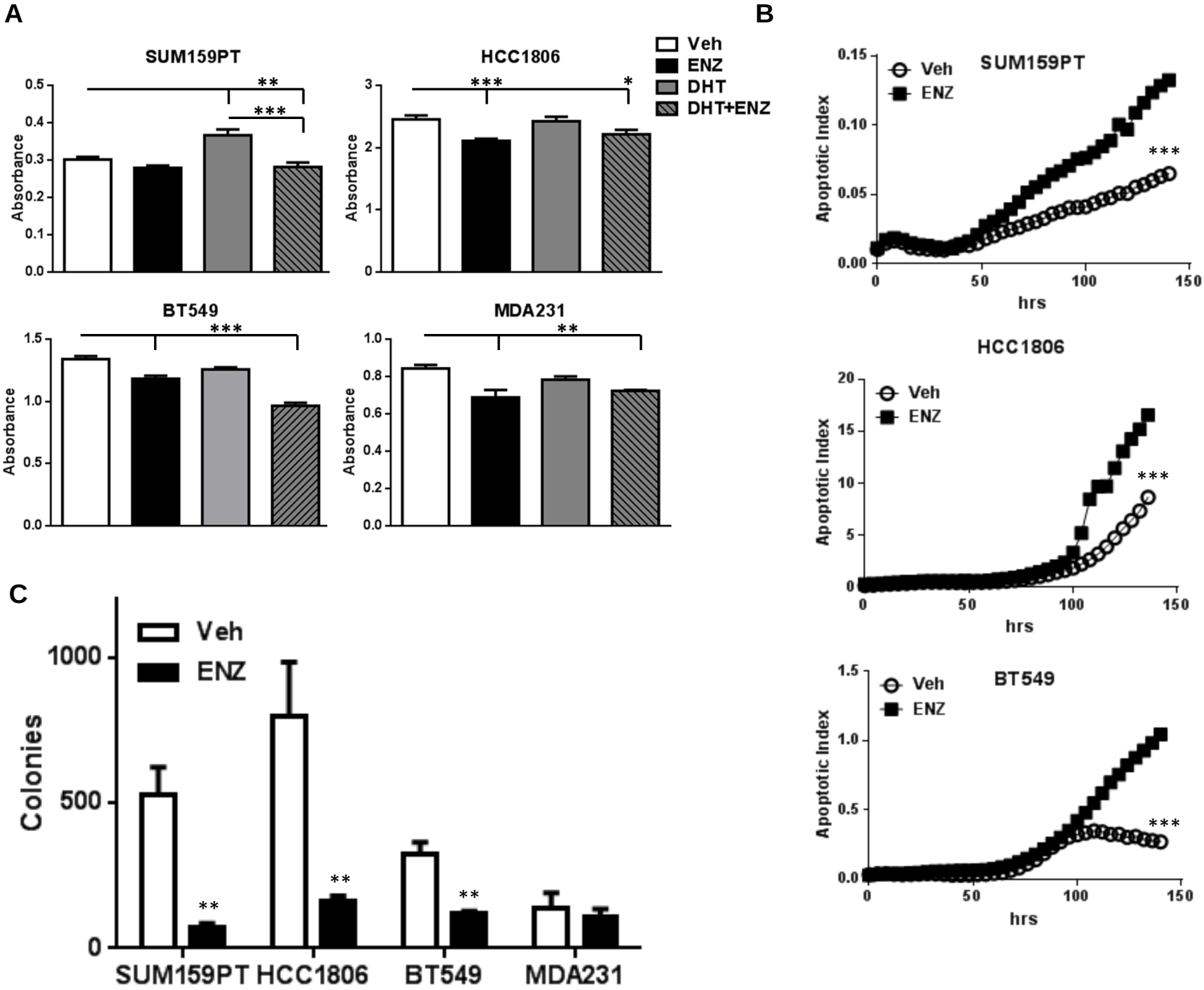
A
SUM159PT
HCC1806
BT549
MDA231
Veh
ENZ
DHT
DHT+ENZ
Absorbance
B
SUM159PT
HCC1806
BT549
Apoptotic Index
hrs
C
Colonies
SUM159PT
HCC1806
BT549
MDA231

Fig 2

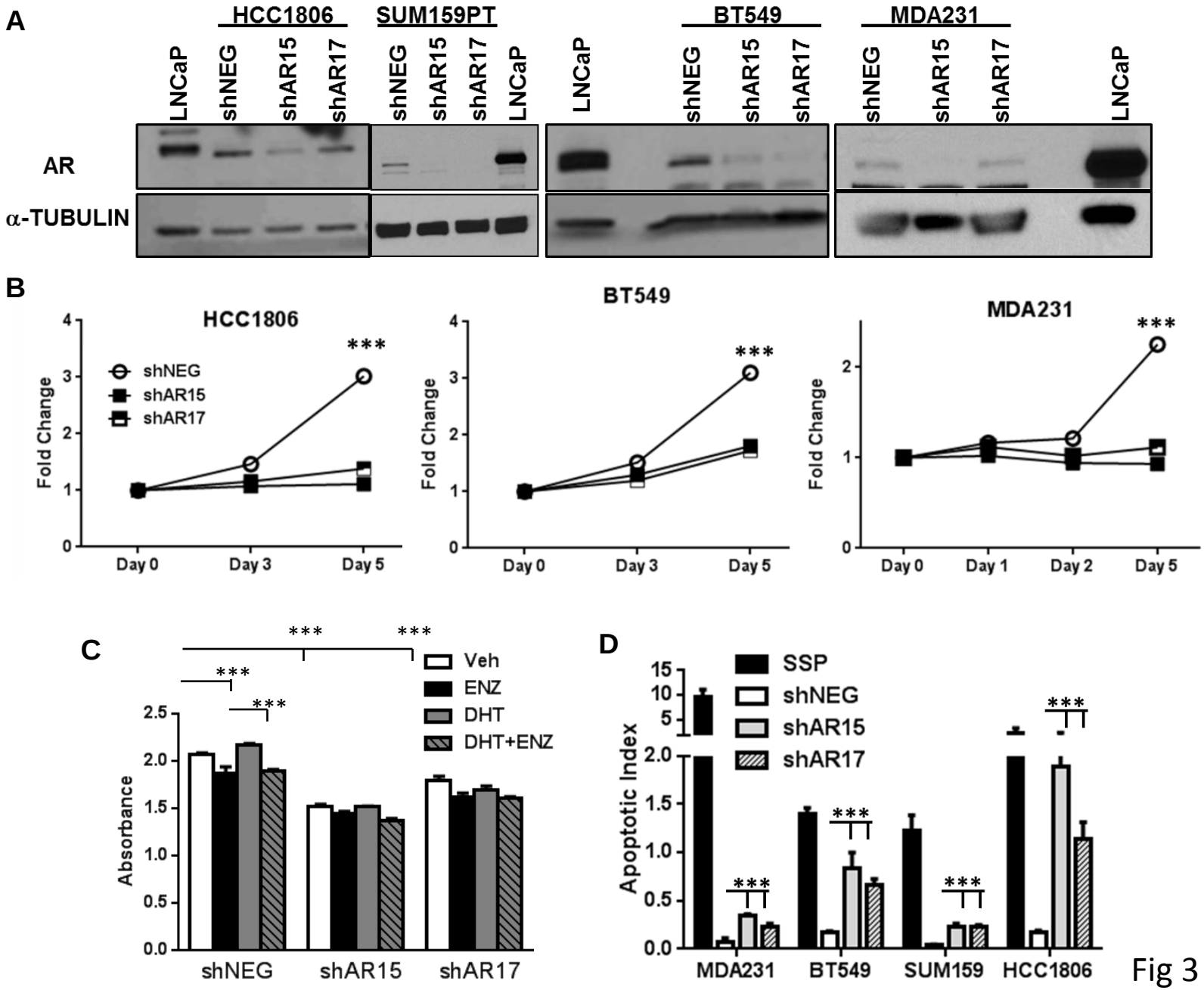
A
HCC1806
SUM159PT
BT549
MDA231
LNCaP
shNEG
shAR15
shAR17
AR
α-TUBULIN
B
HCC1806
BT549
MDA231
shNEG
shAR15
shAR17
Fold Change
Day 0
Day 1
Day 2
Day 3
Day 5
***
C
Veh
ENZ
DHT
DHT+ENZ
Absorbance
shNEG
shAR15
shAR17
D
SSP
shNEG
shAR15
shAR17
Apoptotic Index
MDA231
BT549
SUM159
HCC1806

Fig 3

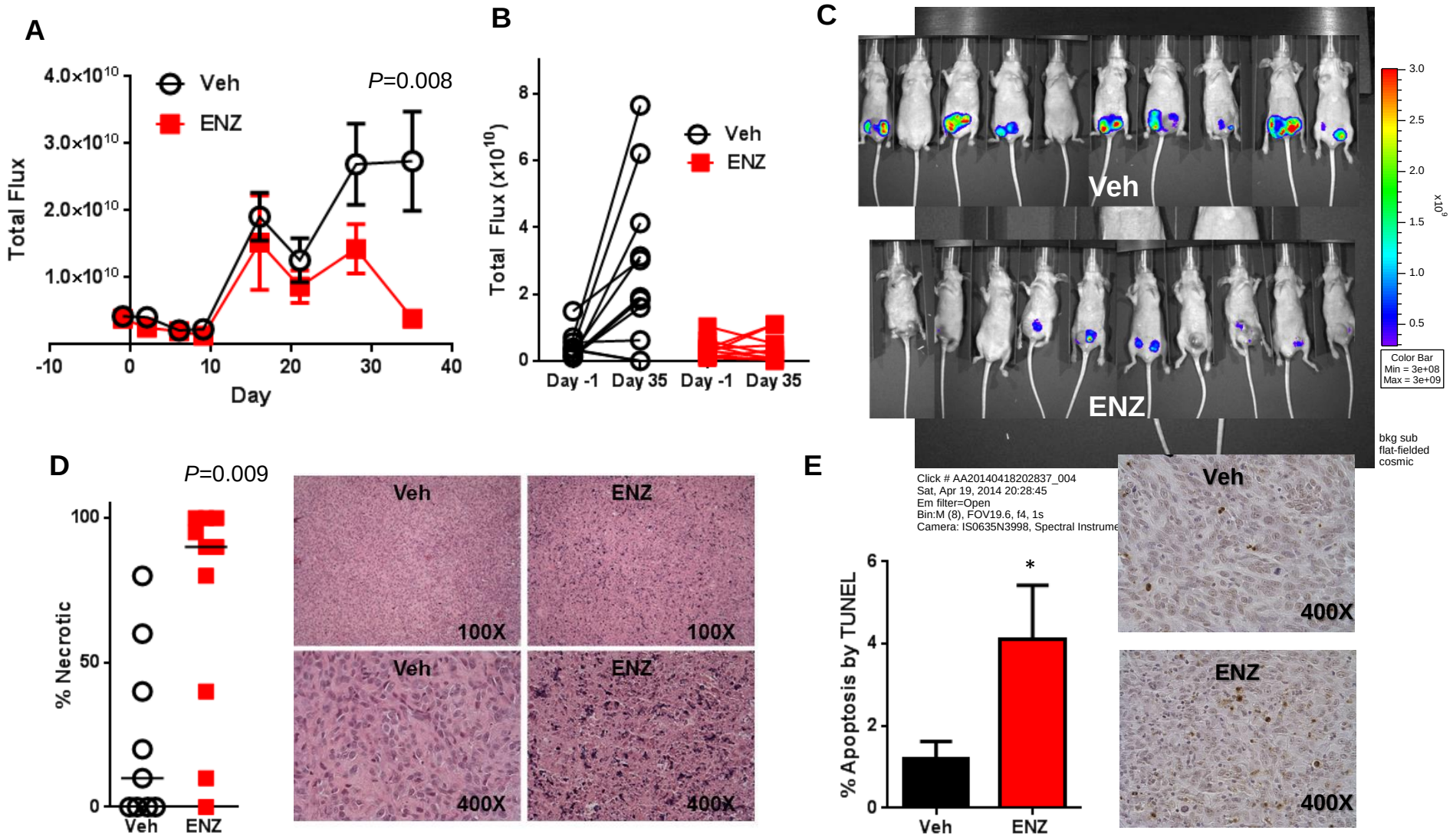
A
4.0x10^10
3.0x10^10
2.0x10^10
1.0x10^10
Total Flux
Veh
ENZ
P=0.008
-10
0
10
20
30
40
Day
B
Total Flux (x10^10)
8
6
4
2
0
Veh
ENZ
Day -1
Day 35
Day -1
Day 35
C
Veh
ENZ
3.0
2.5
2.0
1.5
1.0
0.5
x10^9
Color Bar
Min = 3e+08
Max = 3e+09
bkg sub
flat-fielded
cosmic
D
P=0.009
100
50
0
% Necrotic
Veh
ENZ
Veh
100X
ENZ
100X
Veh
400X
ENZ
400X
E
Click # AA20140418202837_004
Sat, Apr 19, 2014 20:28:45
Em filter=Open
Bin:M (8), FOV19.6, f4, 1s
Camera: IS0635N3998, Spectral Instrume
6
4
2
0
% Apoptosis by TUNEL
*
Veh
ENZ
Veh
400X
ENZ
400X

Fig 4

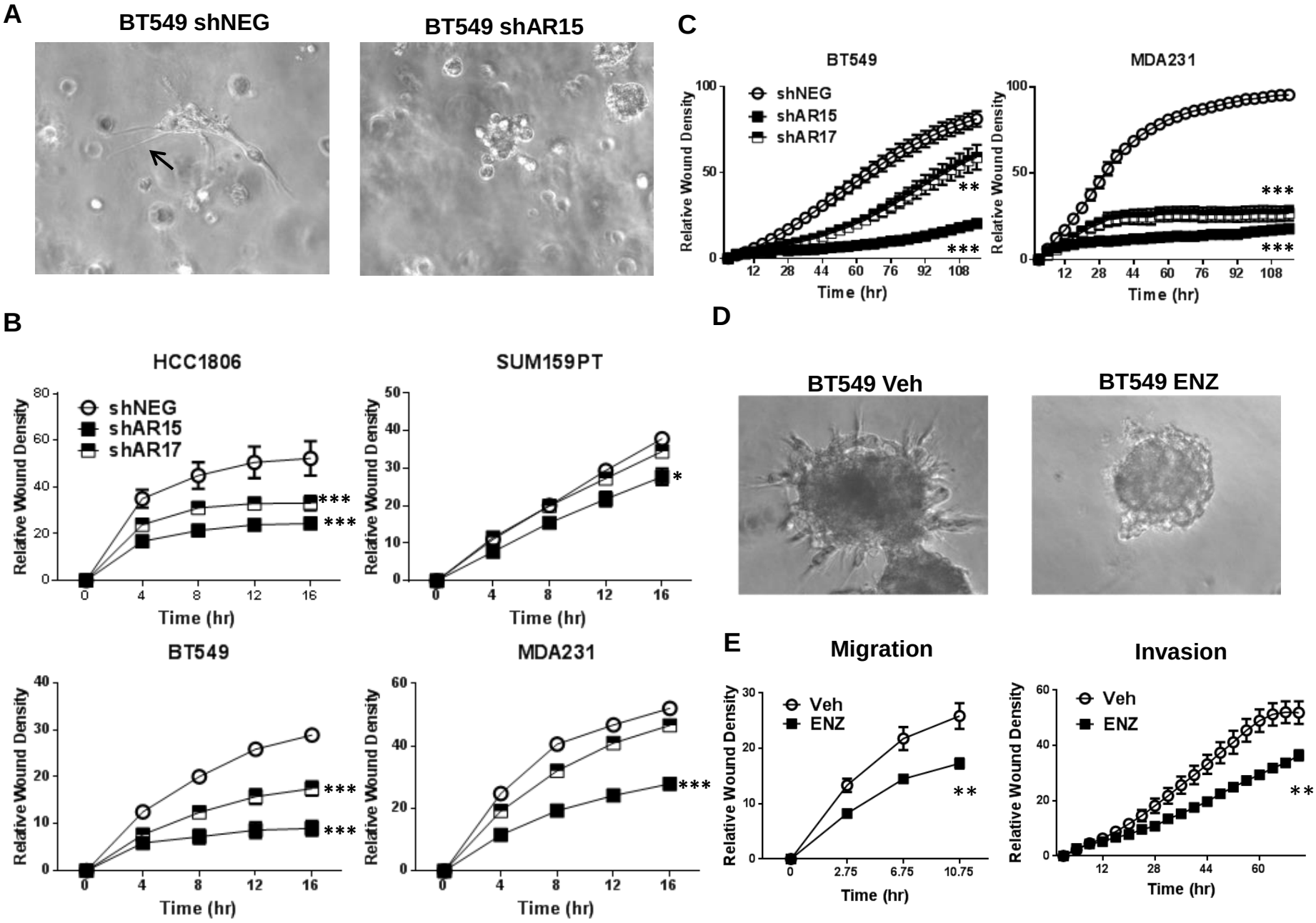
A
BT549 shNEG
BT549 shAR15
C
BT549
MDA231
shNEG
shAR15
shAR17
Relative Wound Density
Time (hr)
B
HCC1806
SUM159PT
BT549
MDA231
D
BT549 Veh
BT549 ENZ
E
Migration
Invasion
Veh
ENZ

Fig 5

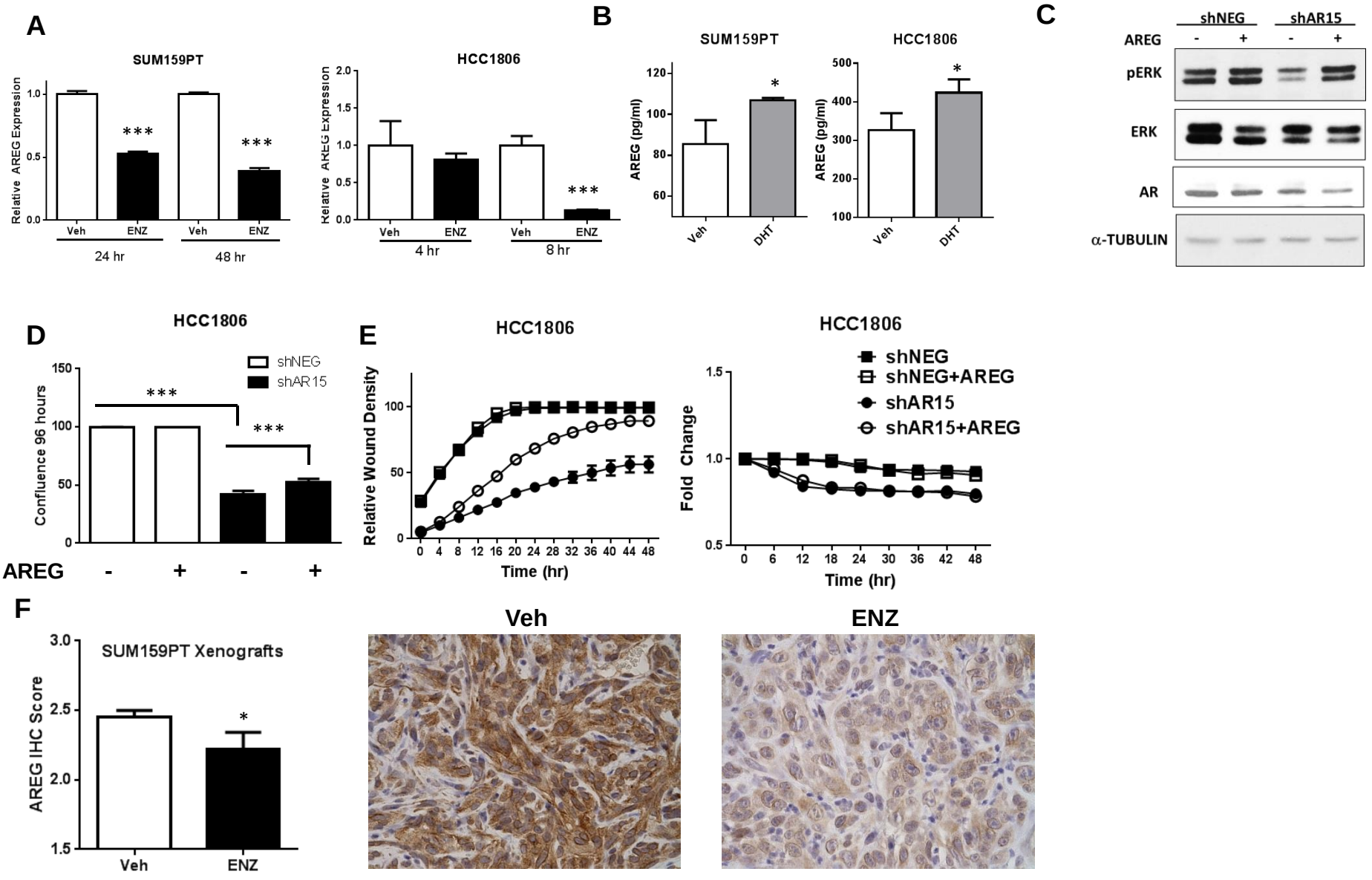
A
SUM159PT
Relative AREG Expression
1.0
0.5
0.0
***
***
Veh
ENZ
Veh
ENZ
24 hr
48 hr
HCC1806
Relative AREG Expression
2.0
1.5
1.0
0.5
0.0
***
Veh
ENZ
Veh
ENZ
4 hr
8 hr
B
SUM159PT
AREG (pg/ml)
120
100
80
60
*
Veh
DHT
HCC1806
AREG (pg/ml)
500
400
300
200
100
*
Veh
DHT
C
shNEG
shAR15
AREG
-
+
-
+
pERK
ERK
AR
α-TUBULIN
D
HCC1806
shNEG
shAR15
Confluence 96 hours
150
100
50
0
***
***
AREG
-
+
-
+
E
HCC1806
Relative Wound Density
100
50
0
0 4 8 12 16 20 24 28 32 36 40 44 48
Time (hr)
HCC1806
shNEG
shNEG+AREG
shAR15
shAR15+AREG
Fold Change
1.5
1.0
0.5
0 6 12 18 24 30 36 42 48
Time (hr)
F
SUM159PT Xenografts
AREG IHC Score
3.0
2.5
2.0
1.5
*
Veh
ENZ
Veh
ENZ

Fig 6

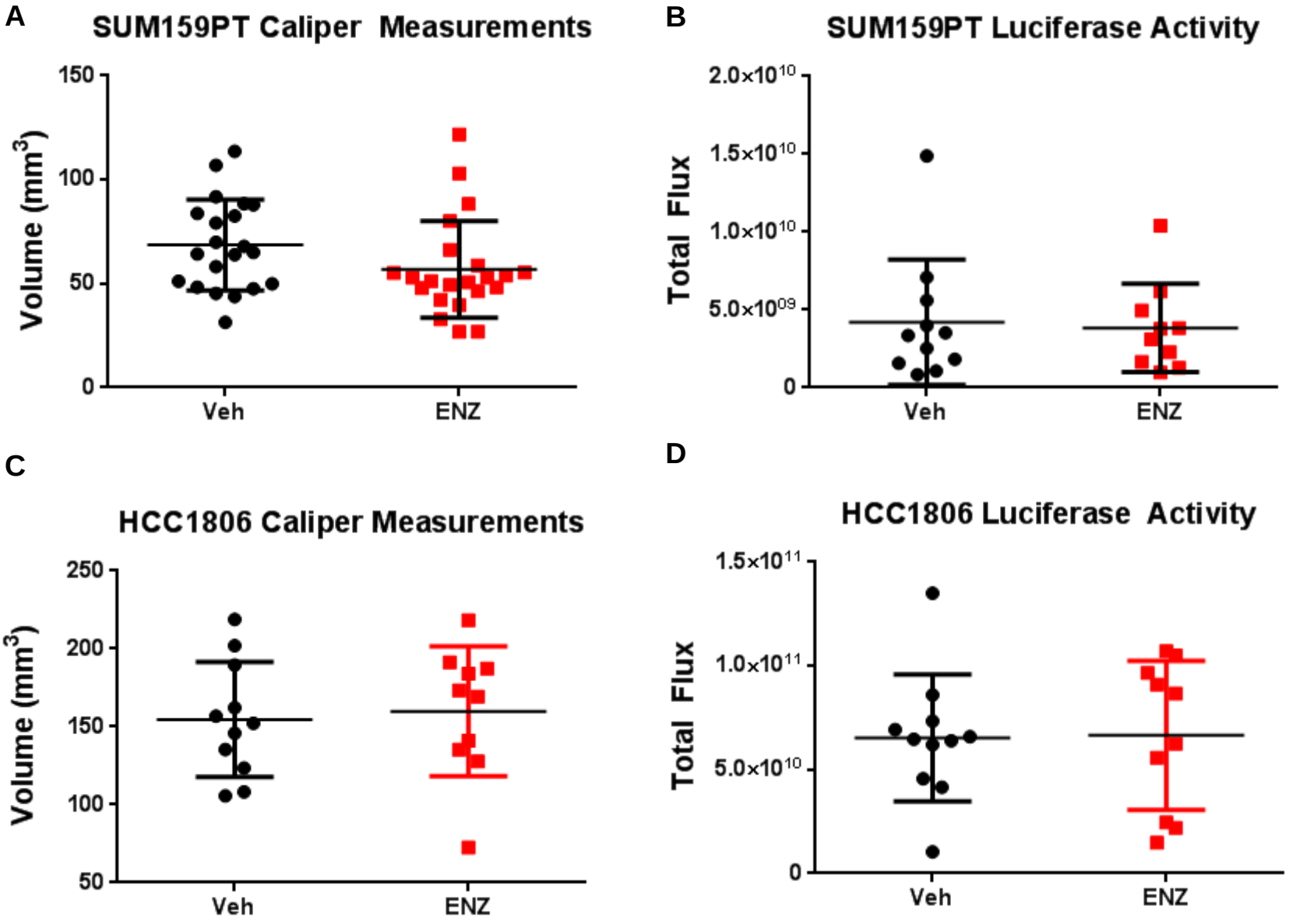
A
SUM159PT Caliper Measurements
Volume (mm3)
150
100
50
0
Veh
ENZ
B
SUM159PT Luciferase Activity
Total Flux
2.0×10^10
1.5×10^10
1.0×10^10
5.0×10^09
0
Veh
ENZ
C
HCC1806 Caliper Measurements
Volume (mm3)
250
200
150
100
50
Veh
ENZ
D
HCC1806 Luciferase Activity
Total Flux
1.5×10^11
1.0×10^11
5.0×10^10
0
Veh
ENZ

Sup Fig. 1

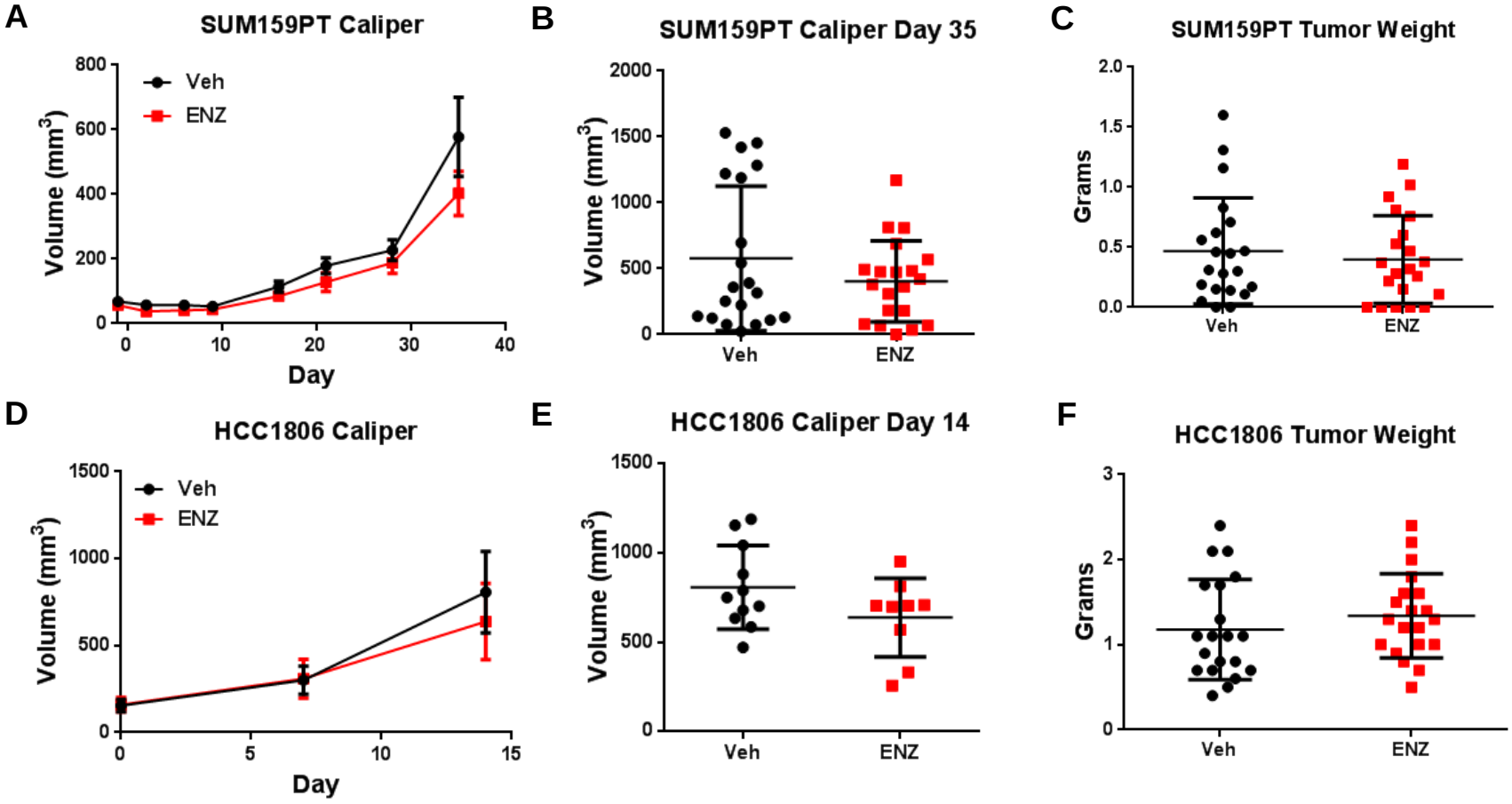
A
SUM159PT Caliper
Volume (mm3)
Day
Veh
ENZ
B
SUM159PT Caliper Day 35
Volume (mm3)
Veh
ENZ
C
SUM159PT Tumor Weight
Grams
Veh
ENZ
D
HCC1806 Caliper
Volume (mm3)
Day
Veh
ENZ
E
HCC1806 Caliper Day 14
Volume (mm3)
Veh
ENZ
F
HCC1806 Tumor Weight
Grams
Veh
ENZ

Sup Fig. 2

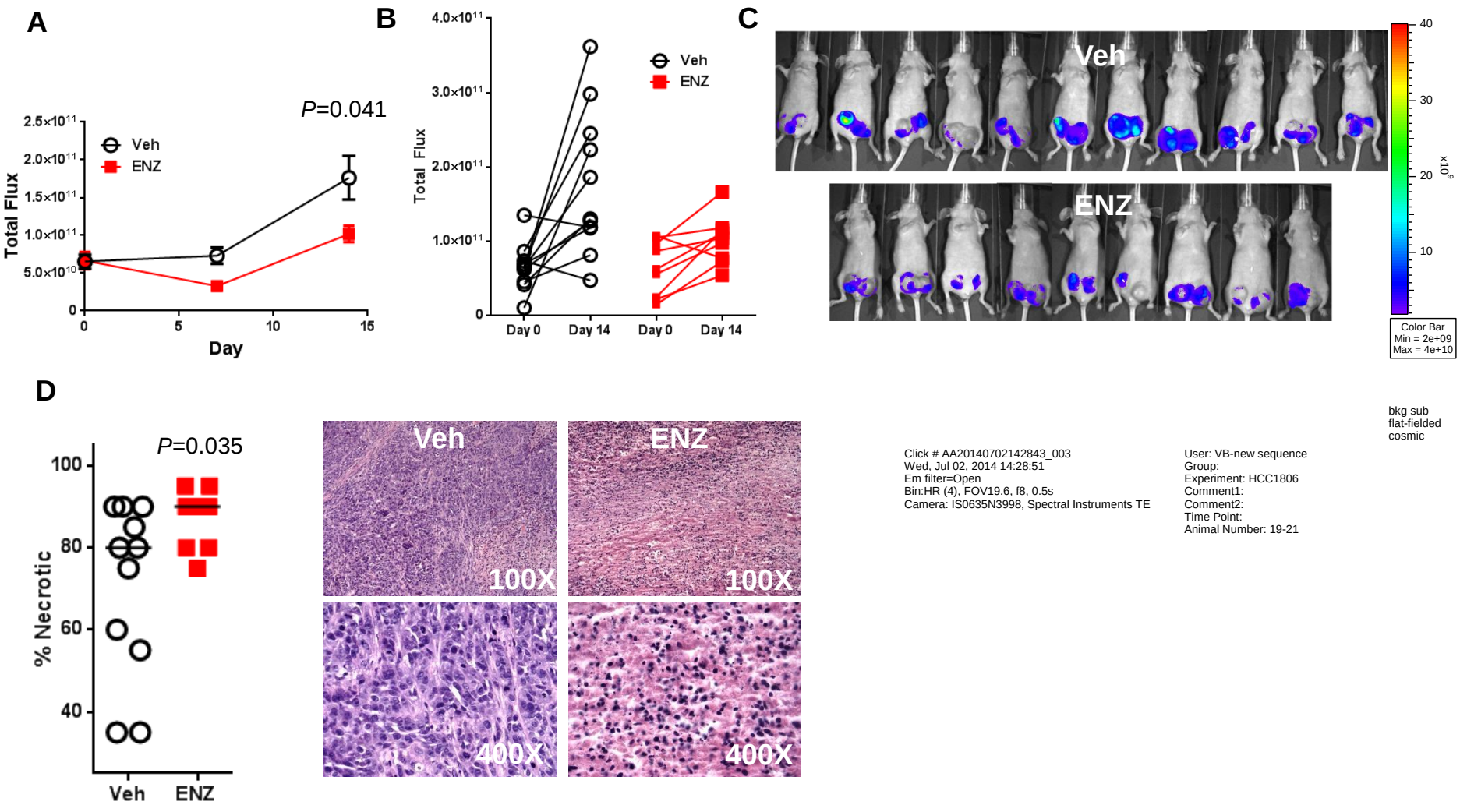
A
P=0.041
Veh
ENZ
Total Flux
Day
B
Veh
ENZ
Total Flux
Day 0
Day 14
Day 0
Day 14
C
Veh
ENZ
Color Bar
Min = 2e+09
Max = 4e+10
bkg sub
flat-fielded
cosmic
Click # AA20140702142843_003
Wed, Jul 02, 2014 14:28:51
Em filter=Open
Bin:HR (4), FOV19.6, f8, 0.5s
Camera: IS0635N3998, Spectral Instruments TE
User: VB-new sequence
Group:
Experiment: HCC1806
Comment1:
Comment2:
Time Point:
Animal Number: 19-21
D
P=0.035
% Necrotic
Veh
ENZ
Veh
ENZ
100X
100X
400X
400X

Sup Fig. 3

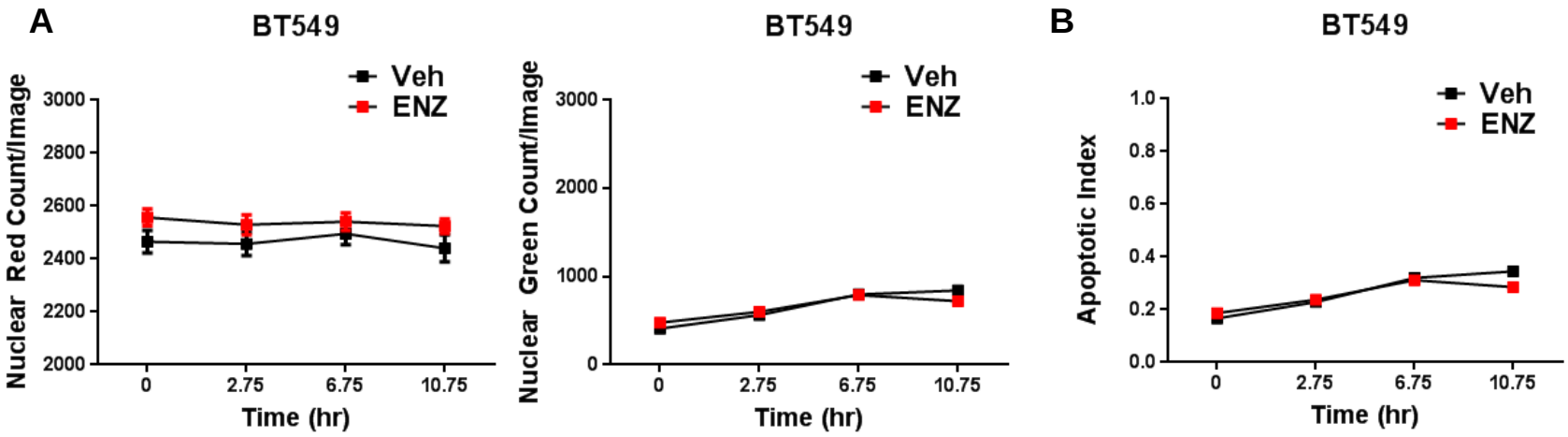
A
BT549
Veh
ENZ
Nuclear Red Count/Image
3000
2800
2600
2400
2200
2000
0
2.75
6.75
10.75
Time (hr)
BT549
Veh
ENZ
Nuclear Green Count/Image
3000
2000
1000
0
0
2.75
6.75
10.75
Time (hr)
B
BT549
Veh
ENZ
Apoptotic Index
1.0
0.8
0.6
0.4
0.2
0.0
0
2.75
6.75
10.75
Time (hr)

Sup Fig. 4